Year : 2023

Characterization of Root Epidermal Cell Wall Modifications in Arabidopsis thaliana

Farahani Zayas Nasim

Farahani Zayas Nasim, 2023, Characterization of Root Epidermal Cell Wall Modifications in Arabidopsis thaliana

Originally published at : Thesis, University of Lausanne

Posted at the University of Lausanne Open Archive http://serval.unil.ch
Document URN : urn:nbn:ch:serval-BIB_1A7F8F04FD864

UNIL | Université de Lausanne
Faculté de biologie et de médecine

Département de Biologie Moléculaire Végétale

Characterization of Root Epidermal Cell Wall Modifications in *Arabidopsis thaliana*

Thèse de doctorat ès sciences de la vie (PhD)

présentée à la

Faculté de biologie et de médecine
de l'Université de Lausanne

Par

Nasim FARAHANI ZAYAS

Master de l'Université de Wageningen, Pays-Bas

Jury

Prof. Laurent Lehmann, Président
Dr. Christiane Nawrath, Directrice de thèse
Dr. Rochus Benni Franke, Expert
Prof. Clara Sanchez Rodriguez, Experte

Lausanne, 2023

UNIL | Université de Lausanne
Faculté de biologie
et de médecine

Ecole Doctorale
Doctorat ès sciences de la vie

Imprimatur

Vu le rapport présenté par le jury d'examen, composé de

Président·e	Monsieur	Prof.	Laurent	**Lehmann**
Directeur·trice de thèse	Madame	Dre	Christiane	**Nawrath**
Expert·e·s	Monsieur	Dr	Rochus	**Benni Franke**
	Madame	Prof.	Clara	**Sanchez Rodriguez**

le Conseil de Faculté autorise l'impression de la thèse de

Nasim Farahani Zayas

Master in Biotechnology, Université de Wageningen, Pays-Bas

intitulée

Characterization of root epidermal cell wall modifications in *Arabidopsis thaliana*

Lausanne, le 26 mai 2023

pour le Doyen
de la Faculté de biologie et de médecine

Prof. Laurent Lehmann

Acknowledgments

These past few years have been the most intense and rewarding of my life, and there are many people I would like to thank for accompanying me on this journey. First, I would like to start by expressing my gratitude to my supervisor Dr. Christiane Nawrath for her guidance, her encouragement, and support. I would also like to thank my mid-thesis and thesis committee for the helpful discussions and guidance. Thank you to Prof. Niko Geldner and his lab for the fruitful lab meetings and always helping me. Thank you to Damien de Bellis for all the beautiful images you took, and to Prof. Matheusz Majda and Nicola Tozzi for assisting me with experiments in the past few months.

Thank you to Aime, Noel, Joaquin, Yifat, Natalia, and Irene for giving me input on this thesis. I would also like to thank my lab mates, former and current: Carolina, Alice, Aurore, Kay, Yifat, and our newest member, John. It has been a pleasure to share the lab with you.

Working at the DBMV has been amazing, I will really miss it. There is such a joyous atmosphere at the department and making it so easy for me to fit in right from the beginning. Through the years people came and left, and so many people have made my Ph.D. years memorable, such as Gioia, Joaquin, Noel, Natalia, Cecilia, Yasmine, and Pedro. A special mention also goes to Debora, the first friend I made in Lausanne, thank you for being a pillar in my life. Throughout these years we, have grown up together and I'm very proud of the woman you are. And Aime, my amazing office mate and go-to person whenever something did not work. I don't have enough words to thank you for all your help and listening to me.

Fabio, thank you for not letting me give up, helping me, and just being there for me. I am so happy and grateful we've met.

The biggest thanks go to my family. Mom and dad, thank you for constantly pushing me to be the best version of myself, I don't think I would have been where I am if it wasn't for all your support and love. I am fortunate to have you as my parents.

Table of Contents

Abstract

During land colonization, plants developed cell wall modifications to isolate themselves from the outer environment. In several species, including onion and soybean, modifications of the outer cell wall of the root epidermis with a "diffuse," non-lamellated form of suberin that can be stained with lipid dyes, such as Fluorol Yellow (FY), have been described. However, little is known about the cell wall modifications in the root epidermis of model plants. Here, we sought to investigate whether there are cell wall modifications in the root epidermis of *Arabidopsis* and characterize their composition and role. In Arabidopsis, the outer epidermal wall is reinforced by molecules that can be stained with Auramine O (AO), but not with FY. AO staining was evaluated in mutants of genes involved in lipid polyester biosynthesis, such as *GLYCEROL-3-PHOSPHATE ACYLTRANSFERASES* (*GPATs*) and *GDSL-MOTIF ESTERASE/LIPASES* (*GELPs*), without giving any indication of the presence of a lipid-based polymer in the outer epidermal cell wall. Pharmacological inhibition of the phenylpropanoid pathway, however, reduced the intensity of AO staining, while exogenous application of lignin monomers and other phenylpropanoids led to increased AO staining of the outer cell wall. We show that *PHENYLALANINE AMMONIA-LYASE 2* (*PAL2*) and *CINNAMATE 4-HYDROXYLASE* (*CH4*), two key genes of the phenylpropanoid pathway, are expressed in the root epidermis, as are several *RESPIRATORY BURST OXIDASE HOMOLOG* (*RBOH*) genes, which are required for the formation of reactive oxygen species (ROS). Analysis of higher-order mutants in monolignol biosynthesis and in ROS formation and the application of peroxidase inhibitors corroborated that a lignin-like polymer is deposited in the outer cell wall of the root epidermis. Interestingly, while Basic Fuchsin strongly stains the lignin of the Casparian strip, it stains the outer root epidermal cell wall very weakly. Conversely, Safranine O, a dye used to detect lignin, stained the outer epidermis stronger than the Casparian strip. This indicated differences in the composition or polymerization grade of the lignin-like polymer. No evidence for a role in cell wall permeability and under abiotic stresses of this lignin-like polymer could be found. However, a higher deposition of the lignin-like compound in trichoblasts than in atrichoblasts was detected, opening the possibility of further studies on the biological role of this lignin-like polymer.

Furthermore, we investigated the potential deposition of a lipid polymer in response to abscisic acid (ABA)-regulated stress responses by studying the spatiotemporal expression pattern of members of the GPAT family. No increase in the expression of GPATs in the root epidermis could be found with ABA treatment, but an intriguing expression pattern in other cell layers was observed, which may be further investigated in the future.

Résumé

Au cours de la colonisation terrestre, les plantes ont modifié leurs parois cellulaires pour s'isoler de l'environnement extérieur. Chez plusieurs espèces, dont l'oignon et le soja, des modifications de la paroi cellulaire externe de l'épiderme racinaire avec une forme "diffuse" et non lamellaire de subérine – pouvant être colorée avec des colorants lipidiques tel que le jaune fluoré (FY) – ont été décrites. Cependant, peu de connaissances ont été acquises concernant les modifications de la paroi cellulaire dans l'épiderme racinaire des plantes modèles. Dans ces travaux, nous avons cherché à savoir s'il existe des modifications de la paroi cellulaire dans l'épiderme racinaire d'Arabidopsis ainsi qu'à caractériser leurs composition et rôle. Chez Arabidopsis, la paroi épidermique externe est renforcée par des molécules qui peuvent être colorées avec l'Auramine O (AO), mais pas avec le FY. La coloration à l'AO a été évaluée chez des individus dont les gènes mutés sont impliqués dans la biosynthèse de polyester lipidique, tels que *GLYCEROL-3-PHOSPHATE ACYLTRANSFERASES* (*GPATs*) et *GDSL-MOTIF ESTERASE/LIPASES* (*GELPs*), sans indiquer la présence d'un polymère à base de lipides dans la paroi cellulaire de l'épiderme externe. L'inhibition pharmacologique de la voie des phénylpropanoïdes a toutefois réduit l'intensité de la coloration AO, tandis que l'application exogène de monomères de lignine et d'autres phénylpropanoïdes a entraîné une augmentation de la coloration AO de la paroi cellulaire externe. Nous démontrons que la *PHENYLALANINE AMMONIA-LYASE 2* (*PAL2*) et la *CINNAMATE 4-HYDROXYLASE* (*CH4*), deux gènes clés de la voie des phénylpropanoïdes, sont exprimés dans l'épiderme des racines, ainsi que plusieurs gènes de la famille des *RESPIRATORY BURST OXIDASE HOMOLOG* (*RBOH*) qui sont nécessaires à la formation de dérivés réactifs de l'oxygène (ROS). L'analyse de mutants d'ordre supérieur dans la biosynthèse des monolignols et dans la formation des ROS, ainsi que l'application d'inhibiteurs de la péroxydase, ont confirmé qu'un polymère semblable à la lignine est déposé dans la paroi cellulaire externe de l'épiderme de la racine. Il est intéressant de noter que si la fuchsine basique colore fortement la lignine de la barrière de Caspary, elle colore très faiblement la paroi cellulaire externe de l'épiderme de la racine. Inversement, la safranine O, un colorant utilisé pour détecter la lignine, a coloré l'épiderme externe plus fortement que la barrière de Caspary. Cela indique des différences dans la composition ou le degré de polymérisation du polymère semblable à la lignine. Aucune preuve d'un rôle de ce polymère dans la perméabilité de la paroi cellulaire et dans les stress abiotiques n'a pu être apportée. En revanche, un dépôt du composé de type lignine a été détecté de façon plus importante dans les trichoblastes que dans les atrichoblastes, ce qui ouvre la voie à des études supplémentaires sur le rôle biologique de ce polymère.

En outre, nous avons étudié le dépôt potentiel d'un polymère lipidique en réponse au stress régulé par l'acide abscissique (ABA) en étudiant le profil d'expression spatio-temporel des membres de la famille GPAT. Aucune augmentation de l'expression des GPAT dans l'épiderme de la racine n'a pu être constatée avec le traitement ABA, mais un schéma d'expression intrigant observé dans d'autres couches cellulaires pourrait faire l'objet d'une étude plus approfondie à l'avenir.

Résumé vulgarisé

Caractérisation des modifications de la paroi cellulaire de l'épiderme racinaire chez *Arabidopsis thaliana*

Présenté par Nasim Farahani Zayas – Département de Biologie Moléculaire Végétale

Au cours de l'évolution, les plantes ont modifié leurs parois cellulaires pour faire face aux pressions environnementales (gel, sécheresse, herbivores, etc.). Les racines des plantes sont composées de plusieurs couches cellulaires, la plus externe étant connue sous le nom d'épiderme. L'épiderme étant la couche cellulaire en contact permanent avec l'environnement, il est concevable que sa paroi cellulaire soit modifiée. En effet, dans les racines d'oignon ou de soja, les parois cellulaires épidermiques sont modifiées par des lipides. Nous avons cherché à évaluer si l'épiderme des racines de l'espèce végétale modèle *Arabidopsis thaliana* était également modifié par des lipides. Nous avons découvert qu'en fait, un type de lignine modifie les parois cellulaires épidermiques d'*Arabidopsis*. La lignine est un polymère organique complexe s'accumulant dans les parois cellulaires de nombreuses plantes, ce qui les rend rigides et hydrophobes. Nos résultats indiquent que la lignine atypique déposée dans la paroi cellulaire externe de l'épiderme racinaire ne semble pas être impliquée dans la perméabilité ni contre les stress abiotiques. D'autres études permettraient d'évaluer le rôle de la lignine atypique dans l'épiderme racinaire d'*Arabidopsis*. Nos résultats ouvrent ainsi un nouveau chapitre dans l'étude des modifications de la paroi cellulaire épidermique chez les plantes.

List of Figures and Tables

List of abbreviations

ABA	Abscisic acid
ABCG	ATP-binding cassette transporters sub-family G
ACC	1-aminocyclopropane-1-carboxylic acid
AO	Auramine O
AFST	Aliphatic suberin feruloyl-transferase
AVG	Aminovinylglycine
BF	Basic Fuchsin
BDG	Bodyguard
CA	Coniferyl alcohol
CIF	Casparian strip integrity factor
CS	Casparian strip
CUS	Cutin synthase
CPC	Caprice
CYP	Cytochrome P450 oxidase
DCF	Deficient in cutin ferulate
DCR	Defective in cuticular ridges
FY	Fluorol Yellow
GL	Glabra
GC-MS	Gas chromatography – mass spectrometry
GDSL	Glycine-aspartic acid-serine-leucine motif
GELP	GDSL-motif esterase/lipase
GFP	Green fluorescent protein
GPAT	Glycerol-3-phosphate acyl transferase
KCS	Ketoacyl-CoA synthase
LAC	Laccase
LACS	Long chain acyl-CoA synthase
LTP	Lipid transfer protein
NLS	Nuclear localized signal
p-CO	*p*-Coumaryl alcohol
PA	Piperonylic acid
PAL	Phenylalanine-ammonia-lyase
PI	Propidium Iodide
PP	Phenylpropanoid
PRX	Peroxidase
RAM	Root apical meristem
RBOH	Respiratory burst oxidase homolog
RCC	Root cap cuticle
RHD	Root hair defective
ROS	Reactive oxygen species
SA	Sinapyl alcohol
TEM	Transmission electron microscopy
TTG	Transparent testa glabra
WT	Wild-type
WER	Werewolf

1. Root: the anchorage of plants to the soil

The emergence of land plants occurred approximately 480 million years ago, and it was a pivotal historical event. Their adaptation to terrestrial life involved several innovations, such as the formation of rooting systems for anchorage, water uptake, and nutrient acquisition (Jones & Dolan, 2012). Moreover, this new environment has new and different biotic and abiotic stresses, such as soil-borne pathogens and, at times, excessive ion concentrations, from which the root must protect itself (Kolattukudy, 2001).

1.1 Root growth and development

Root development is a continuous process in which different cell types originate from individual cells, known as cell initials (**Figure 1**) (Dolan et al., 1993). This event occurs in the root meristem and has been well-studied in the model plant *Arabidopsis thaliana* because of its simple root anatomy and reproducible cell lineage relationships. In *Arabidopsis*, cell initials give rise to all root cell types. The initial cells surround four mitotically less active cells, known as the quiescent center. The region near the cell initials in the root meristem is mitotically active early in root development. However, most cell divisions occur within a short distance above the meristem in an area known as the zone of cell division or the division zone. Upwards from the meristematic zone, is the elongation zone, where cells gradually increase their length. This event drives the expansion of most of the root length, allowing this organ to grow deeper into the soil. The elongation zone is followed by the differentiation zone, in which most cells become mature and specialize (Dolan et al., 1993; Scheres et al., 2002).

1.2 Growth and tissue differentiation of the *Arabidopsis* root

1.2.1 Primary growth

Primary root growth occurs at the root apical meristem (RAM), allowing the root to extend through the soil. To protect the meristematic cells, as the root tip pushes into the soil, the root meristem is surrounded by root cap cells. During primary growth, the RAM gives rise

to the protoderm, ground meristem, and procambium, which differentiate into the epidermis, cortex, endodermis, and vascular system. The complexity of these tissues varies depending on the species. *Arabidopsis* has a relatively simple and well-defined root system consisting of a single layer of epidermis, cortex and endodermis, and multiple vasculature layers. This minimal root system makes *Arabidopsis* an excellent model for studying cellular differentiation and organ development during plant growth (Dolan et al., 1993; Scheres et al., 1995)

The epidermis is the outermost layer of closely packed, thin-walled cells. It is divided into root hair and non-root hair cells. Root hairs increase the absorption area of the root and facilitate the absorption of water and minerals (Jones & Dolan, 2012). The epidermis is followed by the cortex and the endodermis. The endodermis is of central importance for the root function as it acts as an apoplastic barrier for the free diffusion of solutes from the soil to the stele, ensuring selective nutrient uptake (Barberon & Geldner, 2014). It is characterized by the presence of the apoplastic diffusion barrier Casparian Strip, which is composed of lignin, and the cell wall impregnation known as suberin lamellae. Finally, the root vascular system transports water and minerals and comprises the cell tissues pericycle, xylem, and phloem (Lucas et al., 2013).

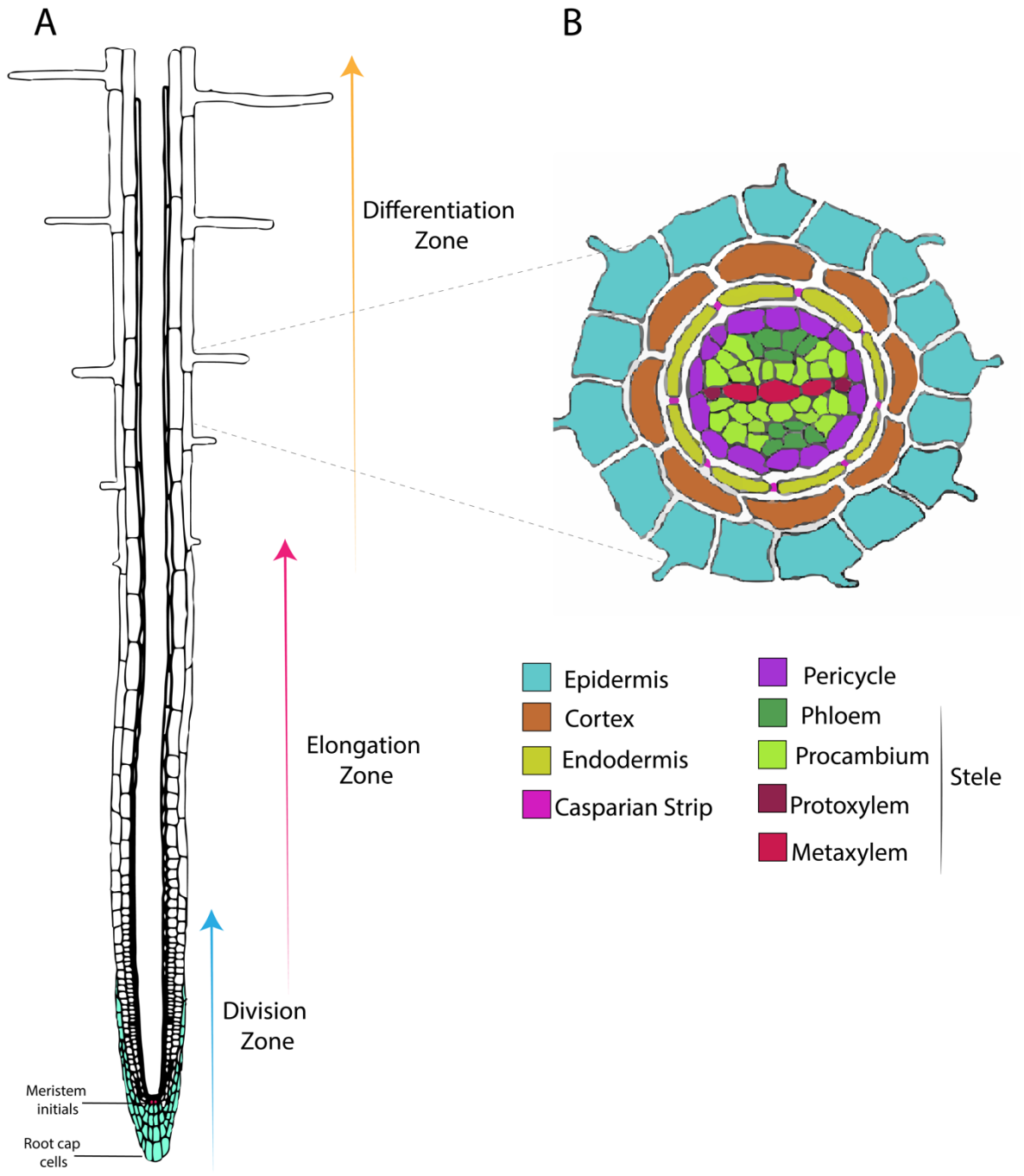

Figure 1. Schematic representation of primary root growth and tissue differentiation. A) Longitudinal view of Arabidopsis root developmental gradient, originating from initial cells with three distinct zones of growth activities: the division zone, where new cells are produced; the elongation zone, where cells undergo rapid elongation; and the differentiation zone, where cells stop rapid elongation. Differentiated structures such as root hairs appear in this zone. B) Schematic overview of an Arabidopsis transversal root section depicting the different root tissues. From the outer to inner layers: epidermis, cortex, endodermis, and vascular stele tissues. Modified from De Smet et al., 2015; Geldner, 2013.

1.2.2 Secondary growth

During development, the root length and maturity of the cells increases, resulting in secondary growth (Spicer & Groover, 2010). This stage is characterized by the development of the periderm, which is composed of three cell types: phellogen, phellem, and phelloderm. The phellogen is produced towards the inside of the phelloderm and the outside of the phellem. In *Arabidopsis,* the periderm is present in the roots and hypocotyl. In the roots, the periderm develops from the pericycle cells in the central cylinder. Then, the epidermal and cortical cells break while endodermal cells undergo programmed cell death. Since phellem cells are continuously produced from the inside, the outer layer constantly peels off (Wunderling et al., 2018).

1.3 Growth and tissue differentiation of roots in angiosperms: the exodermis

In addition to the known root cell tissues, most angiosperms, except *Arabidopsis*, form an additional root tissue with a barrier function known as the exodermis or hypodermis. The exodermis is located between the epidermis and the outermost layer of the cortex (**Figure 2)** (Enstone et al., 2002). In a study where 181 species of angiosperms were surveyed, the exodermis of 86% of the species had been reported to possess either deposits of lignin, suberin, or both (Perumalla et al., 1990). Interestingly, recent studies in *Solanum lycopersicum* show that, unlike the endodermis, the exodermis does not form a Casparian strip (CS). Instead, it forms a polar lignin cap with a barrier equivalent to that of endodermal CS. Furthermore, with seemingly reversed roles, the endodermis of *S. lycopersicum* does not deposit suberin lamellae; instead, the exodermis does (Kajala et al., 2021; Manzano et al., 2022).

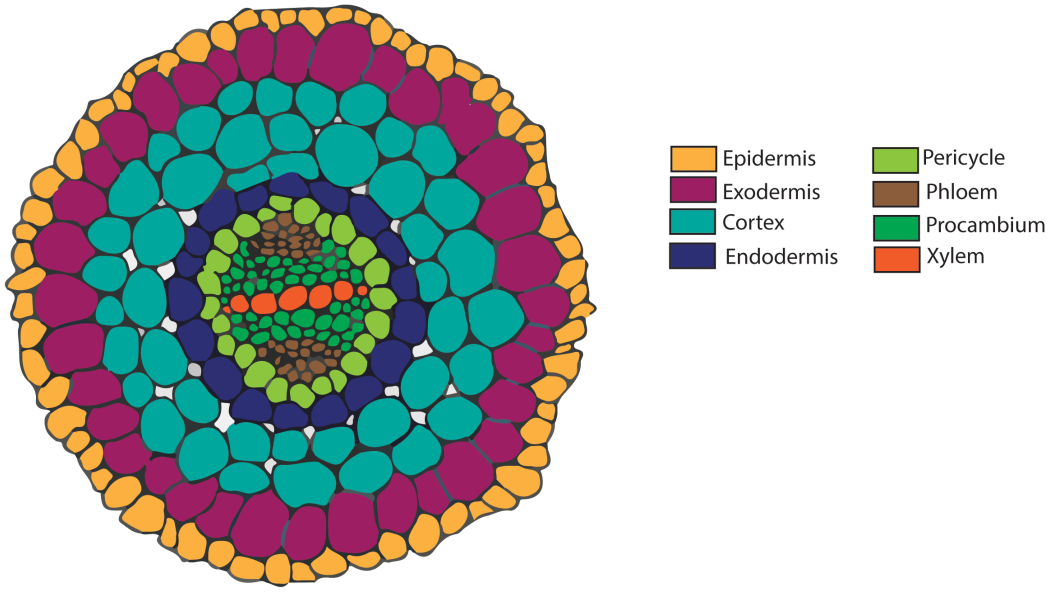

Figure 2. Schematic overview of the different root tissues of *S. lycopersicum.* Drawing of a tomato transversal root section depicting, from the outer to the inner layers, the epidermis, exodermis, cortex, endodermis, and vascular stele tissues: pericycle, phloem, procambium and xylem. Drawing modified from Kajala et al., 2021.

2. The plant cell walls

Every plant cell is surrounded by cell walls, which provide structural support, enabling the root to push through the soil and protecting cells against the environment (Houston et al., 2016). Plant cell walls are mostly composed of three types of polysaccharides: cellulose, hemicelluloses, and pectins. Cellulose consists of para-crystalline microfibrils made of linked (1-4)-β-D-glucose that are synthesized in the plasma membrane by CesA complexes (McFarlane et al., 2014). These microfibrils are the scaffold that maintains the cell wall rigidity and are cross-linked by matrix polysaccharides (Houston et al., 2016). Hemicellulose consists of complex glycans that are entangled with cellulose through hydrogen bonds. Lastly, the pectins form a dense aqueous wall matrix and connect cell wall polymers around and between cells (Somssich et al., 2016).

Primary cell walls are produced during cell growth and division and are thin and elastic (**Figure 3**). After cell differentiation, primary cell walls are reinforced by the production of secondary cell walls. These secondary cell walls are thicker than the primary walls and rigid by nature, thus, providing extra strength and stability to the developing seedling. Structurally,

secondary cell walls differ from primary cell walls as they mainly contain cellulose, xylans, and the polyphenolic compound lignin. Lignin provides extra strength to the cell walls and makes them waterproof (Somssich et al., 2016).

While the main building blocks of the cell walls are similar, the functional needs of the different cells lead to a diverse set of polymers being produced around individual cells. Therefore, cell walls, in different cell layers and along the root axis, vary in polysaccharide content or additional non-polysaccharide modifications that embed or cover the cell walls (Somssich et al., 2016).

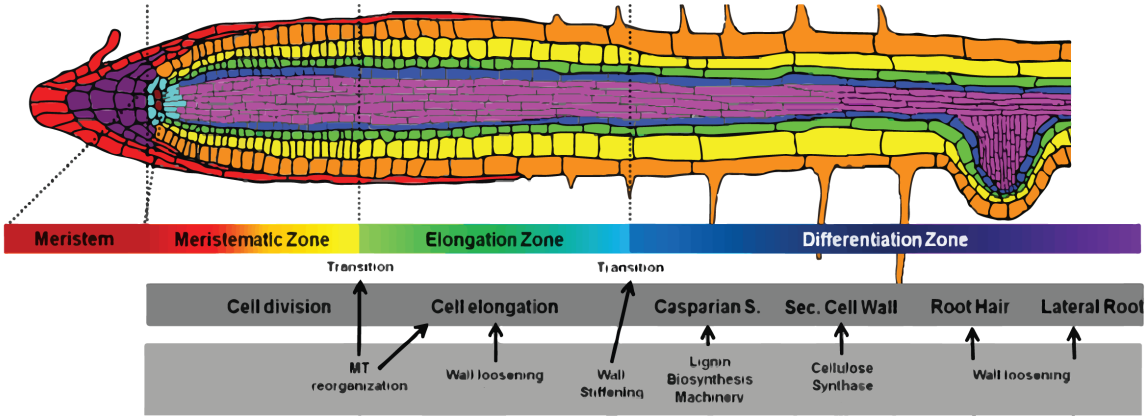

Figure 3. *Arabidopsis* root architecture and cell wall differentiation. Above, the root developmental zones are indicated, ranging from the meristem (dark red) to the differentiation zone (dark blue). In grey: the characteristics of each developmental zone (upper line) and the associated cell wall modifications (lower line). Modified from Somssich et al., 2016.

2.1 Plant cell wall modifications

Root cell walls can remarkably adapt to different environments, nutrient fluctuations, and protect against biotic and abiotic stresses. These adaptations can involve changes in polysaccharide distribution or reinforcement with phenolic compounds or lipids. Since this thesis focuses on young seedlings that have developed only until primary growth, secondary root growth cell wall modifications will not be further discussed.

2.1.1 Polysaccharides

The contents of cellulose, hemicellulose, and pectin are altered by stress. For instance, during phosphate starvation, plants adjust their root architecture and modulate their cellulose content. Indeed, *Arabidopsis* plants grown under phosphate-deficient conditions show increased thickening of primary cell walls (Müller et al., 2015; Zhang et al., 2012).

2.1.2 Phenolic compounds

Cell wall-bound phenolics include two main groups of compounds, hydroxycinnamic acids and lignin, which originate in the phenylpropanoid pathway.

Hydroxycinnamic acids are a class of phenolic compounds characterized for having a phenolic ring and a radical containing a carboxyl group. These molecules are of low molecular weight and may bind to cell wall components. (Gorshkova et al., 2000; Wallace & Fry, 1994). Ferulic acid is the most abundant hydroxycinnamic acid in plants, and in dicots, it can be found covalently linked to polysaccharides and lignin components. Less abundant in plant cell walls are *p*-coumaric acid, caffeic acid, and sinapic acid (Mathew & Abraham, 2004).

Lignin is an aromatic polymer of monolignol units derived from the phenylpropanoid pathway and is one of the main constituents of the secondary-thickened cell wall. It confers strength, stiffness, and hydrophobicity to the cell wall (Boerjan et al., 2003; Gorshkova et al., 2000; Lee et al., 2019; Wallace & Fry, 1994).

2.1.3 The phenylpropanoid pathway

The phenylpropanoid (PP) pathway starts with the α-amino acid phenylalanine, a product of the shikimate pathway (**Figure 4**). From phenylalanine, monolignol biosynthesis proceeds via a series of modifications, including side-chain modifications and ring hydroxylations. The PP pathway also produces several low molecular weight molecules, such as flavonoids, coumarins, hydroxycinnamic acid conjugates, and lignans (Fraser & Chapple, 2011; Vogt, 2010).

2.1.4 General Phenylpropanoid Pathway

The PP pathway begins with three reactions that lead to the conversion of *p*-coumaroyl CoA starting from phenylalanine. Phenylalanine ammonia-lyase (PAL) catalyzes the first step of PP metabolism, in which phenylalanine undergoes deamination to yield *trans*-cinnamic acid and ammonia. Afterward, the enzyme cinnamate 4-hydroxylase catalyzes the hydroxylation of cinnamate to produce *p*-coumaric acid. 4-coumarate: CoA ligase (4CL) catalyzes the ATP-dependent formation of the CoA thioester *p*-coumaroyl CoA. This step is followed by the transfer of the *p*-coumaroyl group to shikimate by the hydroxycinnamoyl-coenzyme A shikimate: quinate hydroxycinnamoyl-transferase (HCT). The 3'-hydroxylation of *p*-coumaroyl shikimate is catalyzed by *p*-coumaroyl shikimate 3'-hydroxylase (C3'H) to form caffeoyl shikimate. Subsequently, HCT catalyzes the transfer of the caffeoyl to Coenzyme A, forming caffeoyl-CoA. The subsequent synthesis of feruloyl CoA is catalyzed by the enzyme caffeoyl CoA 3-*O*-methyltransferase (CCoAOMT) (Chen et al., 2011; Fraser & Chapple, 2011; Vogt, 2010).

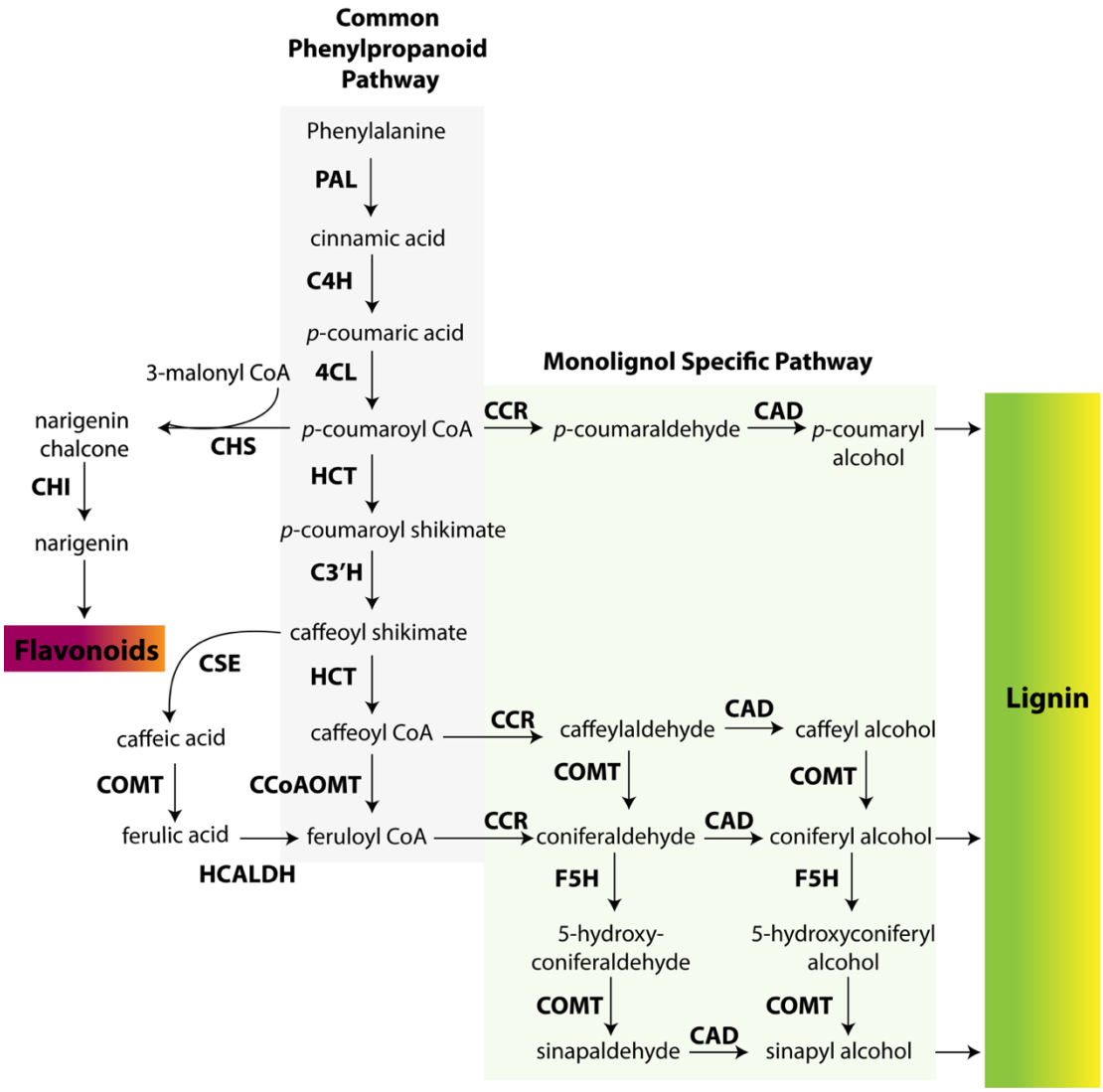

Figure 4. The Phenylpropanoid Pathway. Gray rectangle: common PP pathway. Green rectangle: monolignol-specific ramification with a highlight of the main enzymes. White area: flavonoid biosynthesis-specific pathway. CAD, Cinnamyl Alcohol Dehydrogenase; 4CL, 4-Coumarate: CoA ligase; C3'H, *p*-Coumarate 3-Hydroxylase; C4H, Cinnamate 4-Hydroxylase; CHI, Chalcone Isomerase; CHS, Chalcone Synthase; CSE, Caffeoyl Shikimate Esterase; CCoAOMT, Caffeoyl-CoA O-Methyltransferase; CCR, Cinnamoyl-CoA Reductase; COMT, Caffeic Acid O-Methyltransferase; HCT, *p*-Hydroxycinnamoyl-CoA:Quinate Shikimate *p*-Hydroxycinnamoyltransferase; HCALDH, Hydroxycinnamaldehyde Dehydrogenase; F5H, Ferulate 5-Hydroxylase; PAL, Phenylalanine Ammonia-Lyase; SAD, Sinapyl Alcohol Dehydrogenase. Adapted from Boerjan et al., 2003; Fraser & Chapple, 2011; Vogt, 2010.

2.1.5 Lignin biosynthesis and deposition

Lignin biosynthesis is one of the most extensively characterized branches of the PP pathway. Lignin is generated by radical coupling of hydroxycinnamyl subunits called monolignols (*p*-coumaryl alcohol, coniferyl alcohol, and sinapyl alcohol), which are

synthesized through a monolignol-specific pathway. The steps leading to monolignol formation mainly involve hydroxylation of the aromatic ring, phenolic O-methylation, and reduction of the carboxyl group to an alcohol group (Boerjan et al., 2003).

After their synthesis, monolignols are transported from the cytosol to the cell wall. In *Arabidopsis,* the ATP-binding cassette transporter *ABCG29* has been characterized as a major transporter of *p*-coumaryl alcohol in the root endodermal cell wall (Alejandro et al., 2012). Nevertheless, monolignols may also be transported by other ABCG transporters, yet to be elucidated (Takeuchi et al., 2018).

Once monolignols are transported to the cell wall, they must be oxidized and polymerized into lignin. Lignin polymerization requires monolignol oxidation which is mediated by reactive oxygen species (Mnich et al., 2020)(**Figure 5**). Reactive oxygen species, such as the superoxide, are generated by NADPH oxidases (respiratory burst oxidase homologs (RBOH)). In *Arabidopsis*, the NADPH oxidases RBOHA to RBOHE are expressed in the root in different cell layers and play an important role in root development. *RBOHC* (also called *ROOT HAIR DEFECTIVE 2* (*RHD2)*) is expressed in root hairs and is required for root hair elongation (Foreman et al., 2003), while RBOHF is specifically required for CS formation (Lee et al., 2013). Moreover, RBOHC, RBOHD, RBOHE, and RBOHF control primary root elongation and lateral root emergence (Zhou et al., 2020).

The superoxide formed by the NADPH oxidases must be dismutated into H_2O_2, which often involves catalytic conversion through apoplastic dismutases (SOD) (Karlsson et al., 2005; Karpinska et al., 2001). H_2O_2 will be used to oxidate the monolignols and incorporate them into the lignin polymer. It has been proposed that this process is catalyzed by proteins such as peroxidases, laccases, or other phenol oxidases (Önnerud et al., 2002). The type of peroxidases (PRX) involved in lignin polymerization is class III, with 73 identified homologs, most of which remain uncharacterized (Tognolli et al., 2002). In roots, PRX64 is recruited to form the CS (Rojas-Murcia et al., 2020). Laccases such as LAC4, LAC11, and LAC17 are also involved in root lignin polymerization (Zhao et al., 2013).

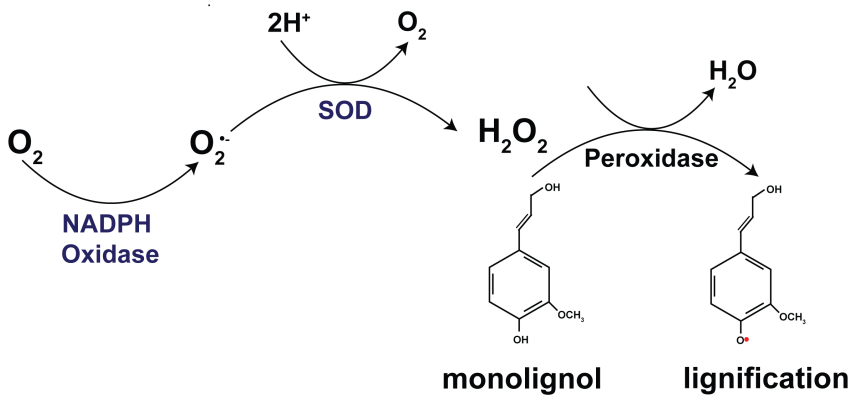

Figure 5. Schematic representation of the steps required for NADPH oxidase-mediated polymerization of lignin. NADPH oxidases produce superoxide, which is subsequently dismutated into peroxide. Peroxide is utilized by peroxidases to catalyze the oxidative coupling of monolignols. Adapted from Lee et al., 2013.

2.1.6 Flavonoids biosynthesis

Several intermediates of the PP pathway serve as branching points towards other pathways, leading to the production of a wide range of secondary metabolites, including flavonoids (Vogt, 2010). Flavonoids are ubiquitous secondary metabolites and key molecules involved in pathogen deterrence, reduction of damage from reactive oxygen species (ROS), and development regulation (Buer et al., 2010). The flavonoid biosynthesis pathway branches from *p*-coumaroyl-CoA and further specific steps result in the synthesis of several metabolites, including flavones, flavonols, and anthocyanins (Lepiniec et al., 2006).

2.1.7 Lignin depositions in different root tissues

An innovation in vascular plants is the deposition of large amounts of lignin in the secondary cell walls of xylem vessels. Lignified xylem provides plants with two vital functions. First, it allows the transport of water and nutrients from roots to shoots. Second, it provides the mechanical support necessary for plants to grow tall (Barros et al., 2015; Cornelis & Hazak, 2022; Emonet & Hay, 2022).

In addition to the deposition of lignin in the secondary cell walls of the vasculature, lignin is deposited in the primary cell walls of endodermal cells for CS formation in the form of a ring-like cell wall modification(Geldner, 2013; Naseer et al., 2012). Endodermal lignification

blocks the apoplastic flow. Therefore, mutants with defects in CS formation lack the apoplastic diffusion barrier that is formed by the CS (Naseer et al., 2012) and show major shoot ionomic changes and reduced fitness (Doblas et al., 2017; Reyt et al., 2021)

In the past it has been hypothesized that the exodermis also forms a CS, mostly due to the autofluorescence of the radial walls of exodermal cell walls. Moreover, CS can be typically recognized because, after plasmolysis, the protoplast does not separate from the radial wall, and this is the case for the exodermal radial walls (Hose et al., 2001; Perumalla et al., 1990; Peterson & Emanuel, 1983). Interestingly, it has been recently described that at least in *S. lycopersicum*, the exodermis does not form a CS. Instead, it forms a polar lignin cap with an equivalent barrier function to the endodermal CS (Manzano et al., 2022).

2.2 Lipidic compounds

Cutin and suberin are insoluble lipid polymers that originate from the fatty acid biosynthetic pathway. Cutin is composed of oxygenated long-chain fatty acids and a small proportion of phenylpropanoids, such as ferulic acid and coumaric acid (Fich et al., 2016). Cutin is a key component of the cuticle, typically described as being present only covering the epidermal cells of aerial parts of the plant. However, it has been shown that in the root cap of young seedlings, a cuticle-like polymer is deposited, named root cap cuticle (Berhin et al., 2019).

Suberin is a poly(acylglycerol) polyester composed of fatty acids and their oxidized derivatives, glycerol, and ferulic acid, linked by ester bonds (Serra & Geldner, 2022). Ferulic acid is the primary aromatic monomer of suberin and a product of the phenylpropanoid pathway (Graça et al., 2015).

Regarding the composition, cutin and suberin are very similar. Their difference arise regarding their location. Cutin is deposited on the outside of the primary cell wall of epidermal cells and is visualized by TEM as an electron-dense layer. On the contrary, suberin forms suberin lamellae that are deposited as a secondary cell wall between the plasma membrane and the primary cell wall. Suberin lamellae can be observed by TEM as an electron-dense

and translucent lamellar structure comprising alternating light and dark bands (Beisson et al., 2012; Bernards, 2002; Fich et al., 2016; Serra & Geldner, 2022)

2.2.1 Cutin and suberin biosynthetic pathway

Aliphatic cutin and suberin precursors are derived from C16 and C18 fatty acids. C16 and C18 fatty acids are synthesized in the plastid and transported to the endoplasmic reticulum, where they undergo key modifications, such as acyl activation, elongation, oxidation/reduction, and esterification to glycerol (**Figure 6**) (Fich et al., 2016; Serra & Geldner, 2022).

C16 and C18 fatty acids are activated by a long-chain acyl-CoA synthase (LACS family), forming an acyl-CoA. The *Arabidopsis* genome contains nine *LACS* genes, two of which (*LACS1* and *LACS2*) are required for cutin formation (Lü et al., 2009; Schnurr et al., 2004). In suberin biosynthesis, only LACS2 has been described to be involved in seed and endodermal suberin formation (Ayaz et al., 2021; Renard et al., 2021).

Next, acyl-CoA intermediates undergo aliphatic chain elongation catalyzed by 3-ketoacyl CoA synthase (KCS) at the fatty acid elongase (FAE) complex. Fatty acid elongation is related to suberin and root cap cuticle formation (Berhin et al., 2019; Serra & Geldner, 2022). KCS2, KCS20, and KCS6 catalyze the formation of very long-chain fatty acids (VLCFA) (Franke et al., 2009; Lee et al., 2009; Serra et al., 2009).

Subsequently, the addition of a hydroxyl group at the terminal or midchain position of the acyl chain is catalyzed by members of the P450 family (Beisson et al., 2012; Fich et al., 2016). The subfamily CYP86A is associated with both suberin and cutin formation (Höfer et al., 2008; Li-Beisson et al., 2009), CYP77 is associated with cutin formation (Li-Beisson et al., 2009), and the subfamilies CYP86B and CYP94B are linked to suberin formation (Krishnamurthy et al., 2021).

Glycerylated precursors are generated by the transfer of the acyl group from acyl-CoA to glycerol-3-phosphate by glycerol-3-phosphate acyltransferase (GPAT) enzymes (Serra & Geldner, 2022). In *Arabidopsis,* GPAT1 to GPAT8 show sn-2 activity (Yang et al., 2012).

Members of the GPAT family can be grouped by the presence or absence of an additional phosphatase domain. GPAT4, GPAT6, and GPAT8 possess an additional phosphatase domain and are involved in cutin precursor formation, as they catalyze a dephosphorylation reaction during condensation between glycerol and fatty-acyl co-A chains (Fich et al., 2016; Yang et al., 2010). However, this role is not exclusive, as, it has been shown recently that GPAT4, GPAT6, and GPAT8 are also involved in suberin formation (Gully et al., unpublished). GPAT5 and GPAT7 lack a phosphatase domain and play a role in suberin precursor synthesis (Beisson et al., 2007; Yang et al., 2012). GPAT1, GPAT2, and GPAT3 also do not have phosphatase activity. GPAT2 is required for the formation of very long-chain FAs into the cutin polymer of the root cap cuticle (Berhin, unpublished), and GPAT1 plays a key role in the tapetum and pollen development (Zheng et al., 2003). The role of GPAT3 in cutin or suberin formation remains elusive.

In parallel, characteristically in suberin formation, fatty acyl-CoA reductases (FAR) reduce the carboxyl group to alcohols, yielding suberin primary alcohols (Domergue et al., 2010; Serra & Geldner, 2022).

Before export to the cell wall, cutin and suberin precursors can be altered by members of the BAHD acyltransferase family (Moghe et al., 2023). The *Arabidopsis* genome encodes 61 putative BAHD acyltransferases, most of which remain uncharacterized (Yu et al., 2009). Several BAHD acyltransferases are involved in either cutin or suberin formation. The incorporation of ferulate-CoA into ω-hydroxy fatty acids and fatty alcohols in suberin is catalyzed by the ALIPHATIC SUBERIN FERULOYL TRANSFERASE (ASFT)(Molina et al., 2009). In contrast, in cutin, DEFICIENT IN CUTIN FERULATE (DCF) catalyzes the transfer of ferulate-CoA to ω-hydroxy fatty acids (Rautengarten et al., 2012). Furthermore, DEFECTIVE IN CUTICULAR RIDGES (DCR) is a diacylglycerol transferase with a specific function in cutin formation. DCR is hypothesized to play a role in the transfer of acyl-CoA to the free OH group of a diacylglycerol to form triacylglycerol (Panikashvili et al., 2009; Rani et al., 2010).

Cutin and suberin precursors must then be transported across the plasma membrane. Members of the ATP-binding cassette (ABC) transporter have been identified as cutin and

suberin precursor transporters. ABCG11, ABCG13, and ABCG32 are implicated in cutin precursor transport. And ABCG1, ABCG2, ABCG6, ABG16, and ABCG20 are involved in transporting suberin precursors (Fich et al., 2016; Panikashvili et al., 2010; Serra & Geldner, 2022). Moreover, extracellular vesiculo-tubular bodies (EVBs) have recently been associated with suberin export (de Bellis et al., 2022).

After transport to the apoplast, cutin precursors must be carried out through the cell wall to the cuticle layer, where they are polymerized. Lipid-transport proteins (LTP) have been suggested to mediate the movement of both precursors across the cell wall to the outer surface (Deeken et al., 2016; Fich et al., 2016; Serra & Geldner, 2022). Moreover, it has also been suggested that the movement of cuticular lipids across the apoplast is likely a passive process involving the diffusion of cutin precursors through the cell wall in a physicochemical phase-separation process (Philippe et al., 2022)

Cutin precursors are polymerized by the Gly-Asp-Ser-Leu motif (GDSL) lipase/hydrolases called cutin synthases (CUS). CUS1 and CUS2 activity in polymerization was confirmed (Girard et al., 2012; Hong et al., 2017). Members of the α/β-hydrolase BODYGUARD (BDG) family could also play a role in cutin polymerization, although their function remains unclear (Fich et al., 2016; Kurdyukov et al., 2006; Shih et al., 2019).

Suberin precursors are polymerized in the inner side of the cell wall. GDSL esterase/lipase (GELP) enzyme family members, GELP22, GELP38, GELP49, GELP55, and GELP72, are involved in suberin polymerization (Ursache, et al., 2021a).

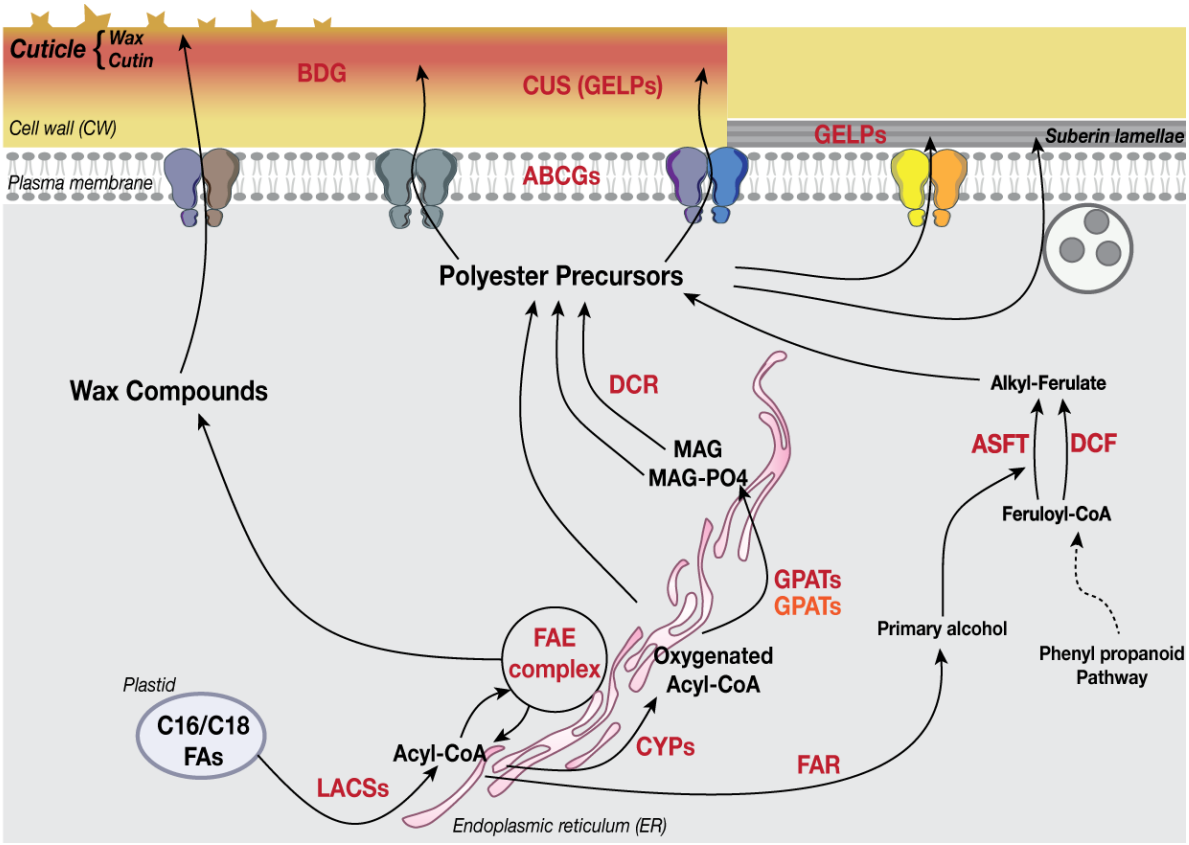

Figure 6. Schematic representation of cutin and suberin biosynthetic pathway. Pathway describing the different steps involved in the formation of cutin and suberin precursors. Enzymes involved in the pathways are highlighted in red. DCF, Deficient in Cutin Ferulate; ASFT, Aliphatic Suberin Feruloyl Transferase; FAR, Fatty Acyl-CoA Reductase; FA, fatty acid; DCR, Defective Cuticular Ridges; FAE complex, Fatty Acid Elongase complex; CYP, Cytochrome P450 Oxidase; GPAT, Glycerol-3-Phospate Acyltransferase; LACS, Long-chain Acyl-CoA Synthase; ABCG, ATP-binding Cassette Transporter; CUS, Cutin Synthase; BDG, Bodyguard; GELPs, GDSL esterases/lipases; MAG, Monoacylglycerol. Pathway drawn by Dr. Aurore Guerault.

2.2.2 Lipidic cell wall modifications of the root

In young seedlings, the root cap cuticle is present only at the first root cap layer during the early development of the primary or lateral roots. Its central role is to protect the root meristem during seedling establishment, e.g., against hyperosmotic conditions or salt stress (Berhin et al., 2019).

In their second developmental stage, endodermal cells are impregnated with suberin (Geldner, 2013; Nawrath et al., 2013). Suberin deposition starts randomly, leading to a “patchy” area that later develops into a continuous suberization, covering the entire endodermal cell except for the regions occupied by plasmodesmata (Geldner, 2013). Most

endodermal cells are suberized, with exception of certain cells adjacent to the xylem pole, named passage cells (Andersen et al., 2015). The impregnation of endodermal cells with suberin plays a crucial role in plant nutrition by forming barriers to the free diffusion of water and nutrients. Enhanced suberization is controlled by salt treatment or potassium deficiency via the abscisic acid (ABA) signaling pathway. While the reduction of suberization is associated with iron, manganese, and zinc deficiency via the ethylene signaling pathway (Barberon et al., 2016).

3. The epidermis: the root outermost layer

The epidermis is the outermost cell layer of young roots and, as so, is constantly in contact with the soil environment. This environment comprises ions, water, and a rich and diverse microbe community (Walker et al., 2003). Thus, the position of the epidermis determines its essential roles, such as water and nutrient uptake and as a defense barrier against harmful microbes (Üstüner et al., 2022).

3.1 Differentiation of epidermal cells

In the mature root epidermis, two cell types can be distinguished: root hair-bearing cells (trichoblasts) and non-hair-bearing cells (atrichoblasts) (**Figure 7A**). Their formation pattern is position dependent. Epidermal cells positioned outside a periclinal cortical cell wall (“N” position) that are in contact with a single cortical cell differentiate into non-hair cells. Epidermal cells located over an anticlinal cortical cell wall (“H” position) in contact with two underlying cortical cells differentiate into hair cells. Since in *Arabidopsis,* the cortex is a ring of eight cells, trichoblasts are always arranged into eight-cell files and, thus, rarely directly neighboring (Dolan et al., 1993; Dolan et al., 1994; Dolan & Roberts, 1995).

Epidermal cell patterning is established during embryogenesis, which is relatively far from the first signs of epidermal cell differentiation. Expression of *GLABRA2*, a transcription factor involved in the specification of the atrichoblast cell fate, can already be detected in the

heart stage embryo (Lin & Schiefelbein, 2001). In addition to being regulated differently, atrichoblasts and trichoblasts also show morphological differences already in the meristematic zone: trichoblasts are shorter, have a denser cytoplasm, and display a higher cell division rate (Balcerowicz et al., 2015; Dolan et al., 1994)

Several genes are involved in epidermal cell fate regulation (**Figure 7B**). One of the key components of this network is TRANSPARENT TESTA GLABRA 1 (TTG1), which forms a complex with the transcription factors GLABRA3 (GL3) and ENHANCER OF GLABRA3 (EGL3)(Esch et al., 2003; Payne et al., 2000; Zhang et al., 2003). Loss-of-function mutants of these genes show excessive trichoblast production, as they inhibit the formation of atrichoblasts (Zhang et al., 2003).

The activity of the GL3/EGL3/TTG1 complex depends on the abundance of the MYB transcription factors WEREWOLF (WER) and CAPRICE (CPC), that act in opposition to each other. The specific epidermal cell fate is a consequence of *WER* activity being concentrated in cells in the future “N” position. In contrast, *CPC* is only active in cells in the future “H” position (Song et al., 2011). When the WER protein binds to GL3/EGL3/TTG1, the root hair-inhibitory complex becomes active and promotes the expression of GLABRA2 (GL2). Then, GL2 inhibits transcription of the transcription factor ROOT HAIR DEFECTIVE 6 (RHD6), leading to the expression of atrichoblast-specific genes and specification of the non-hair cells fate (Masucci & Schiefelbein, 1994).

In addition to the above-mentioned genetic cascades, hormones also can influence epidermal cell fate. Pharmacological studies have shown that treatment with aminoethoxyvinylglycine (AVG), an ethylene biosynthesis inhibitor, abolishes root hair formation (Masucci & Schiefelbein, 1994; Tanimoto et al., 1995). Alternatively, treatment with 1-aminocyclopropane-1-carboxylic acid (ACC), an ethylene precursor, leads to ectopic root hair formation (Tanimoto et al., 1995).

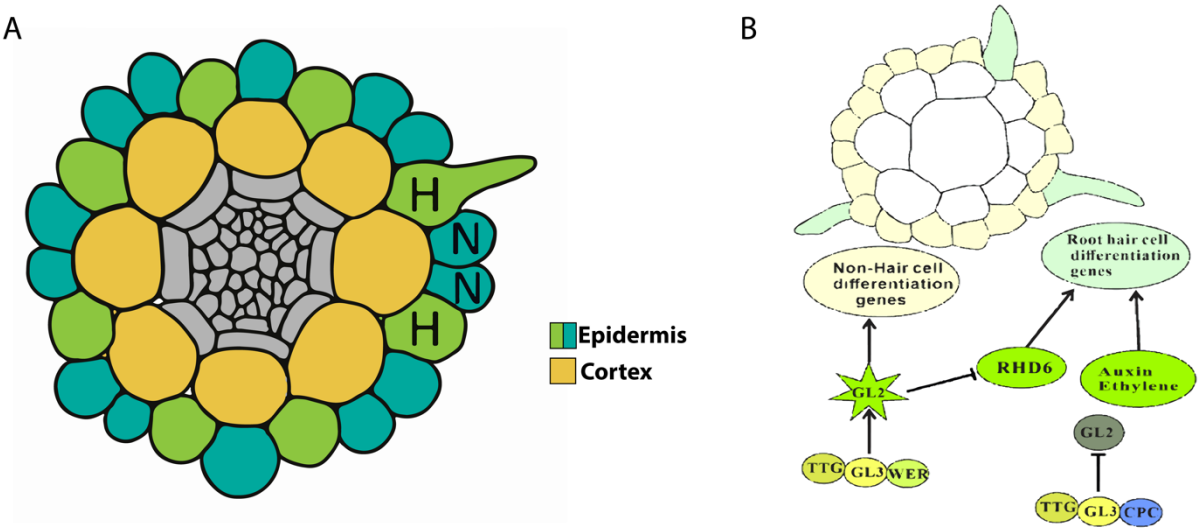

Figure 7. Cellular organization of the *Arabidopsis* root and model for the root epidermal cell-fate determination. A) A) The diagram illustrates the arrangement of trichoblast (H) and atrichoblast (N) cells as seen in a cross-section of an *Arabidopsis* root. B) The model depicts the molecular pathways involved in root hair and non-root hair cell fate. The positions of H and N have different components involved in root-hair formation. Some components shuttle to different cell types and converge at RHD6. Upon activation, RHD6 regulates the differentiation and formation of root hair cells. Additionally, auxin and ethylene play a positive role in root-hair formation via ROS. The arrowhead line indicates a stimulation effect, while the "T"-shaped line indicates inhibition. CPC, Caprice; GL, glabra; RHD, Root Hair Defective; TTG, Transparent Testa Glabra. Modified from Balcerowicz et al. (2015) and (Zhou et al., 2020).

3.2 Root epidermal cell wall modifications

The root epidermal cell wall has received minimal attention, particularly regarding non-polysaccharide cell wall modifications of the epidermis itself. Over the years, studies have primarily focused on root hair evolution, development, and functionality, as well as the patterning of root epidermal cells (Dolan & Roberts, 1995; Jones & Dolan, 2012; Masucci & Schiefelbein, 1994; Shibata & Sugimoto, 2019; Tanimoto et al., 1995).

Cell wall modifications of the root epidermis have been analyzed in non-model species and without genetic approaches. Root epidermal autofluorescence has been reported in species such as *Allium cepa* (onion) (Peterson et al., 1978) and *Glycine max* (soybean) (Thomas et al., 2007). The epidermis of these species could also be stained with the lipidic stains Sudan Red 7B and Fluorol Yellow, respectively (**Figure 8A-B**). Moreover, in the outer

and radial walls of epidermal cells, discreet alternating bands could be observed by TEM in the roots of *A. cepa* (Peterson et al., 1978) (**Figure 8B**). Since the alternating bands typical of suberin are deposited in an atypical location and no suberin lamellae could be detected, this was termed diffuse or non-lamellar suberin. The presence of typical suberin components in the epidermis could be corroborated by chemical analyses in *G. max* (Thomas et al., 2007). Additionally, the amount of diffuse suberin in the epidermis has been correlated to susceptibility to the pathogen *Phytophthora sojae* (Ranathunge et al., 2008) (**Figure 8A**).

In *Arabidopsis,* genes involved in the fatty acid biosynthesis pathway are expressed in the root epidermis. The glycerol-3-phosphate acyltransferases *GPAT2* and *GPAT3* are expressed all along the root epidermis. *GPAT2* might be involved in the formation of the root cap cuticle (Berhin, unpublished). *GPAT7* is also expressed in the root epidermis and is involved in suberin formation (Gully et al., unpublished.; Yang et al., 2012). Finally, crucial for suberin polymerization, GDSL esterase/lipases *GELP22* and *GELP49* are expressed in the root epidermis (Ursache et al., 2021a). The expression of fatty acid biosynthetic genes in the root epidermis suggests a possible lipid deposition in this cell layer.

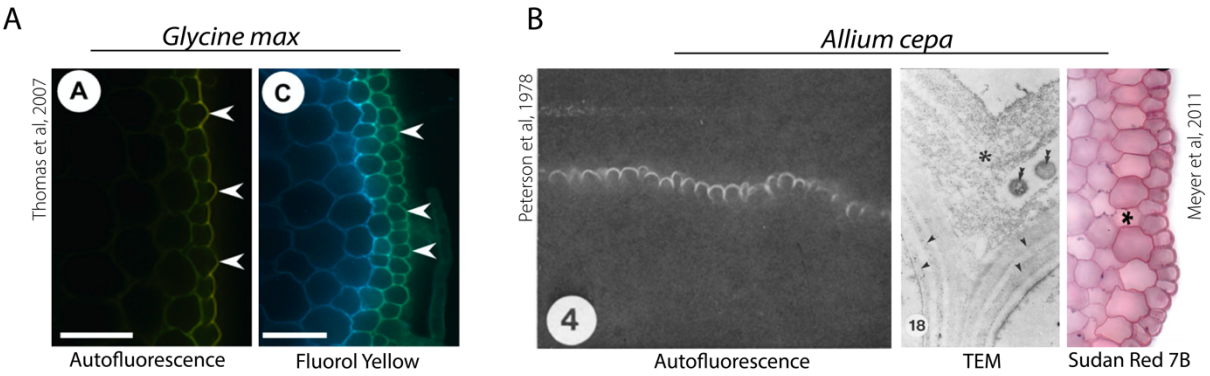

Figure 8. Diagram depicting cell wall modifications in the root epidermis in soybean root and onion root. A) Free-hand cross sections of soybean roots. Autofluorescence of outer epidermal walls (arrowheads) and yellow green fluorescing walls of epidermis stained with the lipidic stain Fluorol Yellow (arrowheads). Adapted from Thomas et al., 2007. B) Autofluorescence of the outer tangential and radial walls of the onion root epidermis. Electron microscopy imaging of onion roots. Tissue fixed in glutaraldehyde-ferric chloride and has not been post-stained. Binding of ferric ions in the extracellular material (*). Arrows indicate intercalating electron-dense layers above the epidermal outer cell wall. Double headed arrows indicate microorganisms within the extracellular material. Cross-section of the mature zone of onion adventitious roots stained with Sudan red 7B, suberin lamellae in red, exodermal cells highlighted (*). Adapted from Meyer et al., 2011; Peterson et al., 1978.

As described in this introduction, limited knowledge exists regarding the cell wall modifications of the root epidermis. Therefore, the objective of this thesis was to better characterize the epidermal cell wall of roots of *Arabidopsis* seedlings. In **Chapter I**, the presence and composition of a non-polysaccharide cell wall modification of the root epidermis of Arabidopsis was assessed through histochemical characterization, pharmacological complementation, and reverse genetics. In **Chapter II**, further investigation was conducted to determine whether a lipid-derived polymer might be deposited in the root epidermal cell wall in response to ABA-regulated stresses.

Chapter II: Characterization of the root epidermal cell walls modification in *Arabidopsis*

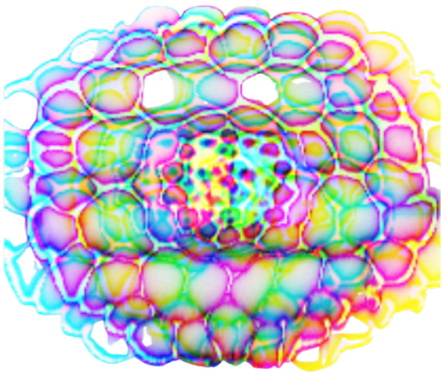

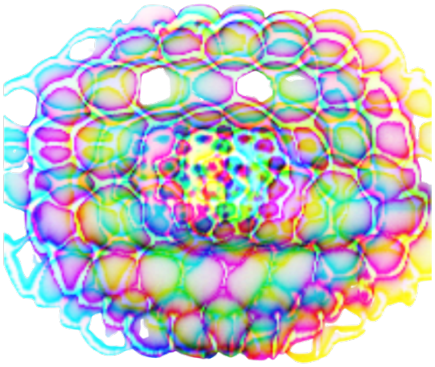

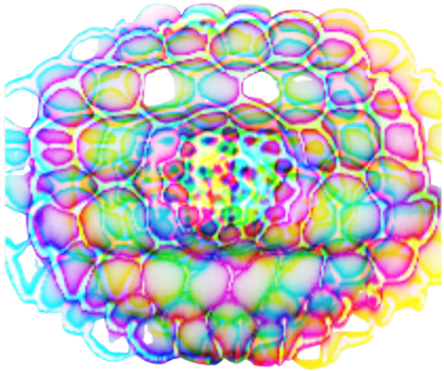

1. Goal and approach

In *Arabidopsis*, cell wall modifications in the endodermis have been thoroughly documented and correlated with physiological functions (Barberon et al., 2016; Naseer et al., 2012). The reinforcement of the endodermis, with suberin and lignin, acts as a checkpoint for nutrients and protects the vasculature from pathogen invasion (Barberon & Geldner, 2014; Geldner, 2013). Nevertheless, the possibility of cell wall modifications in other root cell layers should be considered. Because the epidermis is the first layer in contact with the environment, a modification of its cell wall is conceivable. In *Arabidopsis*, the outer cell wall of the epidermis also shows autofluorescence, indicating the presence of phenolic compounds (Franke et al., 2005) (**Figure 9A**). Moreover, it has been reported that berberine stains the root epidermis, suggesting the presence of lipid polyesters, leading the authors to hypothesize that diffuse suberin could be deposited in this cell layer (Kramer et al., 2007) (**Figure 9B**).

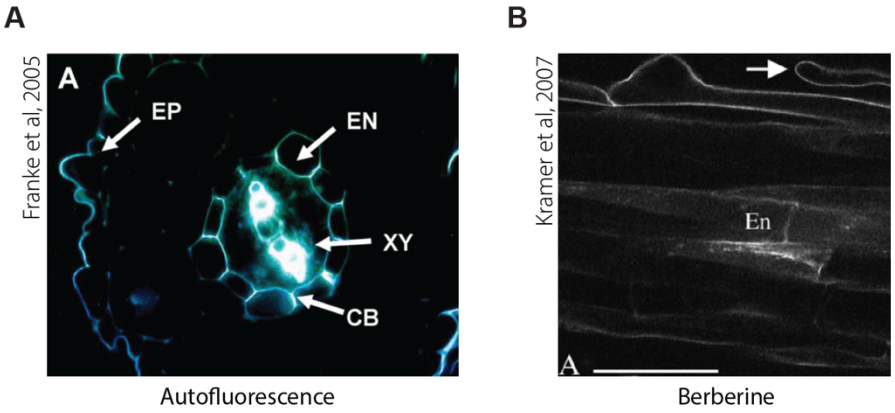

Figure 9. *Arabidopsis* outer epidermal cell wall histological characteristics. A) Autofluorescence is observed in a cross-section of a primary root when excited with UV-light (k=365 nm) (Franke et al., 2005). B) Confocal imaging highlights hydrophobic cell wall modifications in the mature zone, visualized by staining with berberine Note the stained epidermis and root hair (arrow) (Kramer et al., 2007). Ep, epidermis; en, endodermis; xy, xylem, cb, Casparian strips.

The possibility of cell wall modifications in the root epidermis has been previously explored in non-model plant species and solely by histological stains (Meyer et al., 2011; Peterson et al., 1978; Thomas et al., 2007; Wilson & Peterson, 1983). Therefore, throughout this chapter, I aim to test the presence, characterize the composition, and clarify the role of

cell wall modifications in the root epidermis of *Arabidopsis*. This was done via experimental manipulations of suberin production, combined with histochemical and functional assays.

2. Results

2.1 Visualization of epidermal cell wall modifications

2.1.1 The root epidermis outer cell wall is autofluorescent and stains with Auramine O

The root epidermal cell wall composition was examined via a histochemical approach. First, the autofluorescence was analyzed by UV light excitation, which indicates the presence of phenolic compounds (Donaldson, 2020). To further understand the composition of the root epidermal cell wall, roots were stained with Fluorol Yellow (FY) (Naseer et al., 2012), which stains lipid polyesters, and with the lignin-detecting dye Basic Fuchsin (BF) (Dharmawardhana et al., 1992; Ursache et al., 2018). Finally, the dye Auramine O (AO) was used, which stains lipids and lignin (Considine & Knox, 1979; Pesquet et al., 2005; Ursache et al., 2018). Moreover, before investigating the composition of the root epidermis in *Arabidopsis*, we had to define the developmental age of interest. When comparing 5- and 8-day-old roots, we observed that the autofluorescence signal was more apparent in the latter. Hence, the subsequent experiments were done on 8-day-old seedlings.

Microscopic observation of 8-day-old roots in their primary developmental stage revealed a strong autofluorescence in the outer cell wall of the epidermis (**Figure 10A**), indicating the presence of aromatic compounds. The lack of FY staining suggested the absence of lipid polyesters in the epidermis (**Figure 10B**). BF, a typical lignin stain, dyed weakly the epidermis (**Figure 10C**). AO strongly stained the outer cell wall of the epidermis, leading to a clear difference between the outer and inner cell walls of the epidermis, suggesting the presence of lignin and lipid polyesters (**Figure 10D**). Because AO strongly stained the epidermis, subsequent experiments were carried out with this stain.

Roots were segmented into five zones to characterize the accumulation of AO-stainable compounds in the epidermis along the root axis. This segmentation ensured full coverage of

the growth and differentiation zones of the cells of the primary root before the beginning of the secondary growth zone (**Figure 10E**). Starting from the first epidermal elongating cell (Zone +0), ten cells were counted towards the next zone. This procedure was repeated until Zone +50 was reached.

Accumulation of AO-stainable compounds was first visible in Zone +10, where root hairs are initiated. The CS and protoxylem cells become lignified, and root hairs outgrow between Zones +10 and +20. Coincidentally, between those stages, the accumulation of AO-stainable compounds increased significantly, while, from Zone +20 onwards, the AO intensity remained similar (**Figure 10F-G**). Zone +20 harbors fully differentiated epidermal cells, so the remaining experiments were carried out in this root section.

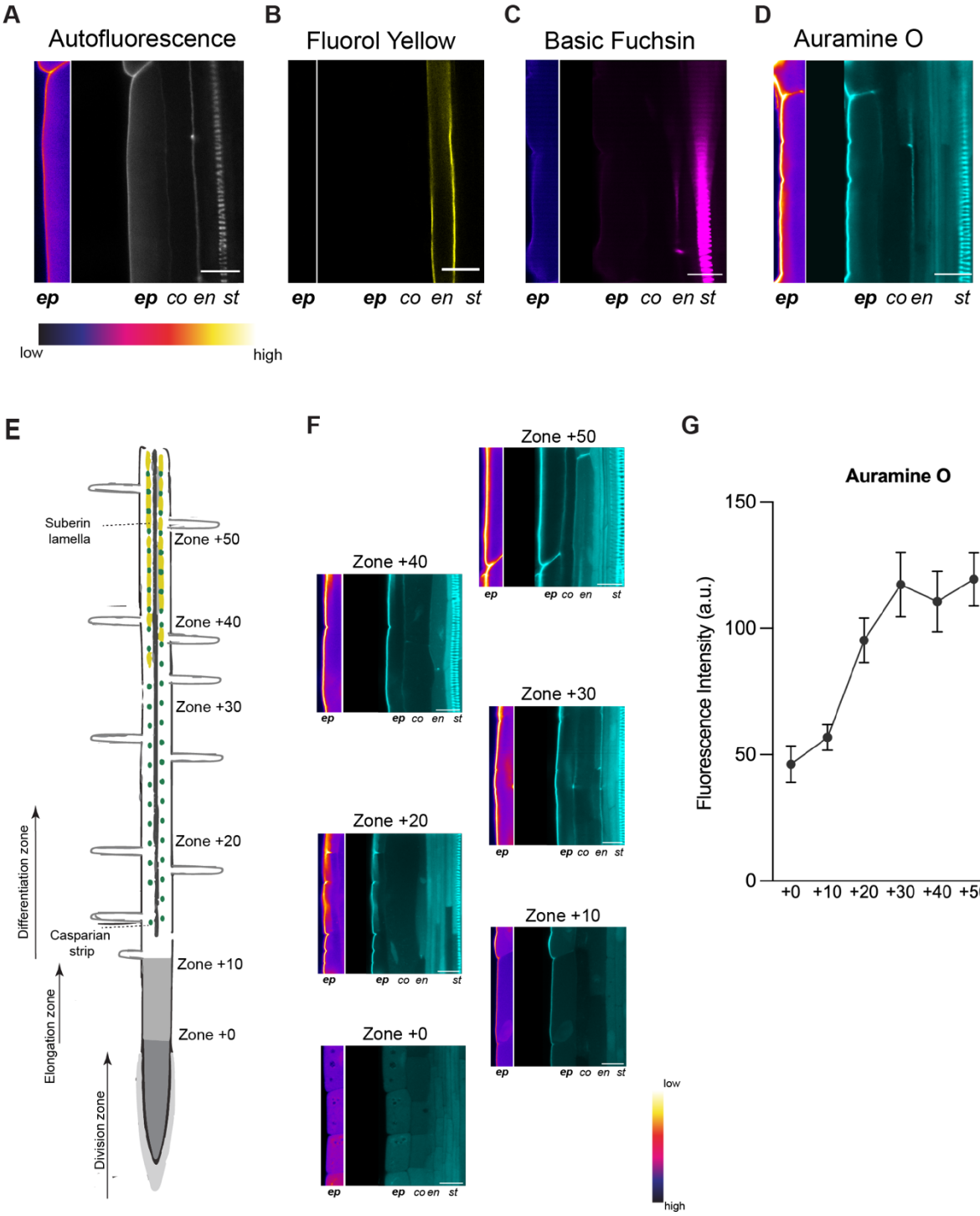

Figure 10. Histochemical investigation of the root epidermis of 8-day-old roots. All pictures are longitudinal, median optical sections of the primary root, of which only half the root is represented. To the left of every root picture, there is a cut-off showing only the epidermis, in which the intensity of the staining can be visualized (>yellow, high intensity; < yellow, lower intensity). A) Autofluorescence in a longitudinal view of a primary root after excitation with UV light (λ = 488 nm), note that xylem vessels and the CS can also be visualized. B) Fluorol Yellow does not stain the root epidermis, only staining the endodermal suberin. C) Basic Fuchsin stains weakly the epidermis, and strongly stains the CS and xylem vessels. D) Auramine O stains the outer cell wall of the root epidermis and, the CS and xylem. E) Schematic diagram of a primary root, highlighting the developmental zones and cell wall modifications. Dark grey, division zone; light grey, elongation zone; white, differentiation zone; green,

Casparian strip; yellow, endodermal suberin; grey line, vasculature. The root was segmented in six zones, in which zone +0 represents the start of the first elongating epidermal cell, which was twice the length of a meristematic cell. The following zones were reached by counting ten epidermal cells each time. F) AO-staining intensity in the different epidermal zones, from zone +0 to zone +50. G) Quantification of the AO staining intensity in the outer cell wall of epidermal cells in different root regions; error bars represent SEM. Scale bars: 20µm. Ep, epidermis; co, cortex; en, endodermis; st, stele.

2.1.2 Epidermal cell wall modifications are not distinguishable with electron microscopy

Our previous investigation regarding the histochemical properties of the root epidermis revealed a gradient of accumulation of AO-stainable compounds. To further understand epidermal cell wall modifications, TEM images were acquired. Potassium permanganate ($KMnO_4$), used to detect lignin (Tamminen et al., 1997), enabled the visualization of the cell walls delimitation. Thus, TEM images were acquired after $KMnO_4$ staining. Since histochemical results showed a gradient of accumulation of AO-stainable compounds between the zones +20 and +50, imaging was done in these regions. Initially, zone +0 was also investigated. However, it was challenging to identify the cell walls due to the mucilage from the root tip. The presence of suberin can be easily recognized by TEM through the presence of alternating bands deposited between the plasma membrane and primary cell wall (Serra & Geldner, 2022). In both root regions, intercalating bands, characterizing suberin lamellae, could not be detected, suggesting that typical suberin is not deposited in the epidermal cell walls (**Figure 11**).

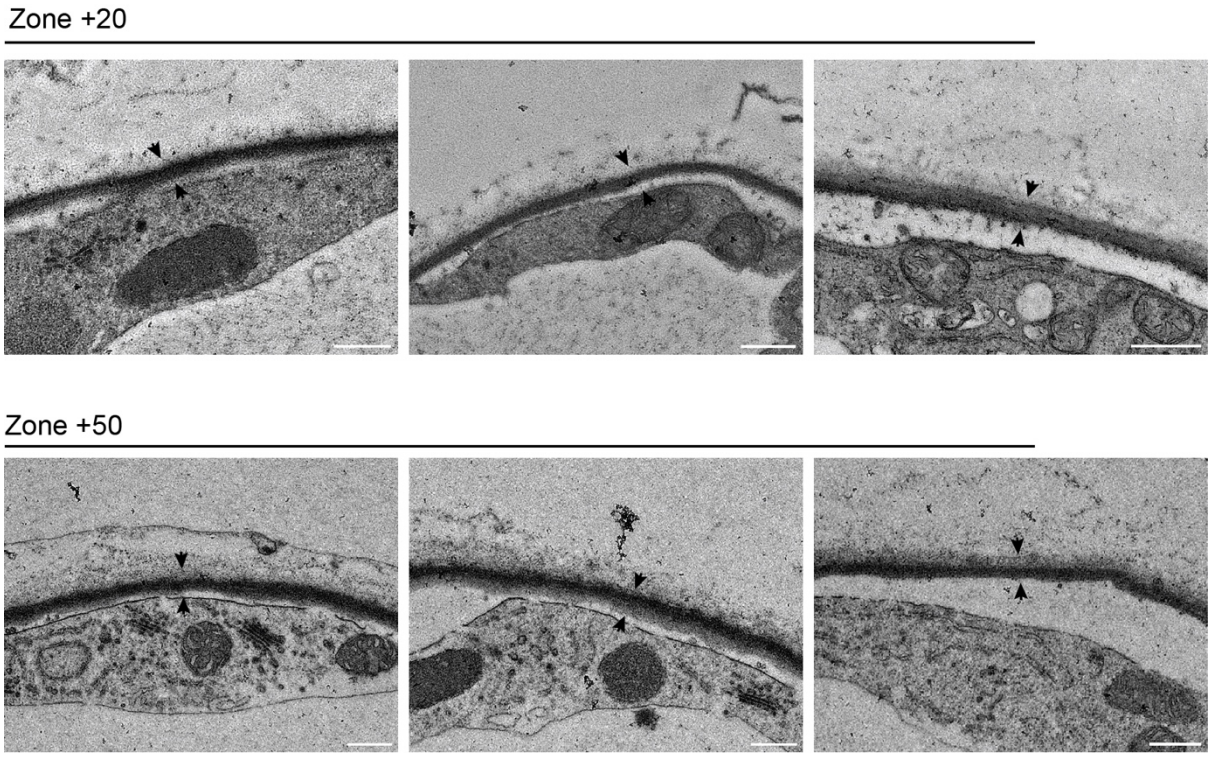

Figure 11. Epidermal cell wall modifications are not visible by electron microscopy. Cross-sections of primary roots visualized by TEM, after staining with $KMnO_4$, focusing on the epidermal outer cell walls. The evaluated zones were +20 (2 mm from the root tip) and +50 (5 mm from the root tip). Three different situations are presented for each analyzed zone due to the variability of the cell wall appearance. Arrows indicate the epidermal outer cell wall. Scale bars: 500 nm.

2.1.3 Epidermal modifications are attached to the cell wall

To further assess the nature of AO-stainable compounds, we addressed whether they are attached to the epidermal cell wall. For this purpose, a methanol treatment was used, in which methanol is known to remove all non-polymerized fatty acids, leaving only polymerized polyester depositions, such as suberin (Berhin et al., 2019). Confocal analysis revealed that the AO staining did not significantly decrease after washing 8-day-old seedlings with methanol for 48h (**Figure 12**). This result suggests that AO-stainable compounds are attached to the epidermal cell wall.

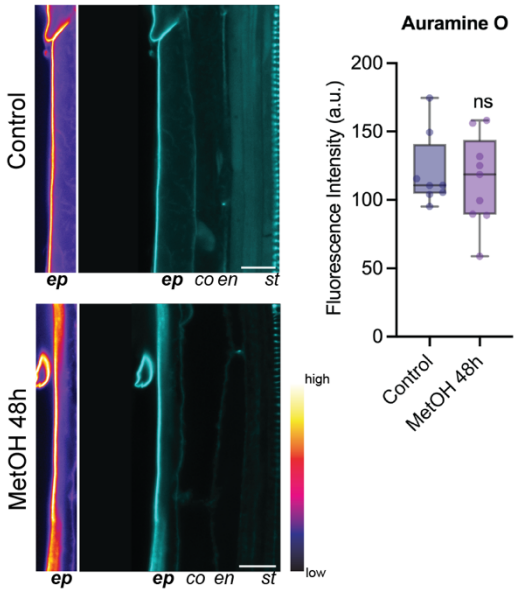

Figure 12. Epidermal modifications are attached to the cell wall. Treatment with methanol for 48 hours does not affect the AO intensity in the root epidermis. The provided pictures are longitudinal median optical sections of the primary root in the +20 zone, in which only half of the root is depicted, along with corresponding quantifications of the staining intensity in the root epidermis. On the left side of each root picture, a cropped section displaying only the epidermis is shown, allowing for the visualization of the staining intensity (>yellow, high intensity; < yellow, lower intensity. Two-tailed Student's t-test versus WT; n=10. Scale bars 20µm. Ep, epidermis; co, cortex; en, endodermis; st, stele.

2.1.4 Epidermal AO-stainable modifications appear at early stages of root development

We went on to test the developmental time point at which AO-stainable epidermal cell wall modifications appear. To this aim, the AO staining in the epidermis was evaluated in 4-, 6-, and 8-day-old seedlings. The zone analyzed was +20 in 8-day-old seedlings. The equivalent zone was assessed in younger seedlings, where the CS and xylem were lignified (**Figure 13**). Visually, the staining intensity in the epidermis was similar in seedlings of the three ages, suggesting that AO-stainable compounds are present from early on during seedling development.

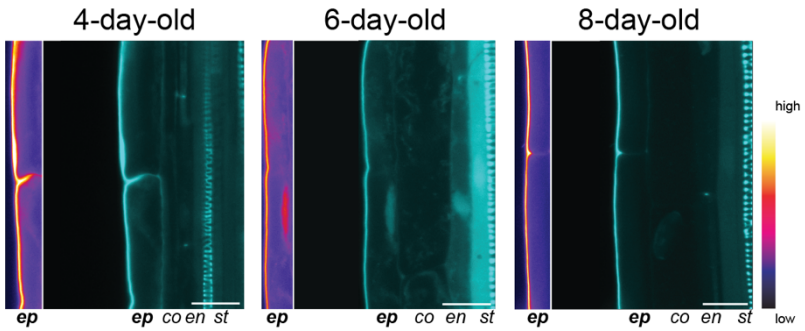

Figure 13. Developmental timeline of AO-stainable epidermal wall modifications. AO staining in the zone +20 or equivalent of primary roots of 4-, 6- and 8- day old seedlings. Pictures are longitudinal, median optical sections of the primary root, in which only half the root is represented. On the left side of each root picture, a cropped section showing only the epidermis is presented, enabling visualization of the staining intensity (>yellow, high intensity; < yellow, lower intensity). Scale bars 20µm. Ep, epidermis; co, cortex; en, endodermis; st, stele.

2.1.5 AO staining is not affected in mutants of the polyester biosynthetic pathway

To test whether the compound stained by AO and deposited in the outer cell wall of the root epidermis is suberin or a suberin-like polymer, we examined lines with mutations in several *GPAT* genes, since this gene family is implicated in lipid polyester formation (Fich et al., 2016; Serra & Geldner, 2022). *GPAT2*, *GPAT3*, and *GPAT7* are expressed along the root epidermis **(Figure 14A)**, suggesting a role in the formation of root epidermal polyesters. Therefore, we used a CRISPR-Cas9 approach to generate loss-of-function mutants of GPAT3, leading to the double mutant *gpat2 gpat3* and the triple mutant *gpat2 gpat3 gpat7*. For the *gpat2 gpat3* mutant lines, *GPAT3* was knocked out via CRISPR on the *gpat2* T-DNA insertional mutant (SALK_118230). We also generated a *gpat2 gpat3 gpat7* mutant line by targeting GPAT3 using the same guides in a *gpat2 gpat7* mutant background (SALK_118230 x SALK_064514). Only one guide worked successfully, generating either insertions or deletions close to the end of the first exon, as described in **Figure 14B**. We selected two alleles from the *gpat2 gpat3* double mutant, namely L1 and L8, and two from the *gpat2 gpat3 gpat7* triple mutant, namely L8 and L27.

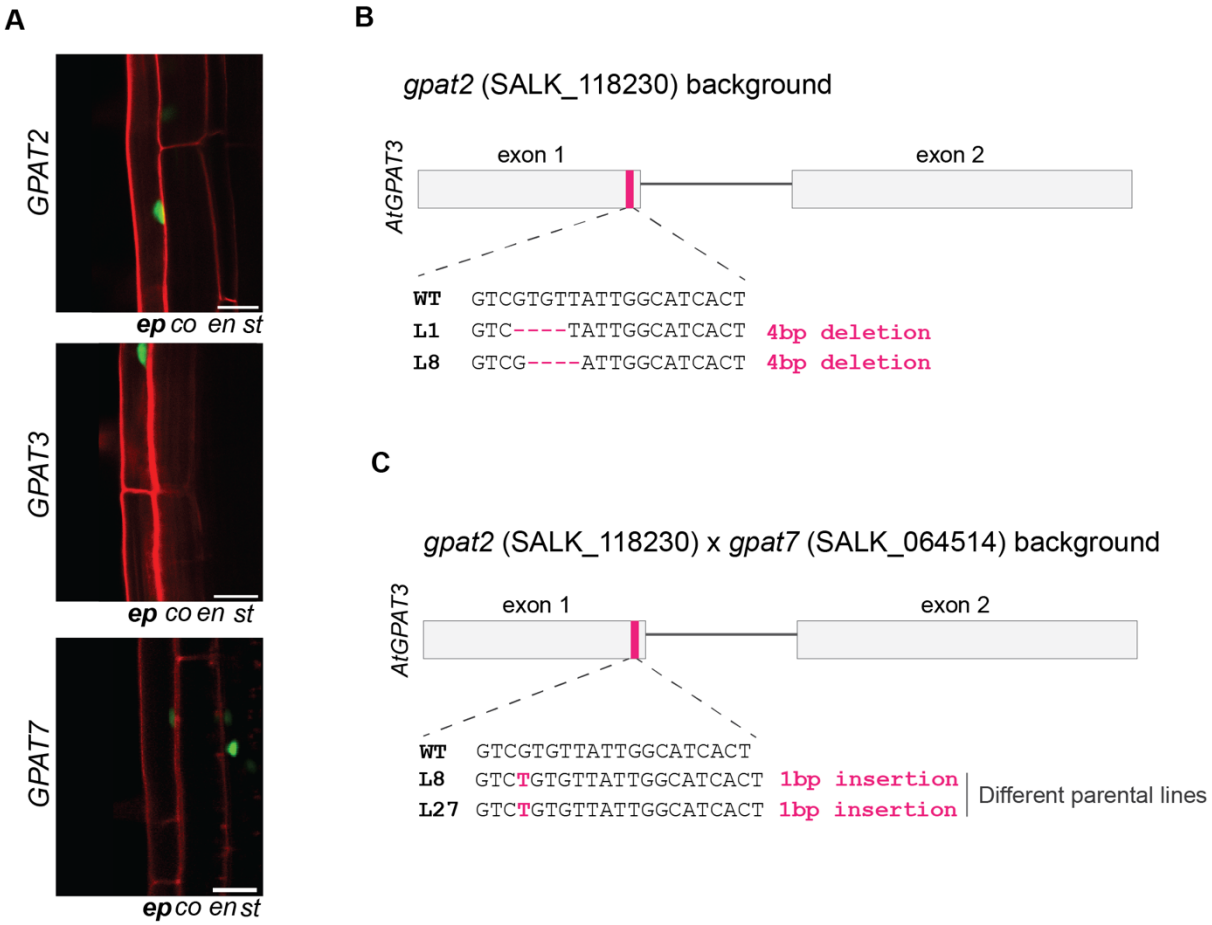

Figure 14. Expression pattern of epidermis expressed GPATs and representation of the CRISPR strategy and outcome. A) Transcriptional reporter lines of the GPATs expressed in the root epidermis of *Arabidopsis*, fused to NLS-GFP. Representation of the different CRISPR lines generated for *GPAT3*, in either the *gpat2* background (B) or the *gpat2 gpat7* background (C). Mutations are indicated in pink. Ep, epidermis; co, cortex; en, endodermis; st, stele. Scale bars represent 50 µm.

Although these *GPATs* are expressed in the differentiated root epidermis, we did not detect any difference in AO staining intensity in the *gpat2 gpat3* mutant compared to the WT (**Figure 15A**). *GPAT7* is involved in suberin formation (Gully et al., unpublished.; Yang et al., 2012). Thus, we also evaluated the intensity of AO staining in the *gpat7, gpat2 gpat7,* and *gpat2 gpat3 gpat7* mutants. Confocal analysis revealed no difference between the mutants and the WT (**Figure 15B**). To gain more insights from other players in suberin polymerization, we also verified the intensity of the AO stain in the *gelp*^{quint} mutant, since it shows defects in suberin polymerization (Ursache et al., 2021a). The *gelp*^{quint} mutant is a quintuple mutant of the GDSL esterases/lipases *GELP22*, *GELP38*, *GELP49*, *GELP55*, and *GELP72.* These five

genes are expressed in the endodermis, and *GELP22* and *GELP49* are also expressed in the epidermis (Ursache et al., 2021a). The *gelp*^{quint} mutant showed a similar signal intensity as the wild-type, suggesting that the AO-stainable compound does not require either *GPATs* or *GELPs* for its synthesis (**Figure 15C**).

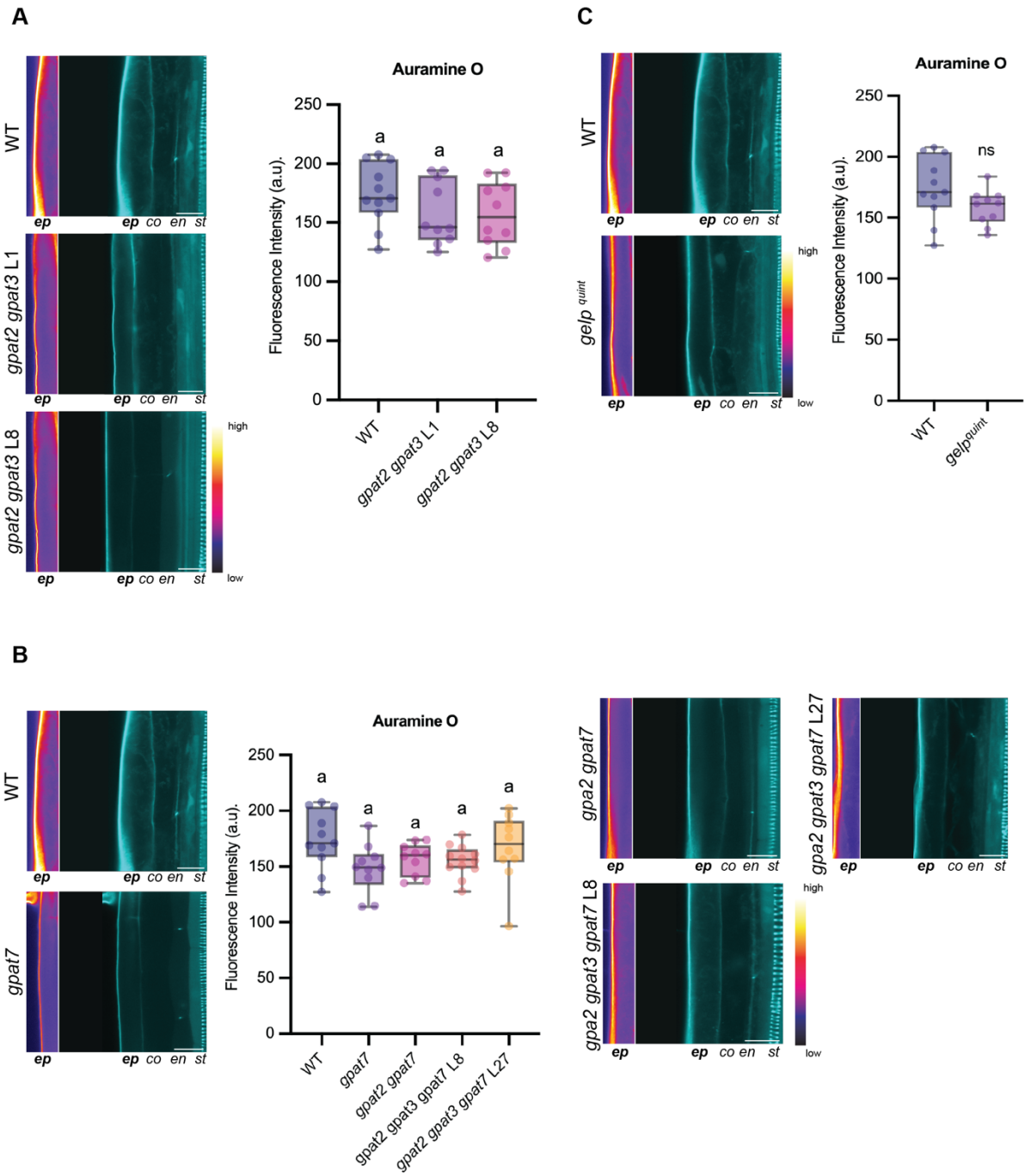

Figure 15. Loss-of-function mutants of *GPATs* and *GELPs* expressed in the root epidermis do not show any significant reduction in the AO staining. A-C) Whole-mount AO staining of WT and mutant seedlings in the zone +20. All pictures are longitudinal, median optical sections of the primary root in the zone +20, of which only

half the root is represented. On the left side of each root picture, a cropped section exclusively showing the epidermis is included, allowing for the visualization of the staining intensity (>yellow, high intensity; < yellow, lower intensity). On the right side, the graph presents the respective quantifications of the staining intensity in the root epidermis. Letters refer to individual groups/treatments in a one-way ANOVA analysis with a post hoc multiple group t-test (Tukey) ($p > 0.05$); ns = $p > 0.05$; two-tailed Student's t-test versus WT; n=10. Scale bars 20µm. Ep, epidermis; co, cortex; en, endodermis; st, stele.

2.1.6 Suberin modulation does not affect the formation of AO-stainable compounds

We went on to test whether modulation of suberin formation affected the formation of AO-stainable compounds. The hormone ABA and the peptide CASPARIAN INTEGRITY FACTOR 2 (CIF2) are positive regulators of root suberization. Endodermal suberization is highly regulated by ABA (Barberon et al., 2016). Moreover, CIF2 treatment leads to ectopic lignification in the endodermis, which enhances the suberization of the endodermal cells as a compensatory mechanism (Doblas et al., 2017; Shukla et al., 2021). After treating the roots with 1µM ABA for two days, confocal analysis revealed that the FY staining intensity was enhanced only in the endodermis, and no staining could be visible in the epidermis (**Figure 16A**). Moreover, defects in the CS integrity were visible upon 24h of 1µM CIF2 treatment, in line with previous reports (Doblas et al., 2017). Still no effect on the intensity of the AO staining in the epidermis was observed (**Figure 16B**). Indicating that the formation of AO-stainable compounds is not modulated by typical suberin formation inducers.

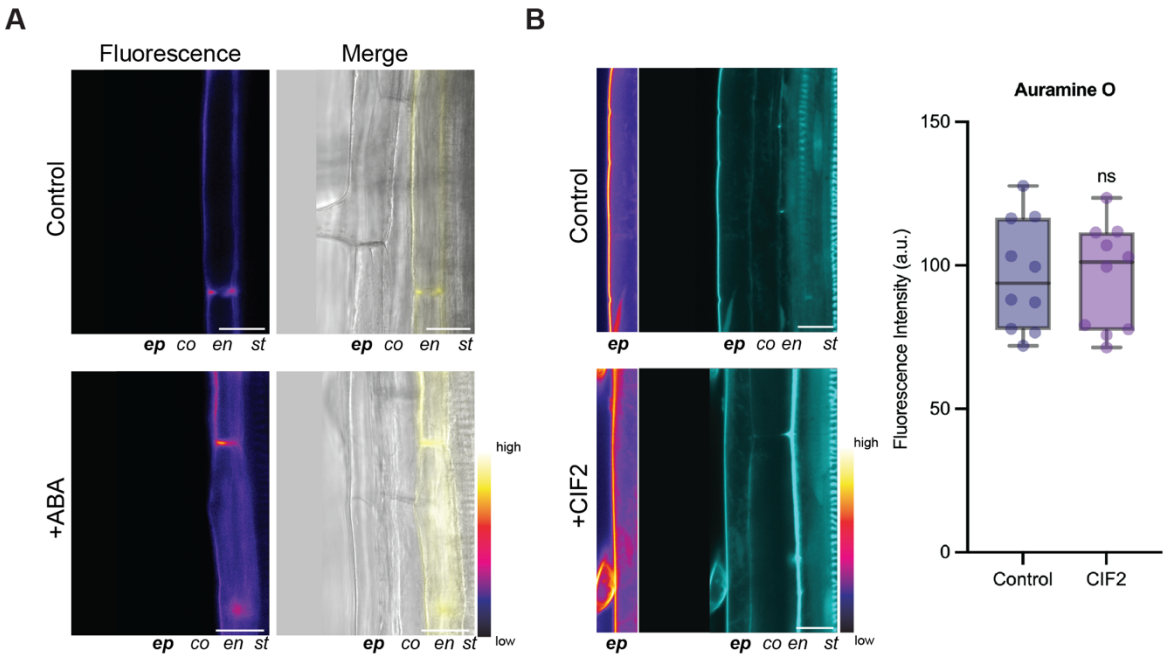

Figure 16. Suberin induction does not induce suberization in the epidermis. All pictures are longitudinal, median optical sections of the primary root, of which only half the root is represented. To the left of every root picture, there is a cut-off showing only the epidermis, in which the intensity of the staining can be visualized (>yellow, high intensity; < yellow, lower intensity). On the right side, the graph presents the respective quantifications of the staining intensity in the root epidermis upon CIF2 treatment. A) FY staining of 8-day-old roots upon 48h of 1µM ABA shows that only endodermal suberin can be enhanced. B) AO staining of whole-mount roots upon 24h of 1µM CIF2 in the epidermis and the respective quantification; n=10, two-tailed Student's t-test versus WT. Scale bars: 20µm. Ep, epidermis; co, cortex; en, endodermis; st, stele.

2.1.7 Inhibition of PP synthesis leads to a reduction of AO-stainable compounds

Ferulic acid is the main aromatic monomer of the suberin polyester (Graça et al., 2015), and is produced by the phenylpropanoid pathway (PP). We sought to investigate whether suberin could be deposited in the root epidermal outer cell wall. To text this hypothesis, the PP pathway was inhibited via the chemical piperonylic acid (PA), which targets C4H, an early-step key enzyme of the PP pathway (Schalk et al., 1998). Seedlings were transferred into a media containing 10µM of PA for 72h (**Figure 17A**), and, as expected (Naseer et al., 2012), this treatment did not interfere with continued root growth (**Figure 17B**). Still, the newly formed part of the root had no PP compounds, including lignin. PA treatment also led to a dramatic reduction of the AO staining intensity in the outer cell wall of the epidermis compared to untreated roots (**Figure 17C-D**). Hence, AO-stainable compounds are linked to the PP

pathway. Next, ferulic acid (FA) was additionally supplied to the PA-treated roots, resulting in the recovery of the intensity of the AO staining in the epidermis (**Figure 17E-F**). The lignified CS and xylem were also visible. To investigate if the FA incorporation may be related to suberin deposition in the root epidermis, the expression of *ASFT* was analyzed using a reporter line previously generated (Naseer et al., 2012). ALIPHATIC SUBERIN FERULOYL TRANSFERASE (ASFT) catalyzes the transfer of ferulic acid onto aliphatic chains (Molina et al., 2009). In 8-day-old differentiated roots, *ASFT* is expressed only in endodermal cells (**Figure 17G**), dispelling the possibility that ferulic acid incorporation into the suberin building blocks is active in the root epidermis.

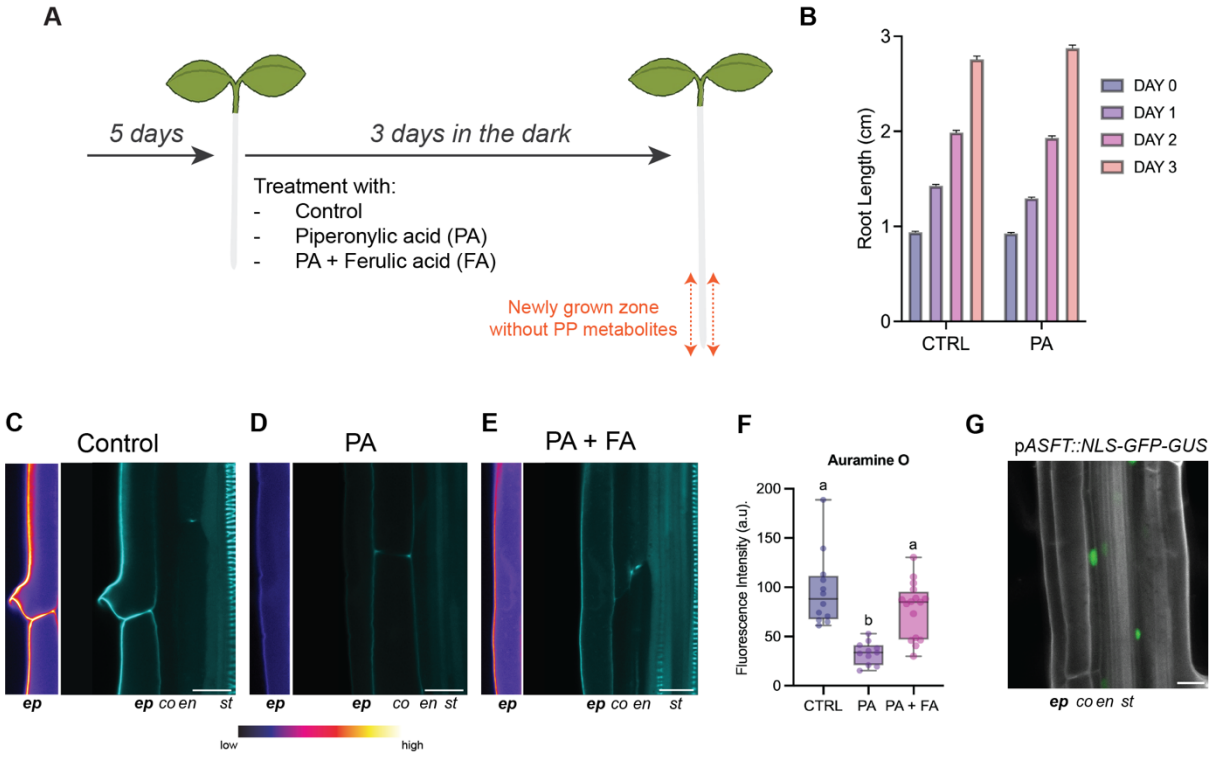

Figure 17. Epidermal AO-stainable compounds deposition is disrupted by inhibition of PP synthesis and complemented by Ferulic Acid. A) The experimental design is depicted in the scheme. WT seedlings were germinated for five days under control conditions and then transferred for three days, in dark conditions, to either a control medium, a medium containing 10 µM piperonylic acid (PA) only, or a medium supplemented with 20 µM ferulic acid (PA + FA). B) Root length measurements were taken for both the control and PA-treated roots, with error bars representing SEM; n=10. C-E) All pictures provided are longitudinal median optical sections of the zone +20, displaying only half of the root. On the left side of each root picture, a cropped section exclusively showing the epidermis is presented, allowing for the visualization of staining intensity (>yellow, high intensity; < yellow, lower intensity). F) Quantification of the epidermal stain intensity; n=10; letters refer to individual groups/treatments in a one-way ANOVA analysis with a post hoc multiple group t-test (Tukey) ($p < 0.05$). Scale bars: 20µm. G) Activity of

nuclear-localized (NLS) GFP-GUS fusion reporters driven by promoter regions of *ASFT*. Scale bars: 50µm. Ep, epidermis; co, cortex; en, endodermis; st, stele.

2.2 Composition of epidermal cell wall modifications: PP-derived compound

Altogether, our results led us to question the likelihood of suberin or a suberin-like compound being deposited in the outer cell wall of the root epidermis of *Arabidopsis*. Nevertheless, we noted that the autofluorescence in the epidermis denotes phenolic compounds, and that most phenolic compounds derive from the PP pathway (Donaldson, 2020; Fraser & Chapple, 2011). Moreover, AO-stainable compounds in the epidermis could also be linked to the PP pathway since AO stains lignin (Pesquet et al., 2005). Finally, the dramatic reduction of the AO staining in the epidermis upon PA treatment indicated that the epidermal cell wall modification might be composed of the PP-derived compound. Therefore, we sought to test the hypothesis that a PP-derived compound is deposited in the outer cell wall of the root epidermis in *Arabidopsis.*

2.2.1 Inhibition of PP synthesis leads to a reduction of autofluorescent compounds

The root epidermal cell wall modification was visible by autofluorescence and AO staining. Since inhibition of the PP pathway reduced the AO staining intensity in the epidermis, we tested whether this inhibition also affected the formation of autofluorescent compounds. Microscopic observation of root autofluorescence was done by exciting the seedlings with UV light. Confocal analysis showed that after 72h of PA treatment, the roots deposited fewer autofluorescent compounds than untreated roots **(Figure 18)**, suggesting that the AO-stainable compounds are likely autofluorescent. Autofluorescent compounds were still left in the epidermal cell wall after PP synthesis inhibition, indicating that not all the compounds in the epidermal walls are linked to the PP pathway.

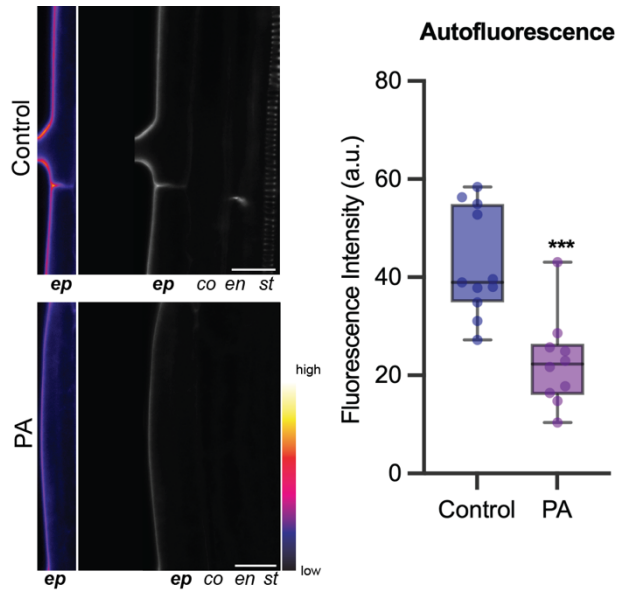

Figure 18. Inhibition of the PP pathway reduces the formation of autofluorescent compounds in the root epidermis. Autofluorescence was observed in 8-day-old control and 10 µM PA-treated roots. The provided pictures are longitudinal median optical sections of the zone +20, displaying only half of the root. On the right side, the graph illustrates the respective quantifications of the autofluorescence intensity in the root epidermis. On the left side of each root picture, a cropped section exclusively showing the epidermis is presented, enabling the visualization of the autofluorescence intensity (>yellow, high intensity; < yellow, lower intensity). n≥10; ***p ≤ 0.001; two-tailed Student's t-test versus the control. Scale bars 20µm. Ep, epidermis; co, cortex; en, endodermis; st, stele.

2.2.2 Key PP-pathway genes are expressed in the root epidermis

After inhibition of the PP pathway, the intensity of the AO staining in the epidermis was drastically reduced. Thus, it is conceivable that PP-derived compounds are deposited in the epidermis. To corroborate this, the expression pattern of *PAL2* and *C4H,* two genes encoding for key enzymes of the PP pathway, was investigated. *Arabidopsis* has four homologs of the *PAL* genes, of which *PAL2* has already been detected in the root epidermis (Andersen et al., 2021), whereas *C4H* has only one homolog. Expression of *PAL2* and *C4H* was evaluated in the zones +0, +10, +20, and +30 using transcriptional reporters generated previously (Andersen et al., 2021). Confocal analysis showed that, in the roots of 8-day-old seedlings, neither *PAL2* nor *C4H* was active in the elongation zone of the epidermis (Zone +0) **(Figure 19)**. From Zone +20 onwards, the expression of both promoters was active and consistent along the root epidermis axis. Thus, key genes of the PP pathway were active in the root epidermis, suggesting that this cell layer can produce PP metabolites. Notably, the gradient

of expression of both genes in the different zones was similar to that of AO-staining along the root axis.

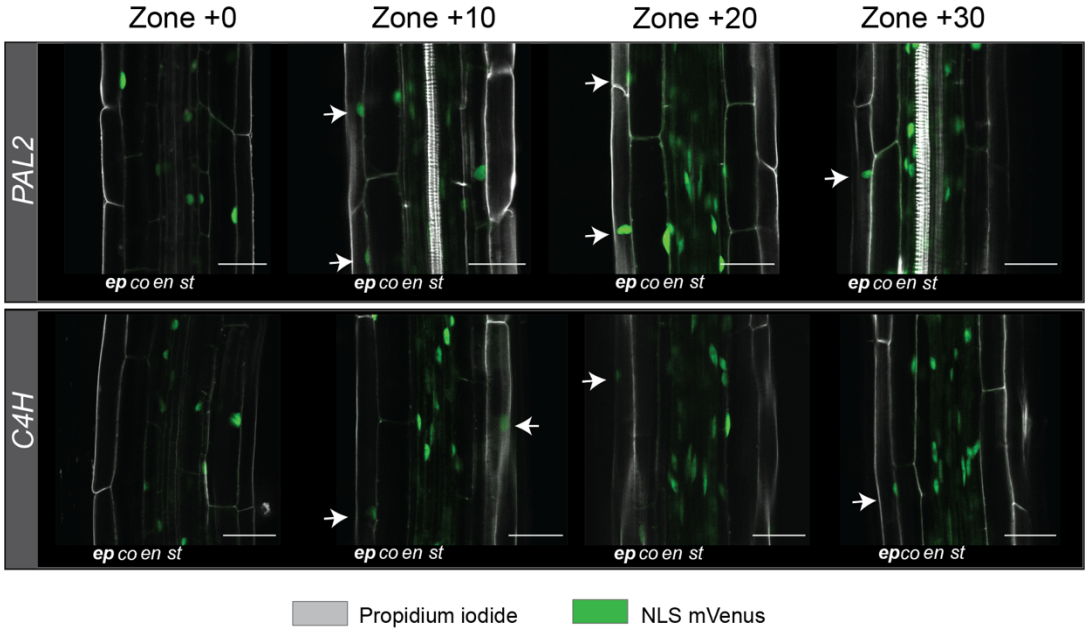

Figure 19. Epidermal cells can synthesize PP metabolites. The activity of nuclear-localized (NLS) Venus fusion reporters driven by promoter regions of root-expressed phenylalanine ammonia-lyase (PAL) and cinnamate 4-hydroxylase(C4H) homologs in *Arabidopsis* roots. The provided pictures are longitudinal median optical sections of the primary root. Expression in 8-day-old roots in elongating epidermal cells (Zone+0) to fully differentiated cells (Zone+30). The cell walls were highlighted with PI staining. Arrowheads indicate epidermal cells displaying reporter activity. Ep, epidermis; co, cortex; en, endodermis; st, stele. Scale bars: 50µm.

2.2.3 Genetic interference with the PP pathway reduces AO staining intensity

In *Arabidopsis*, a semi-dominant mutation of the transcriptional regulatory Mediator complex, *MED5b* (*REDUCED IN EPIDERMAL FLUORESCENCE 4-3* (*ref4-3*)) leads to dwarfism and constitutively repressed phenylpropanoid accumulation (Ruegger & Chapple, 2001; Stout et al., 2008). Similar to PA-treated roots, the *ref4-3* mutant showed a reduction in the AO staining intensity in the outer cell wall of the epidermis (**Figure 20A**). However, there was no visual difference in CS fluorescence intensity compared to the epidermis, suggesting that the *ref4-3* mutant phenotype could be specific to the root epidermis. The functionality of the CS can be visualized with Propidium Iodide (PI), since, in a functional barrier, the diffusion of PI into the inner layers of the stele is blocked upon the appearance of the CS (Naseer et

al., 2012). Counting the number of endodermal cells until PI blocks in the vasculature compared to WT roots showed that the *ref4-3* forms a defective CS barrier. Hence, in this mutant, PP compounds are reduced in the epidermis and endodermis (**Figure 20B**).

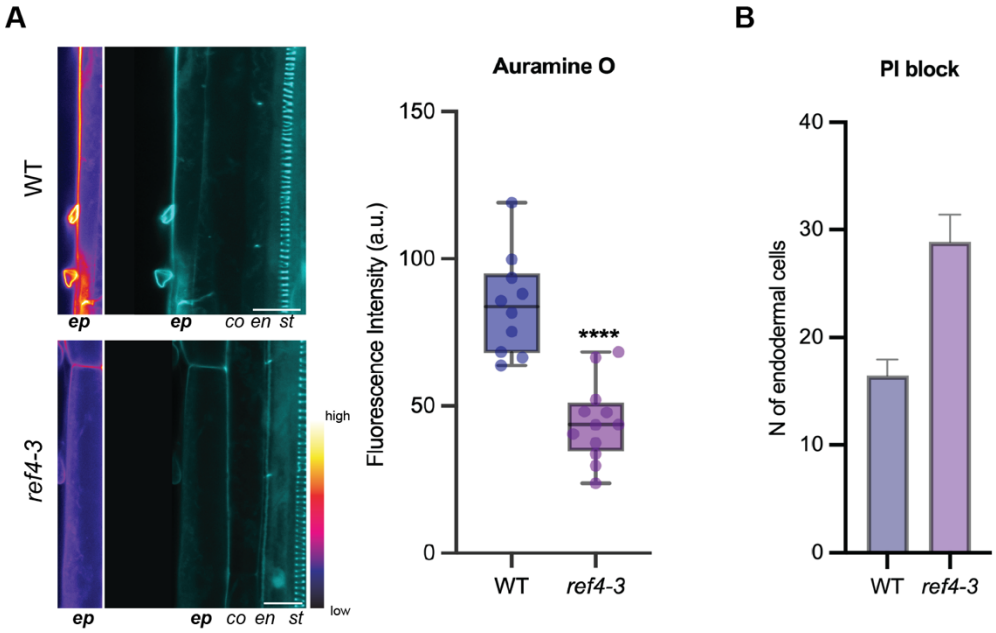

Figure 20. Altering genetically the PP pathway leads to a reduction in the AO staining in the epidermis, but also a defect in CS integrity. The provided pictures are longitudinal median optical sections of the zone +20, displaying only half of the root. On the right side, the graph illustrates the respective quantifications of the autofluorescence intensity in the root epidermis. On the left side of each root picture, there is a cropped section showing only the epidermis, enabling the visualization of the staining intensity (>yellow, high intensity; < yellow, lower intensity). A) Whole-mount AO staining of WT and the *ref4-3* mutant primary roots; n≥10; ****p ≤ 0.0001; two-tailed Student's t-test versus the WT. Scale bars: 20µm. B) Penetration of PI into the stele is blocked at 17 ± 2 endodermal cells after onset of elongation in WT roots and at 29 ± 4 in the *ref4-3* mutant; n=10, error bars represent SD. Ep, epidermis; co, cortex; en, endodermis; st, stele.

2.2.4 Inhibiting flavonoid formation does not affect AO staining intensity

Flavonoid metabolism is an important branch of phenylpropanoid metabolism, giving rise to the largest class of polyphenolic metabolites (Dong & Lin, 2021). The first enzyme specific for flavonoid biosynthesis is chalcone synthase (CHS), which produces chalcone scaffolds from which all flavonoids derive (Falcone Ferreyra et al., 2012). The *TRANSPARENT TESTA 4* (*tt4*) mutant has a lesion in *CHS*, resulting in no flavonoid production (Buer & Muday, 2004). To test whether AO-stainable compounds were composed of flavonoids, the intensity of the AO staining in the root epidermis was analyzed in the *tt4*

mutant. Confocal analysis showed no significant difference when comparing the fluorescence intensity between the WT and the *tt4* mutant. Indicating that AO-stainable compounds of the root epidermis outer cell wall are not linked to flavonoids.

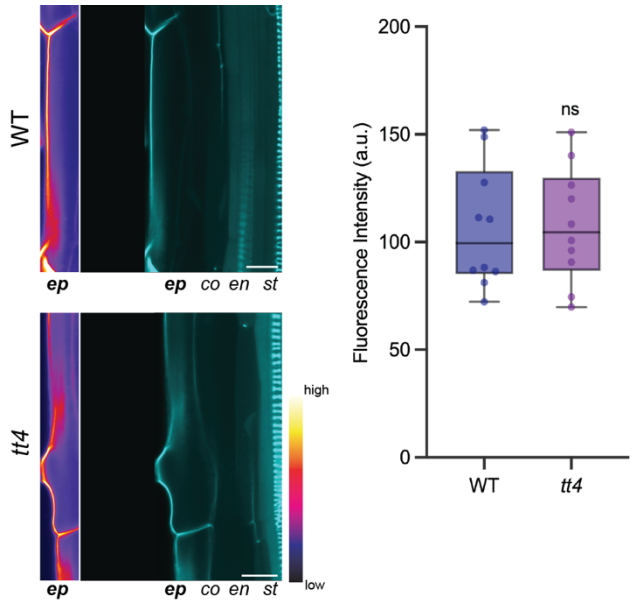

Figure 21. Inhibiting flavonoids formation does not affect AO staining intensity. The provided pictures are longitudinal median optical sections of the zone +20, displaying only half of the root. On the right side, the graph illustrates the respective quantifications of the staining intensity in the root epidermis. On the left side of each root picture, there is a cropped section showing only the epidermis, allowing for the visualization of the staining intensity (>yellow, high intensity; < yellow, lower intensity); n≥10; ****p ≤ 0.0001; two-tailed Student's t-test versus WT; Scale bars: 20µm; ep, epidermis; co, cortex; en, endodermis; st, stele.

2.2.5 Epidermal AO staining intensity correlates with the availability of monolignols

Lignin is the most characterized product of the PP pathway therefore, we sought to test whether lignin could be deposited in the root epidermis. Using a pharmacological approach, the PP pathway was inhibited via PA treatment (**Figure 17**). The PA-treated roots were simultaneously supplied with the monolignols coniferyl, sinapyl, and p-coumaryl alcohols (**Figure 22A**). After 72h of PA treatment supplied together with each monolignol, no perturbance in root growth was observed (**Figure 22B**). Strikingly, the exogenous application of monolignols allowed the recovery of the AO staining (**Figure 22C-D**). This complementation suggested that, even though the epidermis stains mildly with BF, a type of lignin may be

deposited in this cell layer. Then, we aimed to interfere specifically with monolignol biosynthesis. For this pupose, we took advantage of the mutant *cad4 cad5 f5h1 f5h2 ccr1*, in which monolignol biosynthesis is impaired (Naseer et al., 2012). In the *cad4 cad5 f5h1 f5h2 ccr1* mutant, it was possible to observe a clear reduction in the AO staining intensity in the root epidermis, as well as in the CS and xylem (**Figure 22E**). Thus, the deposition of AO-stainable compounds in the epidermal outer cell wall correlates with monolignol availability.

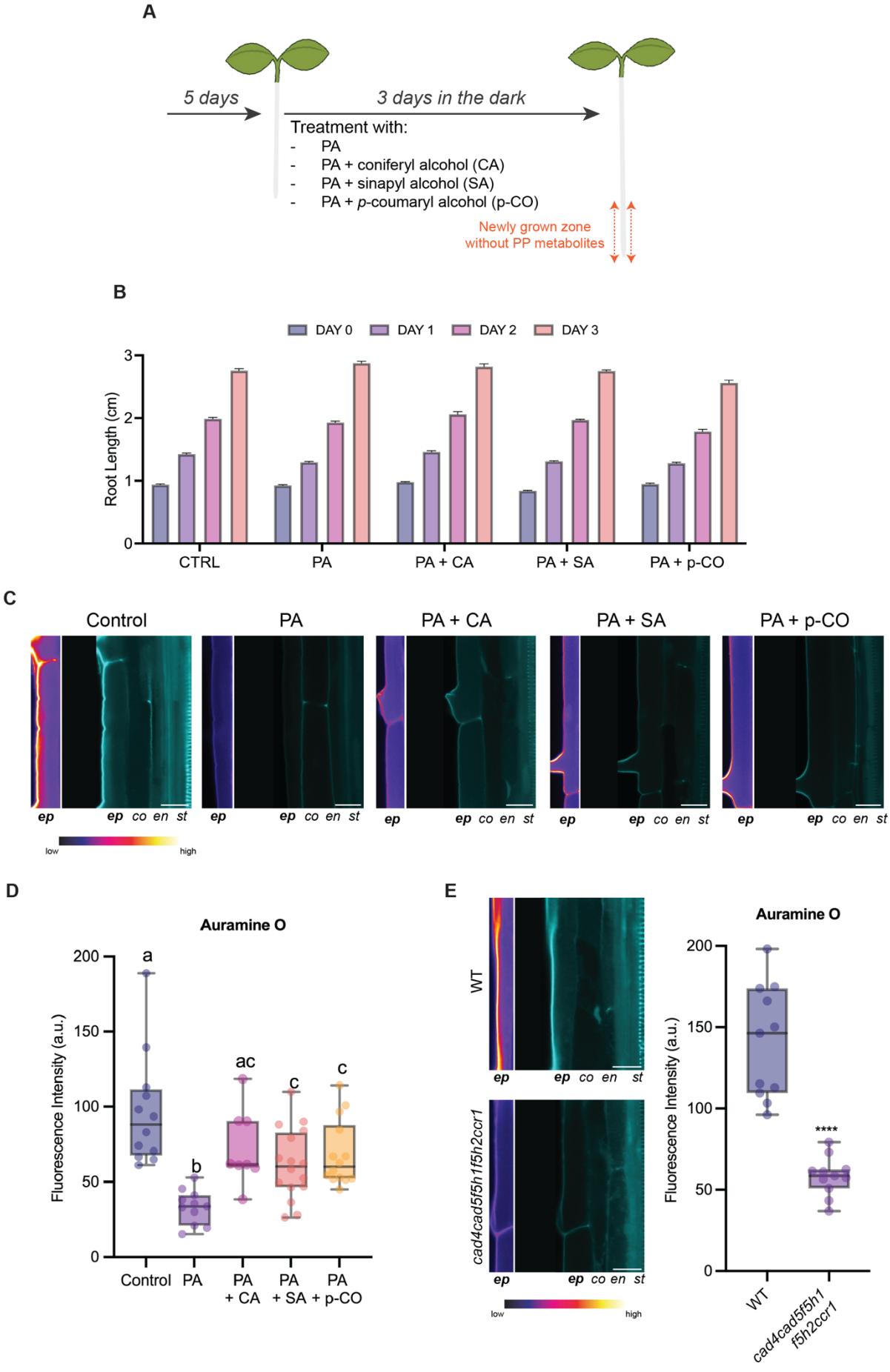
A
5 days
3 days in the dark
Treatment with:
- PA
- PA + coniferyl alcohol (CA)
- PA + sinapyl alcohol (SA)
- PA + p-coumaryl alcohol (p-CO)
Newly grown zone
without PP metabolites
B
DAY 0
DAY 1
DAY 2
DAY 3
Root Length (cm)
CTRL
PA
PA + CA
PA + SA
PA + p-CO
C
Control
PA
PA + CA
PA + SA
PA + p-CO
ep
co
en
st
low
high
D
Auramine O
Fluorescence Intensity (a.u.)
Control
PA
PA + CA
PA + SA + p-CO
E
WT
cad4cad5f5h1f5h2ccr1
Auramine O
Fluorescence Intensity (a.u.)
****
WT
cad4cad5f5h1 f5h2ccr1

Figure 22. Interference with monolignol biosynthesis affects the deposition of AO-stainable compounds. A) Scheme of the experimental design: WT seedlings were germinated for 5 days under control conditions and then transferred for three days to a control medium containing 10 µM piperonylic acid (PA) only or supplemented with 20 µM coniferyl alcohol (PA + CA), 20 µM sinapyl alcohol (PA + SA), or 20 µM *p*-coumaryl alcohol (PA + p-CO). B) Root length measurements for the control and the PA-treated or supplemented with monolignols, n=10, error bars represent SD. C) Whole-mount AO staining of the control and different pharmacological treatments. The provided pictures are longitudinal median optical sections of the zone +20, displaying only half of the root. On the left side of each root picture, there is a cropped section showing only the epidermis, allowing the visualization of the staining intensity. (>yellow, high intensity; < yellow, lower intensity). D) The quantifications of the staining intensity in the root epidermis in control and pharmacologically treated roots; n=10; letters refer to individual groups/treatments in a one-way ANOVA analysis with a post hoc multiple group t-test (Tukey) ($p > 0.05$). E) AO staining intensity was evaluated in a monolignol biosynthesis mutant (*cad4, cad5, f5h1, f5h2, ccr1*). The provided pictures are longitudinal median optical sections of the zone +20, displaying only half of the root. The quantifications of the staining intensity in the root epidermis are included. On the left side of each root picture, there is a cropped section showing only the epidermis, allowing the visualization of the staining intensity (>yellow, high intensity; < yellow, lower intensity); n=10; ****$p \leq 0.0001$; two-tailed Student's t-test versus WT. Ep, epidermis; co, cortex; en, endodermis; st, stele. Scale bars: 20µm.

2.2.6 Accumulation of autofluorescent compounds decreases when monolignol biosynthesis is impaired

PA treatment led to a reduction of both AO staining and autofluorescence. We went on to test whether the genetic interference with monolignol biosynthesis would also reduce the autofluorescence intensity. After evaluating and quantifying the autofluorescence intensity, results showed that the monolignol biosynthesis mutant *cad4cad5f5h1f5h1ccr1* deposits fewer autofluorescent compounds in the epidermis (**Figure 23**). This was in line with lignin being an autofluorescent polymer (Donaldson, 2020). Same as for the PA-treated roots, where there was still a signal remaining in the root epidermis of the lignin mutant.

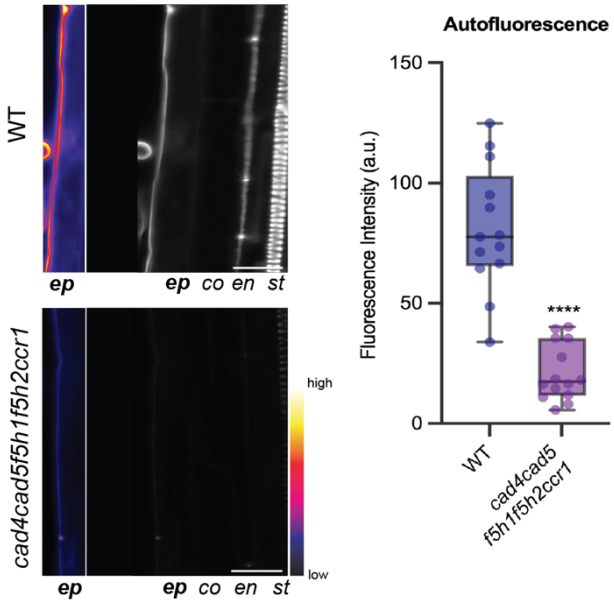

Figure 23. Inhibition of lignin biosynthesis reduces the formation of autofluorescent compounds in the root epidermis. Autofluorescence was observed in whole-mount 8-day-old seedlings of WT and cad4cad5f5h1f5h2ccr1 mutant. The provided pictures are longitudinal median optical sections of the zone +20, displaying only half of the root. On the right side, the respective quantifications of the autofluorescence intensity in the root epidermis are included. On the left side of each root picture, there is a cropped section showing only the epidermis, allowing for the visualization of the autofluorescence intensity (>yellow, high intensity; < yellow, lower intensity); n≥10; ***p ≤ 0.001; two-tailed Student's t-test versus the control. Scale bars: 20µm. Ep, epidermis; co, cortex; en, endodermis; st, stele.

2.2.7 Tissue-specific inhibition of PP synthesis

PA treatment indiscriminately inhibited the PP pathway in all cell types, and PP pathway mutants, including those specific for lignin formation, also developed defects in lignin deposition in the endodermis and stele. Therefore, we wanted to create a genetic tool that allows for tissue-specific repression of PP synthesis. In *Arabidopsis* roots, the transcription factor *MYB4*, which targets *C4H*, has been successfully used as a PP inhibitor in the endodermis (Andersen et al., 2021). To drive the expression of MYB4 in the root epidermis, we used the promoters of *GPAT2* and *GPAT3*, as they are both expressed in this cell layer along the root axis. To avoid pleiotropic effects and to add a temporal control, an estradiol (E2D)-inducible chimeric transcription factor (XVE) was employed (Siligato et al., 2016), generating plant lines expressing either p*GPAT2* or *pGPAT3::XVE>>MYB4-GFP*.

When the roots were exposed to 48h of E2D, it was possible to observe that the translational fusion affected the expression of both promoters. In the differentiation zone, in the roots where expression of *MYB4* was driven by the promoter of *GPAT2*, a GFP signal could be found in some cells (**Figure 24A**). However, in the lines driven by the promoter of *GPAT3*, no GFP signal could be detected (**Figure 24B**). We decided to analyze the AO staining on the roots where the expression of *MYB4* was driven by *GPAT2*. Unfortunately, once the seedlings were transferred to plates with E2D, those with a GFP signal stopped growing. Hence, we could not use these plant lines. (**Figure 24C**).

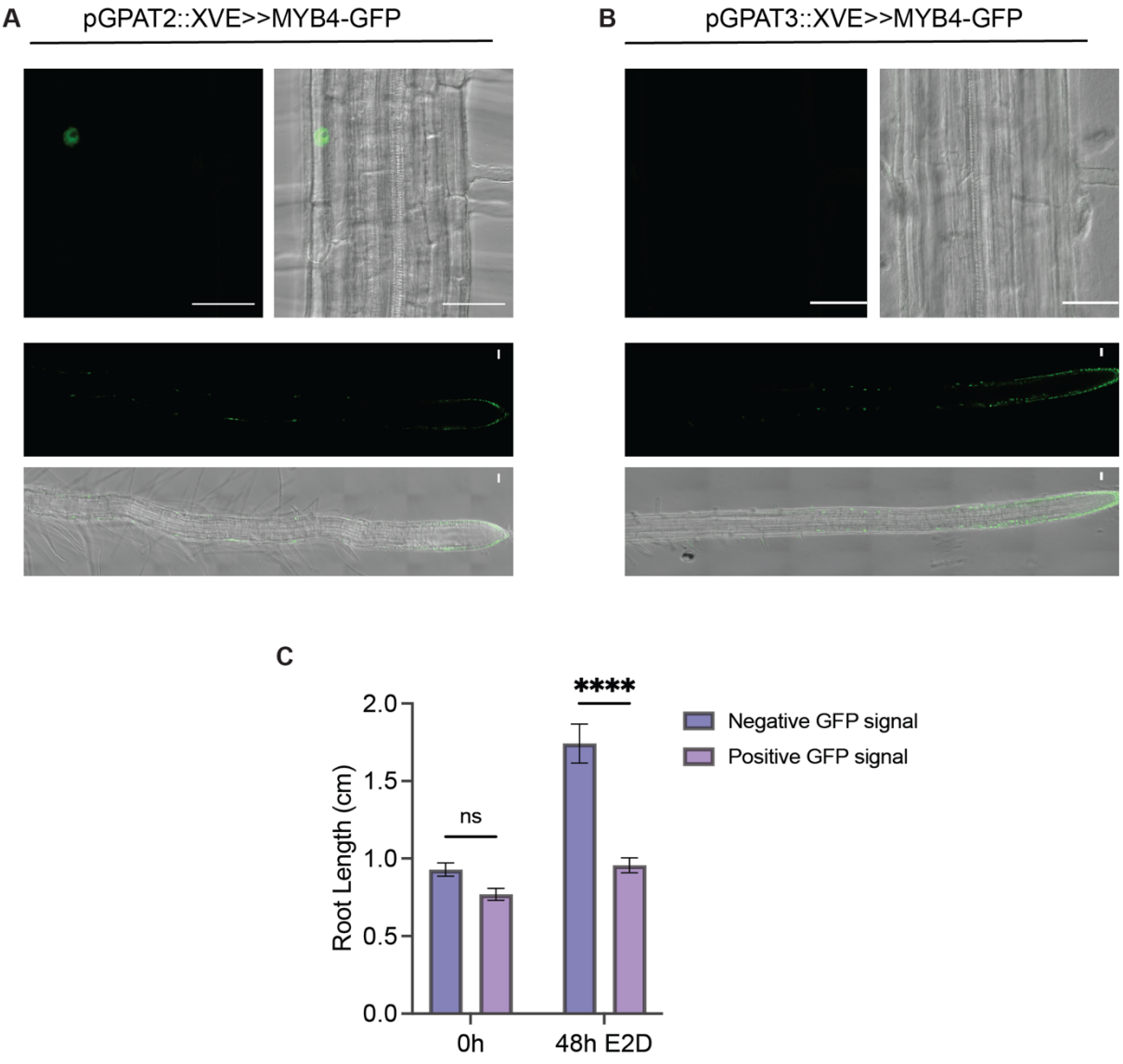

Figure 24. Epidermis-specific expression of MYB4 leads to growth arrest. A-B) The PP-repressive transcription factor MYB4 was expressed using the epidermal-expressed promoters from *GPAT2* and *GPAT3*

coupled with an estradiol (E2D)-inducible chimeric transcription factor. Close-up images of the zone+20 and overview of the root are provided. Scale bars: 50µm. C) Quantification of the root length of the roots expressing p*GPAT2*::XVE>>MYB4-GFP, before and after transferring to E2D; n≥10; error bars represent SD, ****p ≤ 0.0001; two-tailed Student's t-test versus the roots with negative GFP signal.

2.2.8 Lignin deposition is a cell-type specifically regulated event

The CS and xylem lignification were defective in the *cad4cad5f5h1f5h2ccr1* and *ref4-3* mutants and in the pharmacological inhibitions investigated. Therefore, it was essential to understand whether these defects in lignin deposition occur simultaneously or can be regulated independently. To test this, the AO staining intensity in the epidermis was analyzed in CS mutants, in which lignin is deposited in a defective manner in the endodermis, such as *cif1 cif2* (Fujita et al., 2020)*, 5x per* (*per3, per9, per39, per64, per72*) (Rojas-Murcia et al., 2020) and *myb36-2 sgn3-3* (Reyt et al., 2021). Confocal analysis revealed that, in the mutants investigated, the intensity of the AO staining did not decrease significantly (**Figure 25**). To evaluate whether lignin deposition in the vasculature is also cell type-regulated, the AO staining was evaluated in the mutant *arabidopsis histidine transfer protein 6* (*ahp6*). When the *ahp6* mutant is treated with low amounts of cytokinin, the lignification of the xylem is delayed (Mähönen et al., 2006; Naseer et al., 2012). This combination led to a non-lignified vasculature, but the epidermal stain intensity remained unchanged. These results suggest that lignin deposition is cell type-specifically regulated.

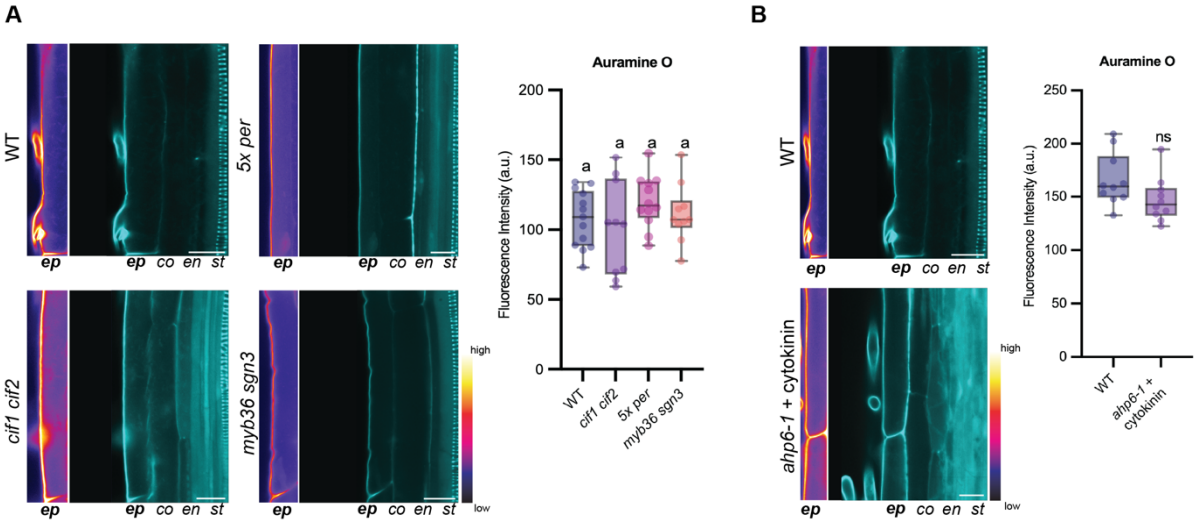

Figure 25. Lignin deposition is a cell-type specifically regulated event. All pictures depict longitudinal median optical sections of the zone +20, showing only half of the root. The respective quantifications of the staining intensity in the root epidermis are presented on the right side. On the left of each root picture, there is a cut-off displaying only the epidermis, allowing visualization of the staining intensity (>yellow, high intensity; < yellow, lower intensity). A) Whole-mount AO staining of WT and CS-specific mutants is shown; n≥10; letters refer to individual groups in a one-way ANOVA analysis with a post hoc multiple group t-test (Tukey) ($p > 0.05$). B) Inhibition of xylem lignification in the *ahp6-1* mutant upon treatment with the 10nM of the cytokinin benzyl-adenine; n=10; two-tailed Student's t-test versus WT. Ep, epidermis; co, cortex; en, endodermis; st, stele. Scale bars: 20µm.

2.2.9 NADPH oxidases are necessary for the formation of AO-stainable compounds

The biosynthesis of PP compounds may be activated under stress conditions (Dixon & Paiva, 1995). ROS is produced by NADPH oxidases and plays a key role in the acclimation of plants to stress (Choudhury et al., 2017). It was previously reported that the NADPH oxidases *RBOHA, RBOHC, RBOHD, RBOHE,* and *RBOHF* are expressed in the root epidermis (Lee et al., 2013). Thus, the intensity of the AO staining was evaluated in *RBOH* mutants (**Figure 26**). In the *rbohF, rbohD rbohF,* and *rbohA rbohB rbohF RBOHE/rbohE* mutants, the formation of the CS was impaired, as previously reported (Lee et al., 2013). In the single mutants of *rbohC, rbohD,* and *rbohF* it was possible to observe a mild reduction of the AO staining intensity in the epidermis. And, in the *RBOH* double and triple mutants *rbohD rbohF* and *rbohA rbohB rbohF RBOHE/rbohE* the reduction of the AO staining was stronger. These results indicate that the formation of AO-stainable compounds is NADPH-dependent.

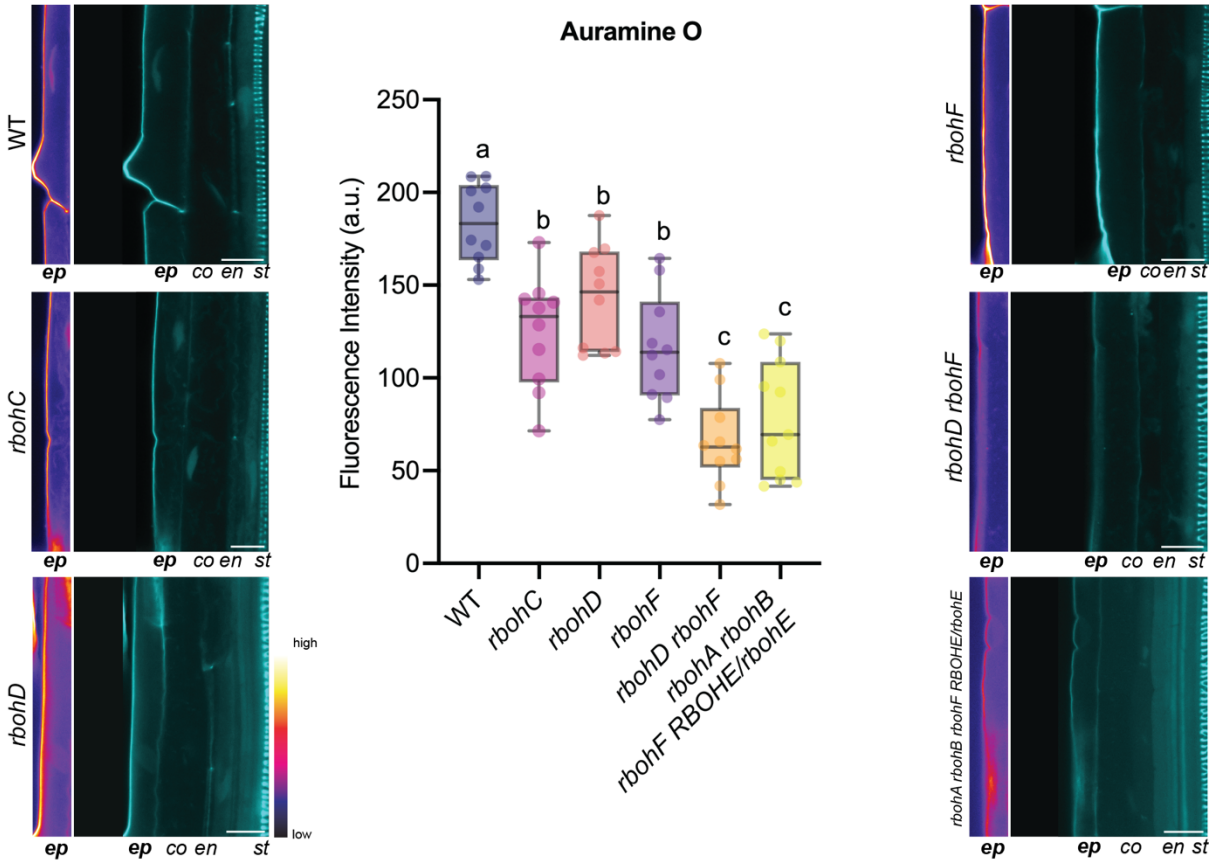

Figure 26. NADPH oxidases are essential for the synthesis of AO-stainable compounds. Whole-mount AO staining of WT and the *rboh* mutants: *rbohC, rbohD, rbohF, rbohDF,* and *rbohABFE*. Pictures are longitudinal, median optical sections of the zone +20, where only half the root is represented. In the middle, the respective quantifications of the staining intensity in the root epidermis are provided. To the left of each root picture, there is a cut-off displaying only the epidermis, allowing visualization of the staining intensity (>yellow, high intensity; < yellow, lower intensity); n≥10; letters refer to individual groups in a one-way ANOVA analysis with a post hoc multiple group t-test (Tukey) ($p > 0.05$). Scale bars: 20µm. Ep, epidermis; co, cortex; en, endodermis; st, stele.

2.2.10 The formation of AO-stainable compounds requires dismutases and peroxidases

Lignin formation requires superoxide formation, which is subsequently dismutated into peroxide, which is used for monolignol oxidation. NADPH oxidases have been pinpointed as major players in superoxide formation. Thus, we sought to test whether all the following steps necessary for lignin formation are also required. Accordingly, each step of lignin formation was inhibited via different pharmacological compounds, using the methodology previously reported (Lee et al., 2013). NADPH oxidases were inhibited by using diphenylene iodonium (DPI) in PA-treated roots. Since DPI is a toxic compound, lignification recovery was tested by supplying additionally the monolignol coniferyl alcohol (CA), in the time frame previously

tested (Lee et al., 2013). Analysis of the fluorescence intensity showed that NADPH oxidases are indeed necessary for the formation of AO-stainable compounds (**Figure 27A**). Moreover, in PA-treated roots, dismutases were inhibited by treating the seedlings with diethyldithiocarbamic acid (DDC) and CA, reducing the AO staining intensity (**Figure 27B**). Disturbing peroxide production with potassium iodide (KI) also led to a reduction in the AO staining intensity (**Figure 27C**). Finally, interference of the peroxidase activity by applying salicylhydroxamic acid (SHAM) to the seedlings reduced the AO staining intensity in the epidermis (**Figure 27D**). The fact that four different manipulations reduced the formation of AO-stainable compounds provides additional support to a model where lignin or a lignin-like polymer is deposited in the root epidermal cell wall of *Arabidopsis*.

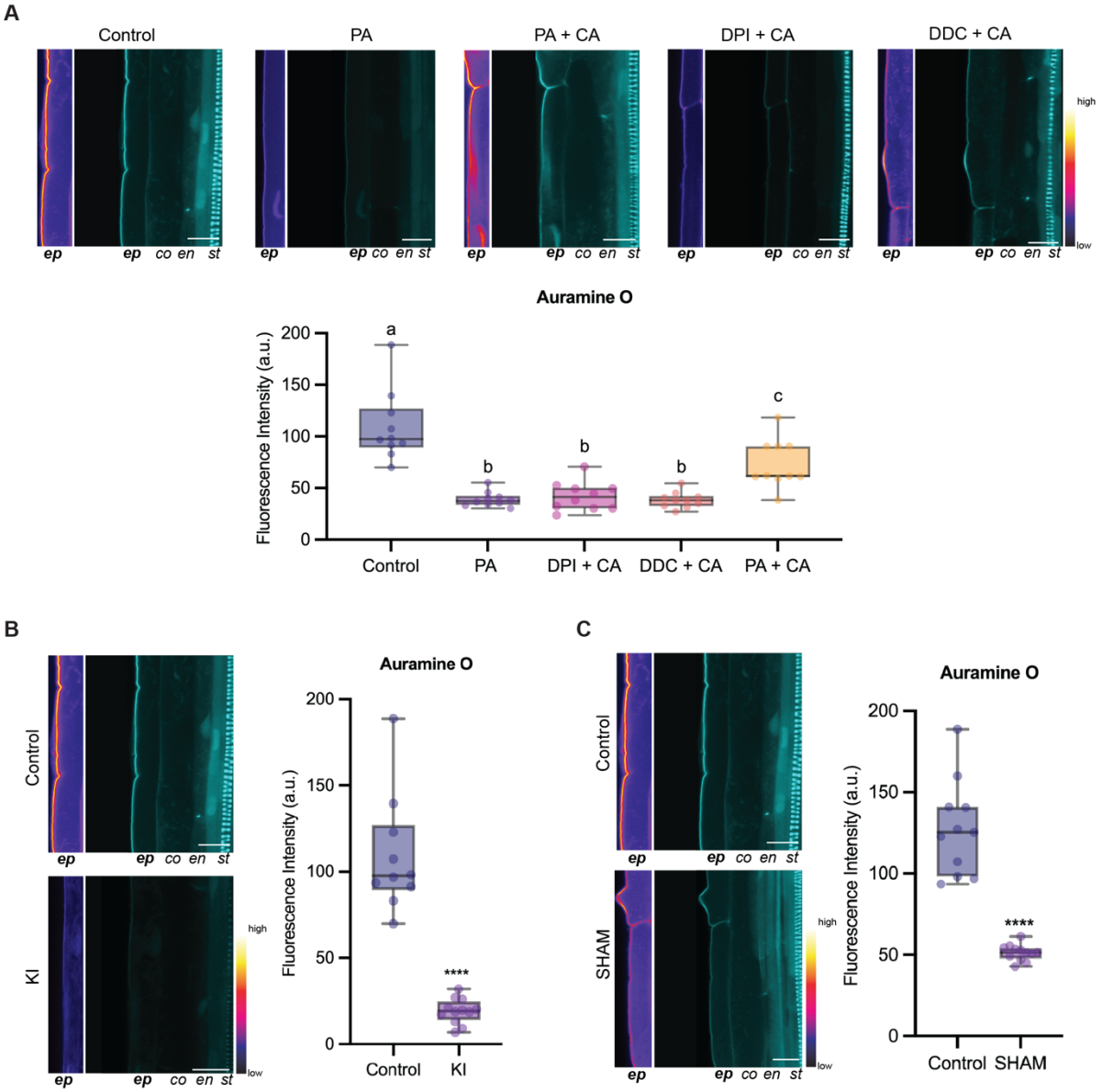

Figure 27. The formation of AO-stainable compounds requires dismutases and peroxidases. All the pictures provided are longitudinal median optical sections of the zone +20, where only half the root is represented. On the right side, the respective quantifications of the staining intensity in the root epidermis are included. To the left of each root picture, there is a cut-off displaying only the epidermis, where the staining intensity can be visualized (>yellow, high intensity; < yellow, lower intensity). A) Inhibition of the NADPH oxidases with 5µM DPI and of dismutases with 250µM DDC, compared to the control, PA, and PA+CA-treated roots; n=10, letters refer to individual groups in a one-way ANOVA analysis with a post hoc multiple group t-test (Tukey) ($p > 0.05$). B) Treatment with 5mM KI resulted in a reduction of AO staining in the epidermis; n=10, ****$p \leq 0.0001$, two-tailed Student's t-test versus the control. D) The inhibition of peroxidases using 50µM SHAM led to a decrease in AO staining intensity; n=10, ****$p \leq 0.0001$, two-tailed Student's t-test versus the control. Scale bars: 20µm. Ep, epidermis; co, cortex; en, endodermis; st, stele.

2.2.11 The lignin stain Safranine O stains the outer cell wall of the root epidermis

All the evidence we gathered pointed towards the premise that lignin or a lignin-like compound is deposited in the epidermal cell wall. To validate this hypothesis, we tested another fluorescent lignin stain. Safranine O is an azo dye commonly used for staining lignified tissues such as the xylem (Baldacci-Cresp et al., 2020; Bond et al., 2008). In control seedlings, Safranine O stained the outer cell wall of the epidermis at a similar intensity as AO (**Figure 28A-B**). After PP-synthesis inhibition with PA, a reduction in the staining intensity of the cell wall was observed in the epidermis. Upon monolignol supply, the staining intensity in the epidermis was partially recovered (**Figure 28A-B**). These findings support the hypothesis that a lignin-like polymer is deposited in the outer cell wall of the root epidermis in *Arabidopsis*. However, this root epidermal lignin-like polymer cannot be distinguished in TEM with the lignin stain $KMnO_4$, and it does not stain with the typical lignin stain BF. Therefore, we have decided to name it atypical lignin.

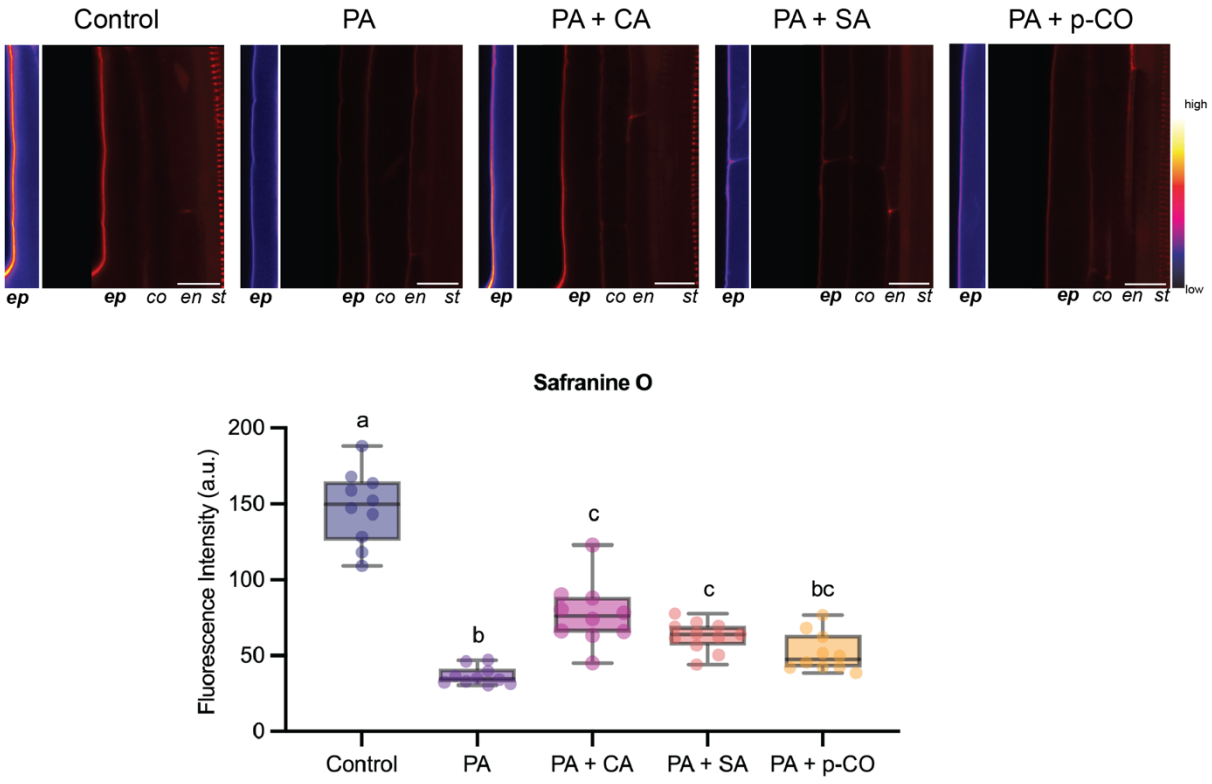

Figure 28. Safranine O stain stains the epidermal cell wall like AO. A) Whole-mount Safranine O staining of the control and upon PP synthesis inhibition and following monolignol supplementation (following the same

experimental procedure as for AO). The pictures presented are longitudinal, median optical sections of the zone +20, where only half of the root is represented. The respective quantifications of the staining intensity in the root epidermis are included on the right side. Additionally, to the left of every root picture, there is a cut-off showing only the epidermis, allowing for visualization of the staining intensity. (>yellow, high intensity; < yellow, lower intensity). PA, piperonylic acid; CA, coniferyl alcohol; SA, sinapyl alcohol; p-CO, *p*-coumaryl alcohol; n=10; letters refer to individual groups/treatments in a one-way ANOVA analysis with a post hoc multiple group t-test (Tukey) ($p > 0.05$). Ep, epidermis; co, cortex; en, endodermis; st, stele. Scale bars: 20µm.

2.3 Close-up analysis: trichoblasts and atrichoblasts

In the previous sections, we analyzed the epidermal cells in general, always observing in the middle root section. However, it was essential to define whether the atypical lignin is deposited in both types of epidermal cells: trichoblasts (root hair cells) and atrichoblasts (non-root hair cells).

2.3.1 Root hair cells deposit more atypical lignin than non-root hair cells

Optical cross-sections of control roots stained with AO revealed a higher deposition of atypical lignin in the trichoblasts compared to the atrichoblasts. Moreover, after PA treatment, the amount of atypical lignin decreases in both types of cells (**Figure 29A-B**). To verify whether the difference in deposition could be reflected in cell wall thickness, control and PA-treated roots were visualized by TEM. Unexpectedly, the outer cell walls of trichoblasts were thicker than those of atrichoblasts, consistent with less deposition of atypical lignin. However, no difference in thickness could be observed after PA treatment (**Figure 29C**). Our results showed that trichoblasts deposit more atypical lignin and have thicker outer cell walls than atrichoblasts. To understand whether the extra atypical lignin deposit could play a role in root hair stability, we sought to inhibit or affect root hair formation pharmacologically or genetically and observe if the staining intensity remains the same. Aminovinylglycine (AVG) is a chemical that inhibits root hair formation (Tanimoto et al., 1995). After treating the seedlings for 24h with AVG, the intensity of the AO staining in the epidermis decreased (**Figure 29D**). To corroborate these results, we analyzed loss-of-function mutants of genes related to root hair elongation (*TRANSPARENT TESTA GLABRA2* (*TTG2*) (Grierson et al., 2014) and *GLABRA1 x ROOT*

HAIR DEFECTIVE 2 (*GL1 RHD2*) (Schiefelbein & Somerville, 1990), both with no reduction on the AO staining intensity. The lack of effect on the AO staining could be linked to the fact that root hair initiation was not affected in the *ttg2* and *gl1 rhd2* mutant lines. Thus, the AO staining was analyzed in the *ROOT HAIR DEFECTIVE 6* (*RHD6*) mutant, which controls the differentiation of trichoblasts into hair cells, leading to a shift in the starting point of root hair emergence (Masucci & Schiefelbein, 1994). The intensity of the AO staining in the *rhd6* mutant also remained unchanged. This could have been because the number of trichoblasts remained unchanged, and only the root hair initiation was affected. Nonetheless, due to the contrast of results, further investigations are needed to uncover the role of the extra atypical lignin deposition in trichoblasts.

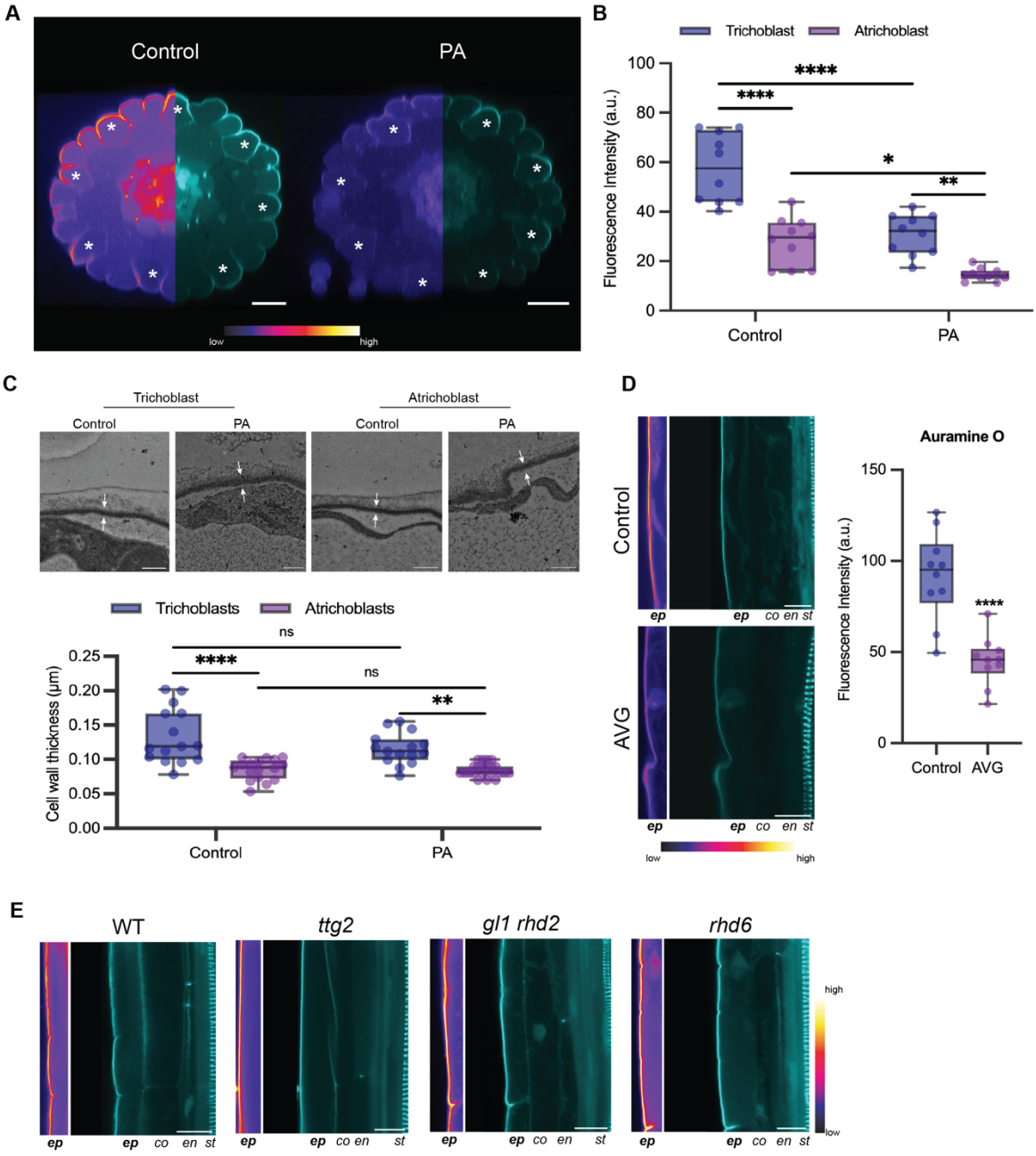

Figure 29. Atypical lignin deposition is higher in trichoblasts. A) Optical cross-sections of AO-stained 8-day-old control and PA-treated roots. To the left of both images, there is a cut-off in which the intensity of the staining can be visualized (>yellow, high intensity; < yellow, lower intensity); asterisks highlight the trichoblasts. B) Quantification of the staining intensity in the outer cell wall of the epidermis upon 10µM PA treatment in trichoblasts and atrichoblasts; n=10, grouped Student T-tests, asterisks denote significance against the control; *p ≤ 0.05, ** p ≤ 0.01, ****p ≤ 0.0001. C) The upper section displays cross-sections of roots imaged by TEM and stained with $KMnO_4$, highlighting the trichoblasts and atrichoblasts. The arrows indicate the epidermal outer cell walls. The lower section provides quantification of the thickness of the epidermis outer cell wall in trichoblasts and atrichoblasts following 10µM PA treatment; grouped Student T-tests, asterisks denote significance against the control; ** p ≤ 0.01, ****p ≤ 0.0001. D) AO staining in control and roots treated with 20µM AVG. The pictures shown are longitudinal, median optical sections of the zone +20, representing only half of the root. On right side, the respective quantification of staining intensity is included. On the left side, there is a cut-off showing only the epidermis, allowing visualization of the staining intensity (>yellow, high intensity; < yellow, lower intensity); n=10,

individual Student T-tests, asterisks denote significance against the control, ****p ≤ 0.0001. E) Wild-type and root hair mutants stained with AO, Pictures are longitudinal, median optical sections of the zone +20, where only half the root is shown. To the left of each root picture, there is a cut-off showing only the epidermis, where the staining intensity can be visualized (>yellow, high intensity; < yellow, lower intensity). Scale bars: 20µm. Ep, epidermis; co, cortex; en, endodermis; st, stele.

2.4 The role of the atypical lignin modification of the epidermal cell wall

Typically, lignin impregnation of a cell confers mechanical strength, rigidity, and hydrophobicity to the latter (Emonet & Hay, 2022). Thus, we executed a set of experiments to unveil the role of the atypical lignin deposited in the epidermal walls.

2.4.1 Permeability of the root epidermis is not affected in seedlings with lower deposition of atypical lignin

Lignin deposition in the CS has a role of apoplastic diffusion barrier (Naseer et al., 2012), thus, we wanted to investigate whether the atypical lignin deposition in the epidermis would also act as a diffusion barrier. For this, the apoplastic tracer propidium iodide (PI) was used. To evaluate whether there was any difference in PI penetration into the cortex radial cell walls between earlier and late differentiating epidermis, Zones +20 and +40 were observed. There was no difference in the PI penetration between the earlier and mature root epidermis (**Figure 30A-B**). If a permeability barrier is linked to the atypical lignin deposition in the epidermis, PA-treated roots should be more permeable to PI. However, there was no difference in PI penetration, either in the younger or later stage of differentiation of the epidermis, after the inhibition of the PP pathway (**Figure 30A-B**). Calcofluor White is a cell wall stain that binds to cellulose and other β-1,4-linked carbohydrates (Ursache et al., 2018; Zhou et al., 2009). We tested whether there was a difference in permeability to Calcofluor White in the PA-treated roots. Strikingly, after 72h of PA treatment, the fluorescence intensity in all the cell walls was stronger, meaning all cell walls were more permeable to Calcofluor White, or the composition of the cell walls changed. Hence, our results indicate that the

atypical lignin deposited in the outer epidermal walls might not have a role in forming of a diffusion barrier in the apoplast.

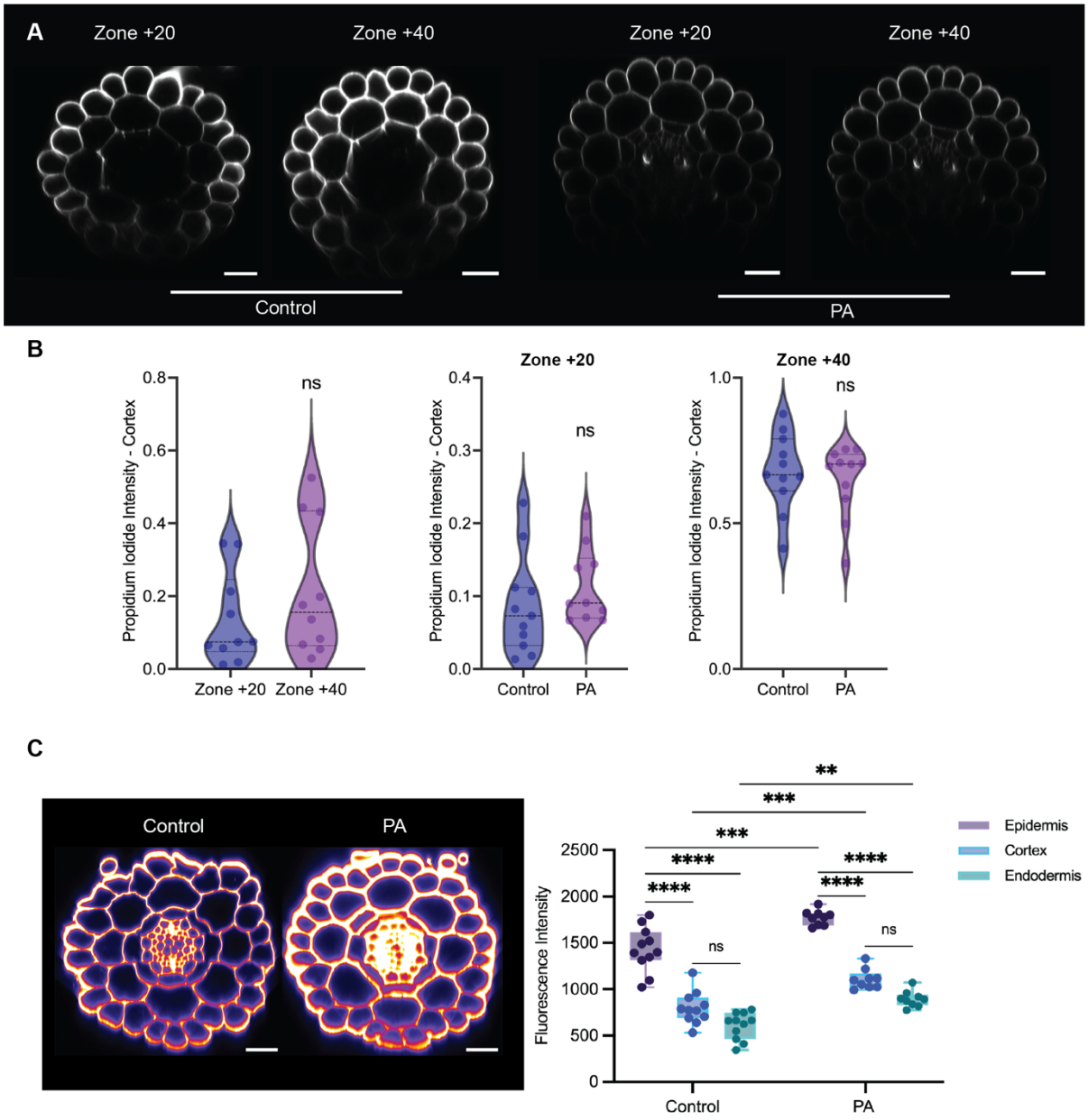

Figure 30. Permeability remains unaffected in roots after PP synthesis inhibition. A) *Arabidopsis* root optical cross-sections from control and seedlings treated with 10µM PA for 72h, in the zones +20 and +40. 8-day-old seedlings were incubated in the apoplastic tracer Propidium Iodide (PI) for 10 minutes; scale bars represent 20 µm. B) Quantification of PI penetration into cortex cells in control and PA-treated seedlings in the zones +20 and +40; n=10; statistical significance was determined by two-tailed Student's t-test. C) Optical cross-sections of control and PA-treated roots fixed and stained with Calcofluor White. The fluorescence intensity in the epidermis, cortex, and endodermis was quantified and presented on the right side.; n=10; statistical significance was determined by Three-Way ANOVA with a post-hoc Tukey HSD test, **p ≤ 0.01,*** p ≤ 0.001,**** p ≤ 0.0001; scale bars: 20 µm.

2.4.2 Abiotic and biotic stresses do not induce atypical lignin formation in the epidermis

In plants, stress resistance is closely related to the increased deposition of lignin. Both osmotic and ionic stress can lead to higher cell wall lignification (Chen et al., 2019; Chun et al., 2019). Mannitol is often used to impose osmotic stress on seedlings (Khandal et al., 2020). Osmotic stress responses are also regulated by ABA (Rowe et al., 2016). Salt is commonly used to impose ionic stress on plants (Chun et al., 2019). Hence, we treated seedlings with either mannitol, ABA, or salt, in different time incubation periods, to investigate if these stresses could induce the deposition of atypical lignin in the root epidermis. After treating the seedlings with mannitol in two different concentrations for 72h, there was no increase in the AO staining intensity in the epidermal cell wall (**Figure 31A**). Moreover, there was also no difference upon ABA or salt treatments (**Figure 31B**).

Lignification can also be induced upon mechanical injuries (Moura et al., 2010), hence, to elicit a damage-related response in the root, we used the *Arabidopsis*-derived plant elicitor peptide 1 (AtPep1). AtPep1 is a damage-associated molecular pattern (DAMP) reported to induce lignin formation in roots (Zhang et al., 2022). Upon treatment for 24h with AtPep1, a higher intensity of the AO staining in the epidermis was observed already in zone +10 (**Figure 31C-D**). However, root hairs were also present in zone +0, and the CS and vasculature were lignified, indicating that the roots differentiated earlier. The staining intensity at zone +20 remained unaltered.

An increase in lignification is also often observed in response to pathogen attacks (Lee et al., 2019; Moura et al., 2010). Thus, we thought of simulating a pathogen attack by using different peptides isolated from pathogens and known as pathogen-associated molecular patterns (PAMPs). One of the most studied PAMPs is a 22-amino-acid fragment of the bacterial flagellin protein (flg22). It has been reported that flg22 induces a signaling cascade, eventually leading to defense responses such as lignin deposition (Chezem et al., 2017; Emonet et al., 2021). Chitin is another well-studied PAMP derived from fungi (Choi & Klessig, 2016). Finally, the endogenous peptide SCOOP12 regulates the defense response against pathogen aggression (Choi & Klessig, 2016). We evaluated the staining intensity of the outer

epidermal cell wall in the zones +10 and +20. We observed that in all the peptide treatments, the root differentiates slightly earlier, as seen by the increase of staining in zone +10 and similar to the the results obtained with AtPep1 (**Figure 31D**). In zone +20, the staining intensity did not increase for any peptide treatment, meaning PAMPs did not elicit a lignification response in the root epidermis. Therefore, altogether, these results show that treatment with both types of peptides does not induce the deposition of atypical lignin in the outer cell wall of the root epidermis.

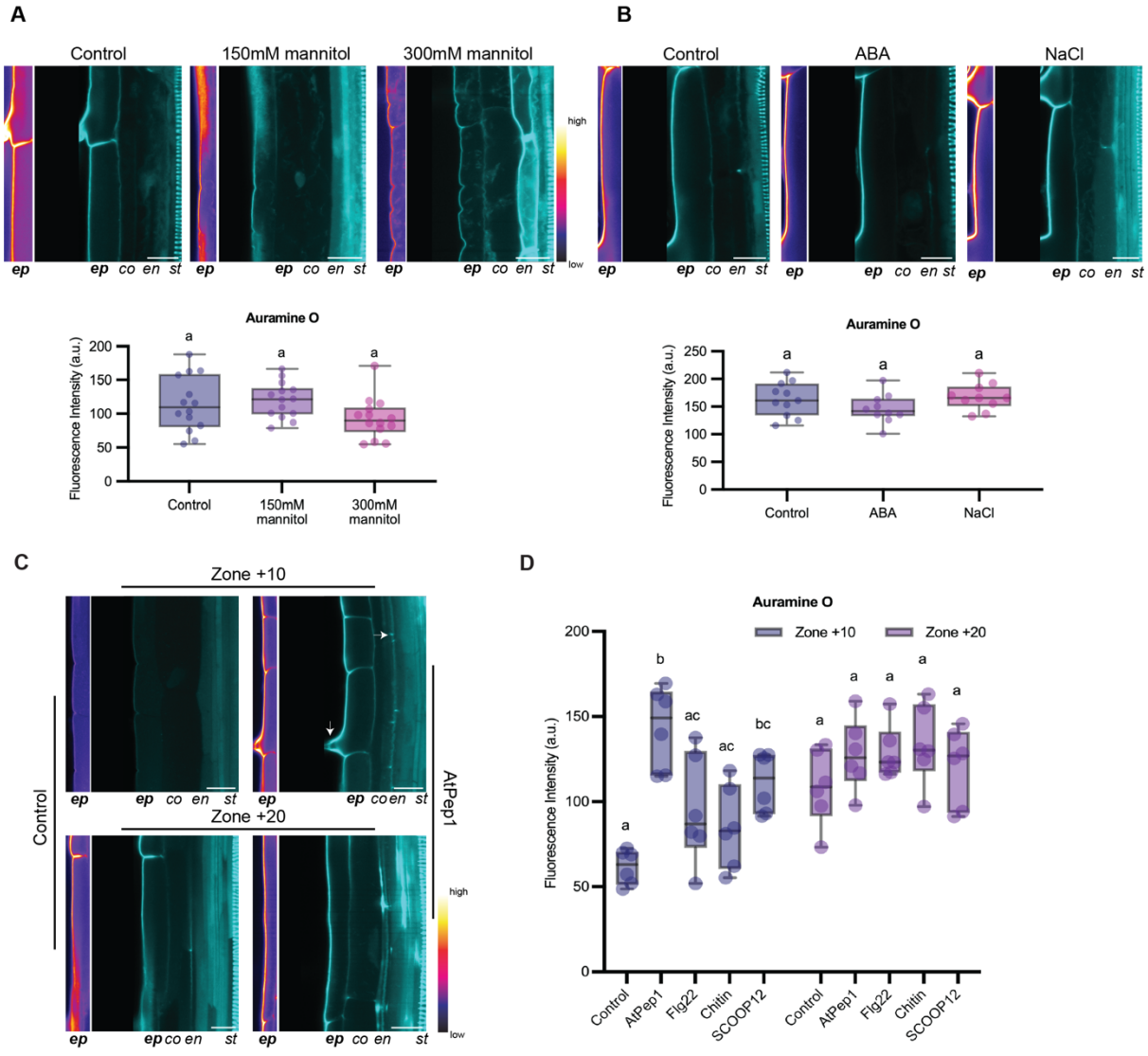

Figure 31. Abiotic and biotic stresses do not induce atypical lignin in the epidermal cell wall. Pictures presented are longitudinal, median optical sections of the zone +20, displaying only half of the root. To the left of each root picture, there is a cut-off section showing only the epidermis, enabling visualization of the staining intensity (>yellow, high intensity; < yellow, lower intensity). A) AO staining of whole-mount roots grown on 150mM

and 300mM mannitol for 72h. The respective quantification is presented below the images; n=10. B) Visualization of the AO staining of roots grown on 48h 1µM ABA or 72h 100mM NaCl. The corresponding quantification is presented below the images.; n=10, letters refer to individual groups/treatments in a one-way ANOVA analysis with a post hoc multiple group t-test (Tukey) ($p > 0.05$). C) Visualization of the root earlier differentiation upon AtPep1 treatment. Arrows point to features of the differentiated root: root hairs and CS. D) Quantification of AO staining intensity in the epidermal cell wall in the zones +10 and +20 of the primary root; n=10; letters refer to individual groups/treatments in a one-way ANOVA analysis with a post hoc multiple group t-test (Tukey) ($p > 0.05$). Ep, epidermis; co, cortex; en, endodermis; st, stele. Scale bars: 20µm.

2.4.3 Preliminary results: mechanical properties of the root epidermal atypical lignin

Typically, lignin enhances plant cell wall rigidity (Liu et al., 2018). We sought to investigate whether the atypical lignin would also enhance cell wall rigidity. Cells shrink due to the loss of turgor pressure in response to a hyperosmotic solution. Thus, cell wall stiffness or elasticity can be measured by measuring cell shrinkage (Liu et al., 2022; Sapala & Smith, 2020). After cell segmentation and area measurement, our results showed that 20 minutes of 0.4% salt stress did not increase shrinkage in the *cad4cad5f5h1f5h1ccr1* mutant and the PA-treated roots (**Figure 32**). These results are preliminary, and the experiment requires further optimizations. Suggestions are given in the discussion.

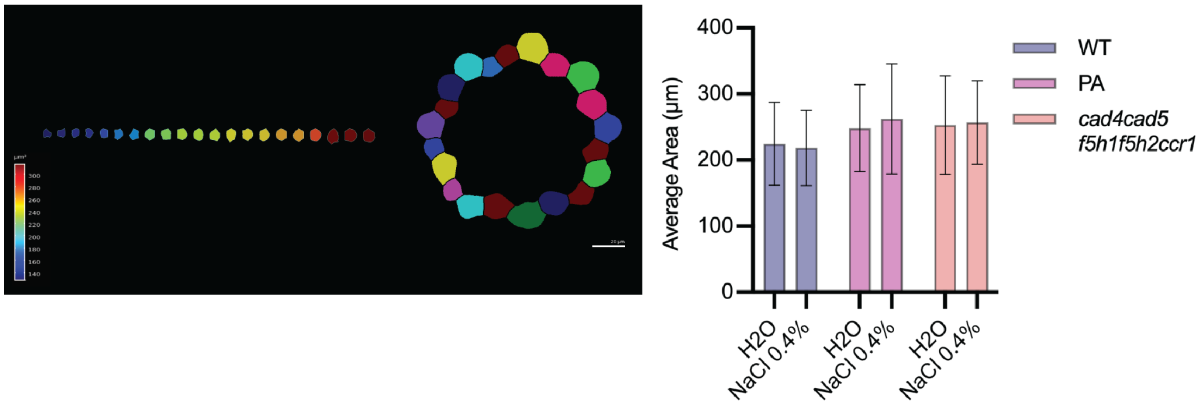

Figure 32. Osmotic stress does not affect cell size. Root epidermal cells were segmented using MorphoGraphX and arranged based on their area size (left side). To the right side, quantification showing the average area size in wild-type, PA-treated, and cad4cad5f5h1f5h2ccr1 mutant roots under both water and 0.4% salt treatments; error bars represent SD. Scale bars: 20 µm.

Cell wall lignification may be induced in response to environmental changes (Barros et al., 2015). With this rationale, we bent wild-type, PA-treated and *cad4cad5f5h1f5h2ccr1*

roots for 6h to simulate an environmental change. Quantifying the bending angle after 6h gave contrasting results over the three biological replicates (**Figure 33A**), but overall, there was little difference between the genotypes/treatments. Moreover, the root length measurements during the bending timeframe also led to diverging results, with little difference among the genotypes/treatments (**Figure 33B**). Since this experimental section is still ongoing, no conclusions could be made.

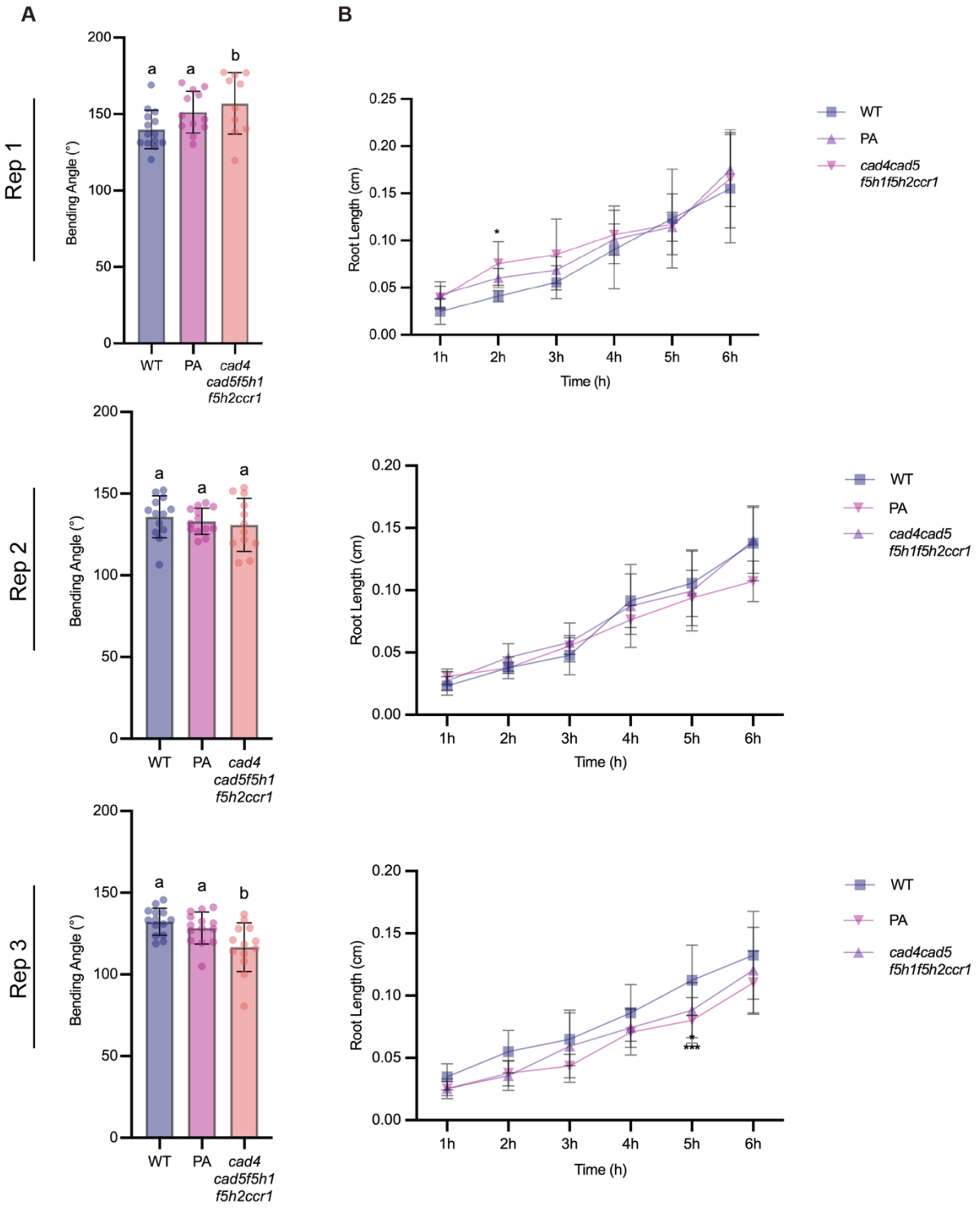

Figure 33. Atypical lignin does not interfere with root bending. A) Three biological repetitions of the bending angle quantification in 8-day-old roots, after 6h of bending; n ≥ 10; One-way ANOVA analysis with a post hoc multiple group t-test (Tukey) ($p > 0.05$), error bars represent SD. B) Measurement of the root length after bending in a 6h timeframe; n ≥ 10; Two-way ANOVA analysis with a post hoc multiple group t-test (Tukey), $^{**}p \leq 0.01$.

3. Discussion and perspectives

In this study, we sought to shed light on the chemical nature and functions of the root epidermal cell wall modification in *Arabidopsis thaliana*. Although previous assumptions postulated the presence of diffuse suberin in the epidermis, we have shown that a lignin-like compound is deposited in the outer cell wall of the root epidermis.

3.1 A lignin-like compound is deposited in the outer cell wall of the root epidermis

Our results demonstrate for the first time the chemical nature of the compound that modifies the outer epidermal cell walls in *Arabidopsis* via pharmacological treatments and loss-of-function mutants. We coined the term atypical lignin since Basic Fuchsin, a typical lignin dye, stains the epidermal cell wall very lightly. Whereas the lignin stain Safranine O stains the epidermal cell wall strongly in comparison to the CS and xylem. Moreover, p-coumaryl alcohol incorporates in the epidermal cell wall, as seen with both Auramine O and Safranine O. Characteristically, in angiosperms, lignin is typically composed of coniferyl- and sinapyl alcohols. *p*-coumaryl alcohol is naturally a minor lignin component, accounting for only 2% of the total lignin in *Arabidopsis* (Higuchi, 1990). Hence, it would be interesting to generate a lignin mutant specific for the root epidermis so chemical analysis can be done via thioacidolysis followed by gas chromatography-mass spectrometry (GC-MS) to evaluate the monomer composition of the epidermal atypical lignin (Naseer et al., 2012). This will be further discussed in Section 3.2. Finally, when imaging with TEM, the atypical lignin deposited in the root epidermis did not stain with $KMnO_4$. In fact, no modification could be visualized in the outer cell walls of the epidermis. This could have occurred because the atypical lignin does not stain with $KMnO_4$ or it does, but the amounts are below the detection limit of the microscopy.

Contrary to the hypothesis that diffuse suberin might be deposited in the epidermal walls in *Arabidopsis*, we have shown that it is rather a lignin-like compound. The possibility of

lignin deposition in the root epidermis was implicit in previous papers, in which authors reported that a compound like the one deposited in the Casparian strips could also be deposited in the epidermal cell walls (Brundrett et al., 1988; Kramer et al., 2007). There were also indications of lignin deposition in the root epidermis *Arabidopsis*. It was reported that an analog of the lignin monomer coniferyl alcohol could be incorporated in the root epidermis. This observation suggested that the root epidermis possesses the machinery required for lignification (Pandey et al., 2015). Furthermore, lignin is deposited in the epidermal walls of the dicot species *Feijoa sellowiana* (Tuladhar et al., 2014). Finally, in a survey of 27 angiosperm species, 14 reportedly stained for lignin in the epidermis (Wilson & Peterson, 1983), showing that lignin can be deposited in the epidermal cell walls. Intriguingly, out of the 14 species, 12 of them were also stained for suberin, meaning that both polymers can be deposited together in the epidermis (**Figure 34**). Suberin and lignin also be found deposited together in endodermal cells (Geldner, 2013). These two polymers share more commonalities than the local of deposition, they also share the same ancestral polymer (Renault et al., 2019). Still, it is particularly intriguing that not all the species deposit both polymers in the epidermis, but this might be an artifact of the techniques previously used to detect each compound. For example, phloroglucinol staining was used to stain lignin, but in the case of *Arabidopsis*, it did not stain the epidermis (Naseer et al., 2012). Thus, it is plausible that all plant species deposit both lignin and suberin in the epidermal cell walls, in different ratios and, perhaps, different monomer arrangements, depending on their environment.

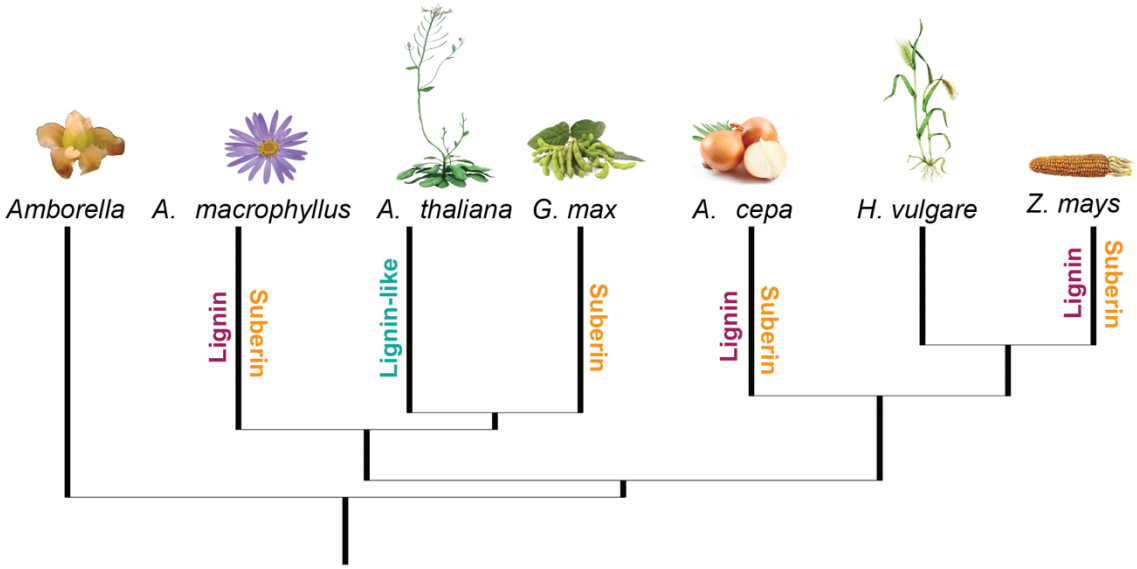

Figure 34. Phylogenetic tree depicting root epidermal cell wall modifications in monocots and dicots along evolution. Staining data was extracted from Thomas et al., 2007 and Wilson & Peterson, 1983. Tree generated on iTOL (https://itol.embl.de), with genomic data imported from National Center for Biotechnology Information (NCBI).

In our study, we did not detect any suberin or suberin-like compounds in the epidermal walls either via histochemical visualizations or loss-of-function mutants. However, this may be a consequence of the detection limit of the confocal microscope or TEM. Our results indicate that after PP synthesis inhibition, compounds remain in the epidermal cell walls, since the epidermal autofluorescence is not completely reduced, as shown previously (Naseer et al., 2012). However, it is unlikely that these compounds are suberin-like since the aromatic domain of suberin has also been removed by PA treatment, and the remaining fatty acids are not autofluorescent. Moreover, almost all autofluorescent compounds are derivatives of the PP pathway (Donaldson, 2020). Thus, it remains an open question what the remaining compounds could be.

Regarding the root epidermis expressed *GPATs* and *GELPs*, we still wonder which role they could play in this cell layer. In addition to the investigated *GELP22* and *GELP49*, more members of this gene family are expressed in the root epidermis: *MVP1* (*AT1G54030*), *AT2G19060*, *AT2G31540*, *AT3G27950*, *AT3G62280* and *AT5G55050* (**Figure 35**). The *GELP* gene family members possess multifunctional properties, meaning that they are not only

involved in polyester formation (Lai et al., 2017). A sextuple mutant of the genes before-mentioned might be useful to assess the role of GELPs in the root epidermis. Finally, the role of *GPAT2*, *GPAT3* and *GPAT7* in the root epidermis will be further discussed in Chapter 3.

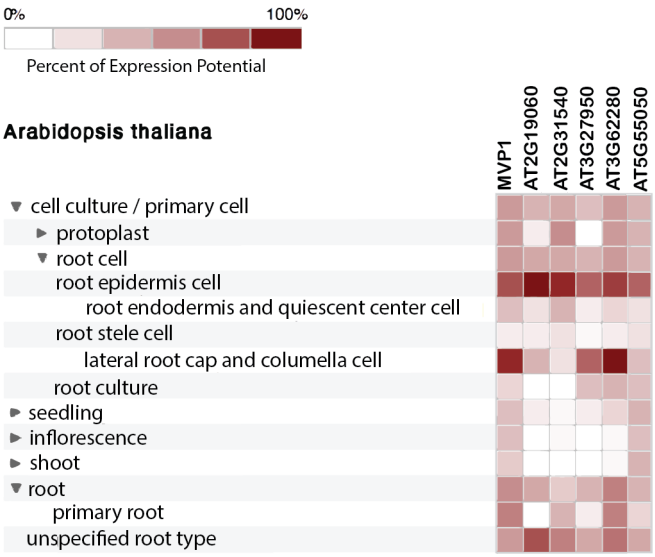

Figure 35. Expression data of root epidermis expressed GELP obtained from Genevestigator (Hruz et al., 2008).

3.2 Generation of a lignin mutant specific for the root epidermis

A challenge in this project was to elucidate the biological role of the atypical lignin due to the lack of epidermis-specific mutants, creating hurdles along the study. First, since the *Arabidopsis* root is fragile, it was not feasible to remove only the epidermis for chemical analysis. Second, this negatively affected finding the role of the atypical lignin deposited in the epidermis since, in all the mutants analyzed, lignification is altered in all root tissues. Below we will discuss and propose new strategies to find or generate a cell-specific loss-of-function mutant.

3.2.1 Unsuccessful inhibition of PP synthesis in the epidermis via *MYB4*

In this study, we attempted to generate an epidermis-specific lignin mutant via the expression of *MYB4* in the epidermis. The logic behind it was the previously reported PP inhibition in the endodermis driven by the promoters of the Casparian strip membrane protein

1 (CASP1) and endodermal lipid transfer protein (ELTP) (Andersen et al., 2021). However, inhibition of PP synthesis in the epidermis via MYB4 expression driven under the *GPAT2* and *GPAT3* promoters led to a root growth halt. Inhibition of PP synthesis via PA treatment does not disrupt root growth. Therefore the growth issues in the p*GPAT2*::XVE>>MYB4-GFP lines are unrelated to the PP pathway. This result builds evidence that MYB4 does not repress C4H exclusively.

3.2.2 Tissue-specific inhibition of lignin biosynthesis

To generate an epidermis-specific mutant for lignin biosynthesis, tissue-specific CRISPR could be used. Tissue-specific CRISPR (CRISPR-TSKO) is an inexpensive technique compatible with GoldenGate vectors. This method allows the combination of Cas9 with a promoter sequence of choice (Decaestecker et al., 2019). The challenge, however, is the lack of strong specific promoters active in the differentiated root epidermis. Therefore, trichoblast cells could be targeted using the promoters of the cell identity genes *COBRA-LIKE 9* (*COBL9*), *SHORT ROOT HAIR 1* (*SRH1*), and *PROLINE-RICH PROTEIN 3* (*PRP3*) could be used. And for the atrichoblasts, the promoter region of *GLABRA 2* (*GL2*) (Bruex et al., 2012). To ease the genotyping of the T1 generation, it would be optimal to target one or two genes involved in lignin formation. Thus, the best strategy would be to generate a double mutant of *RBOHD* and *RBOHF*. Another gene candidate could be *MED5b* (*ref4-3*), however, it might be difficult to control the single amino acid substitution on *MED5b* required to reduce the accumulation of PP metabolites (Stout et al., 2008).

3.2.3 Identification of key players involved in the formation of atypical lignin in the epidermis.

In this thesis, through a reverse genetics approach, we have described genes that play a role in the formation of epidermal atypical lignin. However, in all the mutants studied, root lignin formation is also affected in other tissues, such as the endodermis. Therefore, it would

be interesting to find unique and main players involved in forming the atypical lignin. Through the cell-type-specific transcriptomics data (Wendrich et al., 2020) we can extract possible candidates. Since there is more deposition of atypical lignin in the trichoblasts than in the atrichoblasts, we chose to analyze data from the former cell type. Among the genes highly expressed in trichoblast cells compared to all other cells in the root, we can find lignin-related genes (**Figure 36**). Reporter lines and mutants of the highlighted genes might lead to the discovery of key players in the formation of atypical lignin in the root epidermis. Among the potential key players are the NADPH-oxidases *RBOHG* and *RBOHI* are particularly interesting since members of this gene family are required to form the epidermal atypical lignin, and, the role of these two enzymes has not yet been investigated. Another interesting group of genes are the laccases and peroxidases. Although the role of *LAC8* and *LAC9* remains uncertain, laccases are also typically involved in lignin formation. The peroxidase gene family is multifunctional, and some members can also participate in root hair formation, thus, we have highlighted the enzymes that are also expressed in atrichoblasts. *PER21, PER27, PER45,* and *PER69* are class III peroxidases, which typically are involved in lignin formation. Finally, the Casparian strip membrane domain protein (CASP)-like proteins (CASPLs) *CASPL1D1* and *CASPL4D1* reportedly play a role in lignin deposition upon pathogen infection (Lee et al., 2019). CASPL genes are functionally redundant (Roppolo et al., 2014), therefore, it is worth generating the triple mutant *caspl1d1 caspl4d1 caspl4d2* and investigating the AO staining phenotype.

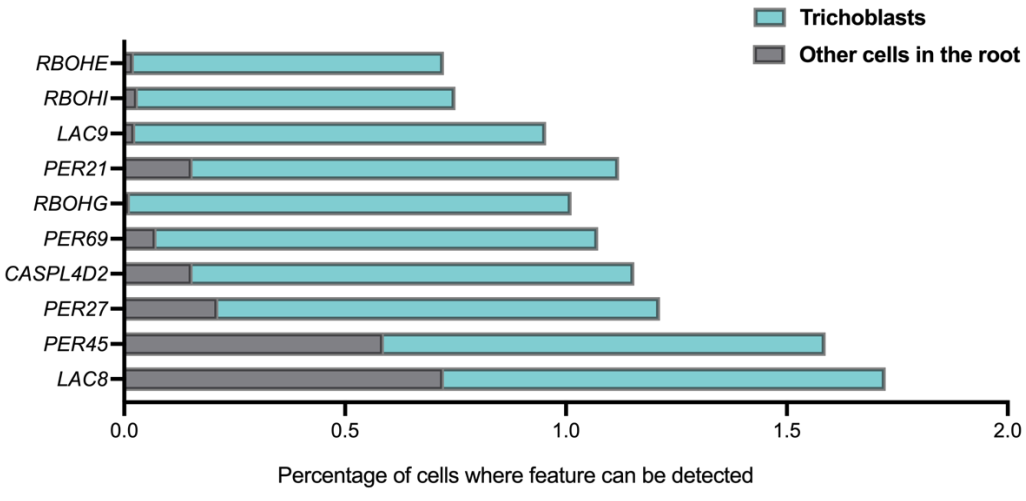

Figure 36. Transcriptomics data showing the epidermal preference of lignin-related genes (Wendrich et al., 2020).

3.3 Trichoblasts deposit more atypical lignin than atrichoblasts

In this study, we have reported a higher deposition of atypical lignin in trichoblasts than in atrichoblasts. Intriguingly, trichoblasts cells of *Zea mays* roots have a stronger autofluorescence than atrichoblasts (Marzec et al., 2013). The authors found no obvious difference in cell wall thickness that could explain the higher autofluorescence. Nonetheless, our results revealed a difference in thickness between the two cell types, with the trichoblasts being thicker. The main difference between these two types of cells is that the trichoblasts form root hairs. Hence, our first hypothesis was that the extra atypical lignin deposition could be linked to root hair support. We investigated root hair elongation and formation mutants to corroborate this theory, with no resulting AO staining phenotype. Nevertheless, when root hair formation is inhibited using a pharmacological approach, the intensity of the AO staining is reduced. The contrasting results could be because in the *rdh6* mutant, even though there are no root hairs in the area of interest, root hairs do initiate at a later point (Masucci & Schiefelbein, 1994). This means that trichoblasts are still present in the region evaluated, and thus, the extra atypical lignin. Whereas with the pharmacological approach, cell differentiation may be affected, altering the epidermal cell fate. Therefore, the role of the additional atypical deposition in trichoblasts should instead be investigated in a mutant where the epidermal cell identity is altered at the meristematic level and no trichoblasts are formed. A fitting mutant could be the *caprice x transparent testa glabra* (*cpc ttg*) double mutant (Long & Schiefelbein, 2020), which is devoid of trichoblasts.

The extra deposit of atypical lignin in trichoblasts may also be an evolutive consequence. *Arabidopsis* belongs to the Brassicaceae, a plant family that lost the ability to establish mycorrhizal symbiosis after the divergence of the Brassicales (Delaux et al., 2014). In the root of *Wollsia pungens*, a species colonized by mycorrhizal fungi, epidermal cell walls

are thicker (Briggs & Ashford, 2001). Further investigations should be made to elucidate the role of the extra atypical lignin deposition in trichoblasts.

3.4 The role of atypical lignin deposition in epidermal cell walls

3.4.1 Permeability of epidermal cells

Our results showed no difference in permeability to PI between younger and older zones of the root epidermis in 8-day-old seedlings. This challenges a previous observation, in which an increasing resistance along the root axis to the fluorescent dye Propidium Iodide (Naseer et al., unpublished data). Moreover, it has been reported that, in *Arabidopsis* roots, there is a difference in permeability to the fluorescent protein carboxyfluorescein between elongating and mature epidermal cells (Kramer et al., 2007). The differences in results could have been due to differences in method sensitivity, especially for the latter. Inhibition of atypical lignin formation did not lead to differences from the control. This was also seen in *S. lycopersicum* roots, in which PP inhibition via PA did not affect the levels of permeability of PI into cortical cells (Manzano et al., 2022). In any case, the likelihood of an apoplastic diffusion barrier in the root epidermis is questionable. The endodermis is a well-established barrier to the free diffusion of solutes from the soil into the stele (Geldner, 2013), and because of this, it could be redundant if the epidermis had the same function.

3.4.2 Abiotic and biotic stresses

Our results showed that neither abiotic stress nor peptide treatment enhanced atypical lignification in the epidermis. Nonetheless, since the epidermis is the first line of contact with microbes, it would be conceivable that these cell wall modifications protect the root against pathogen attack. This has been corroborated in *G. max*, in which diffuse suberin contributes to partial resistance to pathogen infection (Ranathunge et al., 2008; Thomas et al., 2007). Disruption of endodermal barriers also affects the levels of bacterial colonization. This could be seen in the roots of the *myb36 sgn3* mutant, in which the *Pseudomonas simiae* strain

WCS417 colonization is much higher than in wild-type roots (Verbon et al., 2022). Higher colonization of the *Pseudomonas protegens* strain CHA0 was also shown in the *rbohD rbohF* double mutant, which has defects in CS formation (Tsai et al., unpublished data). Since all the mutants analyzed in this study are also defective in CS formation, it was unfeasible to investigate if the atypical lignin deposited in the epidermis could act as a barrier against microbe colonization. Intriguingly, cell laser ablation of epidermal, cortical, and endodermal cells, followed by CHA0 treatment, leads only to colonization once the endodermal barrier is ablated (Tsai et al., unpublished data). Therefore, it is unclear whether the atypical lignin deposited in the outer epidermal cell wall plays a role against biotic stress. Further studies should be done with an epidermis-specific mutant and different types of microbes.

3.4.3 Mechanical properties

We have also explored the mechanical properties that the atypical lignin confers to root epidermal cells via osmotic treatments and bending assays, both with inconclusive or negative data. Regarding the osmotic treatment, further optimization is needed to decrease the sample variability. First, the seedlings must be put in a chamber and, the salt solution should be added directly to the chamber. In this way, the same cells will be followed, maximizing the accuracy of the experiment. Second, the concentration of salt used should be increased and optimized. The current concentration was ideal for the meristematic zone of 3-day-old seedlings. Since we are interested in the differentiated epidermal cells of 8-day-old seedlings, the concentration used was probably suboptimal. Third, the roots should be imaged longitudinally instead of transversally since the direction of cell growth is longitudinal (Liu et al., 2022).

The mechanical properties of epidermal cell walls, such as stiffness, could also be assessed via atomic force microscopy (AFM). In *Arabidopsis*, the properties of root meristematic and elongating epidermal cells have already been evaluated by AFM (Fernandes et al., 2012). However, there is a lack of data regarding the differentiated cells, thus, the output of this experiment would be handy.

4. Collaborators and contributions

In this study, I designed, performed, and analyzed all the experiments except for the TEM preparation of the samples and imaging, which Damien de Bellis executed. Prof. Mateusz Majda and Nicola Trozzi contributed to the bending experiments and analysis of images on MorphoGraphX.

Chapter III: Investigation of the GPATs expression in the root epidermis upon stress

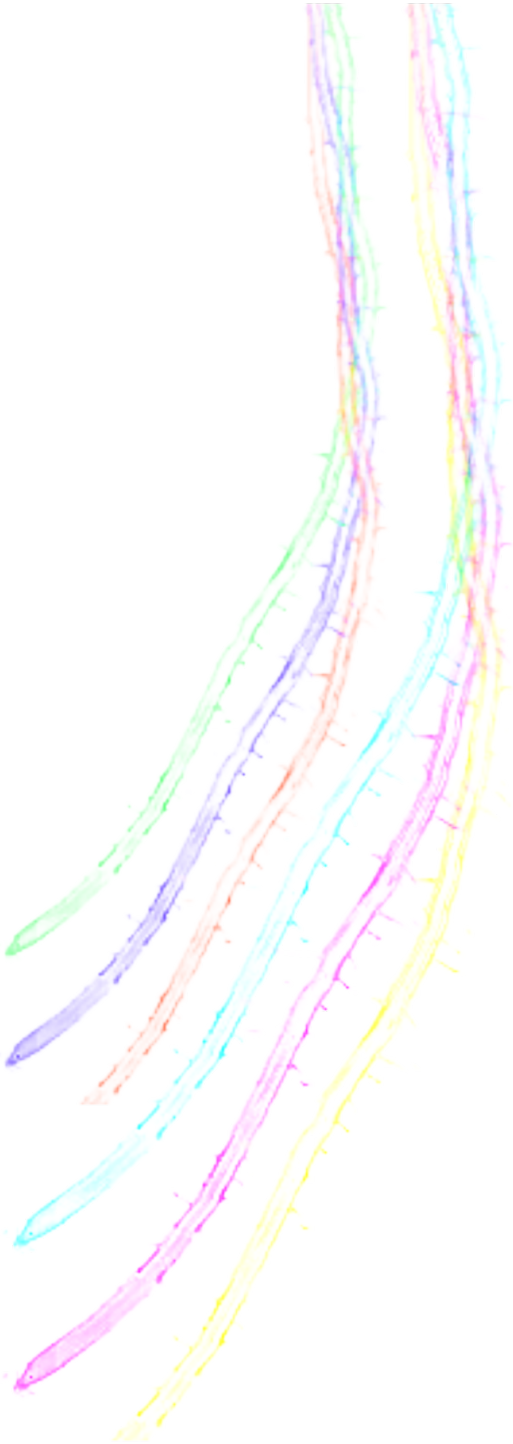

1. Goal and approach

According to our results from Chapter II, *GPAT2*, *GPAT3,* and *GPAT7* are likely not involved in forming the epidermal cell wall modification stainable with AO. Nevertheless, we aimed to characterize better the role they could play in the root epidermis. Phylogenetic relationships suggest that GPAT1 groups with GPAT2 and GPAT3 in *Arabidopsis* (**Figure 37**). This could indicate a similar role; thus, it was interesting to verify whether *GPAT1* is also expressed in the root epidermis.

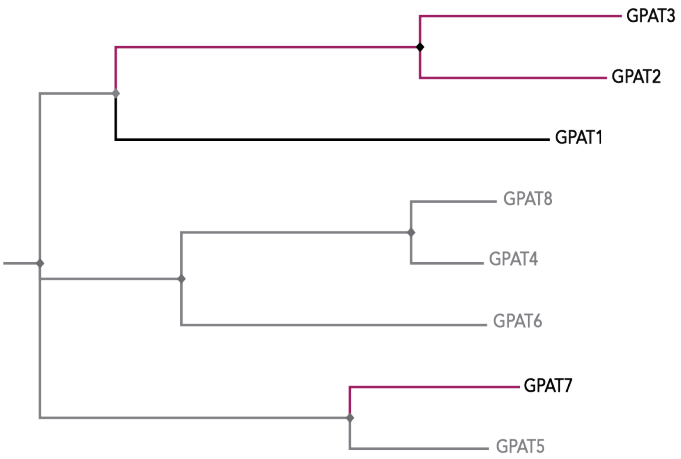

Figure 37. **Overview of the phylogenetic relationships between the land plant GPATs at the protein level**. Highlight on the root epidermal expressed GPATs (pink). The tree was constructed using the MegaAlign Pro tool of the DNAStar software, Clustal Omega.

Given the role of the epidermis as a barrier to environmental stresses, we sought to simulate a stress situation by using ABA. This plant hormone that plays a crucial role in mediating plant responses to adverse environmental stimuli (Swamy & Smith, 1999). Therefore, in this study, we aimed to understand whether the expression of *GPAT2*, *GPAT3,* and *GPAT7* in the root epidermis is enhanced upon ABA. And to test the hypothesis that *GPAT1* is also expressed in the root epidermis. To do so, we examined the spatiotemporal expression of the mentioned *GPATs* in response to ABA.

2. Results

2.1 Expression of *GPATs* is altered upon ABA treatment

The expression levels of *GPAT1, GPAT2, GPAT3,* and *GPAT7* were analyzed via RT-qPCR. *GPAT5* was used as a positive control since its expression in the endodermis is upregulated by ABA (Barberon et al., 2016). RT-qPCR data revealed that the expression of the four investigated *GPATs*, in entire roots of 8-day-old seedlings, was upregulated upon ABA treatment when compared to mock conditions. Strikingly, the expression levels of *GPAT2* had significantly increased four times compared to mock-treated roots (**Figure 38A**). It has been shown that *GPAT2* and *GPAT3* are strongly expressed in the root tip (Berhin, unpublished; Jia et al., 2022), which could influence our results, especially since we were only interested in the differentiated zone of the root. Therefore, the expression of the *GPATs* in roots without root tips was analyzed, better reflecting the differentiated zone. Again, the expression of all the *GPATs* evaluated was upregulated upon ABA treatment (**Figure 38B**).

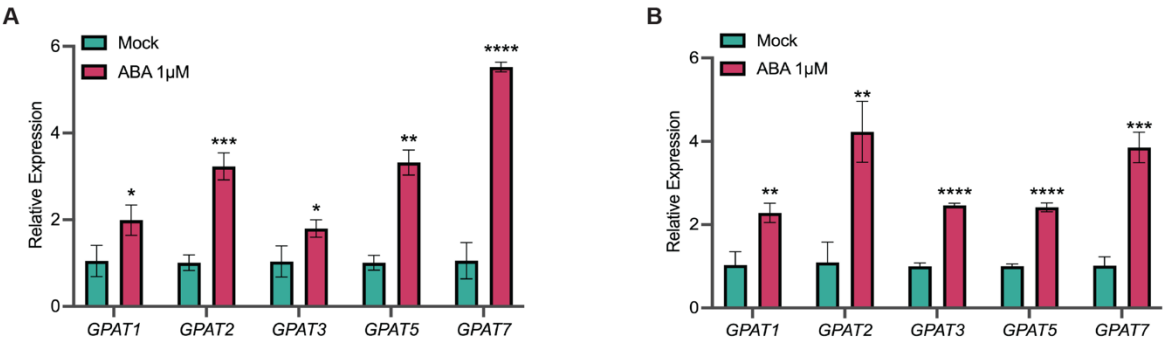

Figure 38. Expression levels of *GPATs* upon ABA treatment. Expression of GPATs was evaluated by RT-qPCR in wild-type seedlings. A) Full roots. B) Roots without the root tip. Six-day-old plants were transferred to a half-strength MS medium containing 1µM ABA or methanol (control) for 48h. The results are presented as the means of fold-changes relative to the respective control, with standard deviation, from three biological replicates. Significant differences were determined by Student's t-test. *, $p < 0.05$ and ***, $p < 0.001$.

To verify the spatial expression of *GPAT1*, *GPAT2*, *GPAT3,* and *GPAT7* upon ABA treatment, reporter lines of each gene were evaluated. In control conditions, in the differentiated zone of 8-day-old roots, *GPAT2* was expressed in the epidermis and cortex, *GPAT3* in the epidermis, cortex, and stele, and *GPAT7* in the epidermis, cortex, and endodermis, fitting to previous data (Berhin, unpublished) (**Figure 39A**). *GPAT1* was not

expressed in the epidermis but only in the stele. Upon ABA treatment, we evaluated the intensity of the GFP signal in the different reporter lines and generated a summary (**Figure 39B**). The expression of *GPAT1* in stele cells was increased upon ABA. Surprisingly, in the *GPAT2* reporter lines, the signal in the epidermis was almost invisible, whereas in the cortex was stronger. In the case of *GPAT3*, the intensity of the GFP signal in the epidermis was barely visible, but the expression in the cortex and stele remained unchanged. Finally, when in the *GPAT7* reporter line, the intensity of the signal in the epidermis also lowered, and the expression in the endodermis was induced.

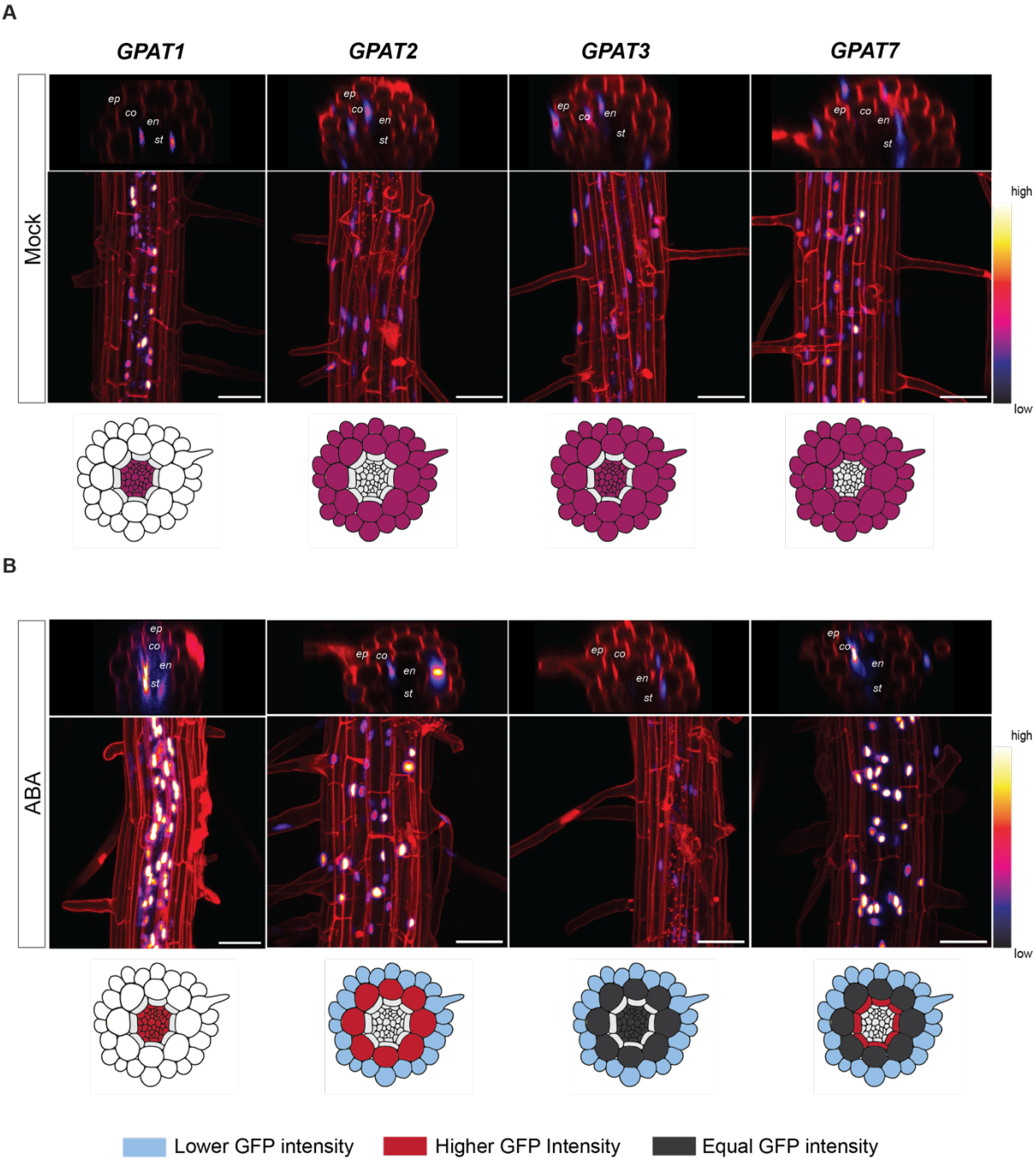

Figure 39. Expression pattern of GPATs upon ABA treatment. *GPATxpro: NLS-GFP-GUS* reporter expression in transgenic 8-day-old *Arabidopsis* seedlings. Six-day-old plants were transferred on a half-strength MS medium containing 1µM ABA or methanol (control) for 48h. Maximum projections of the differentiated zone are shown in the upper panels, accompanied by schematic diagrams of cross-section views in the bottom panels. The GFP signal is represented in purple to white, reflecting the intensity of the signal. Cell walls were highlighted using PI. Ep, epidermis; co, cortex; en, endodermis; st, stele. Scale bars: 50µm.

2.2 The *gpat2* mutant does not show changes in suberization upon ABA treatment

In response to stress conditions, such as ABA stress, tissues that typically do not suberize, such as the cortex, become suberized (Barberon et al., 2016). Since *GPAT2* expression was induced upon ABA stress in the cortex, we were interested in investigating whether *GPAT2* is involved in suberization after ABA treatment. For this purpose, we evaluated the FY staining in 8-day-old roots (**Figure 40**). For the *gpat2* mutant, we analyzed two T-DNA insertion lines: SALK_118230 and SALK_051152. We found no differences in the degree of suberization upon ABA between wild-type and *gpat2* mutant roots. Nevertheless, this experiment should be repeated with a *gpat2 gpat5* double mutant. This will be further discussed.

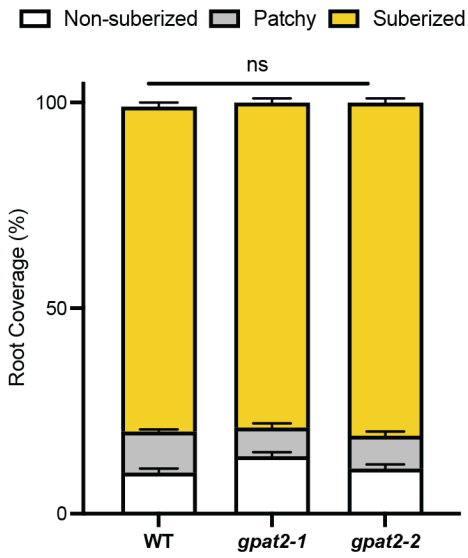

Figure 40. Suberization is not affected in the *gpat2* mutant upon ABA treatment. Six-day-old plants were transferred to a half-strength MS medium containing 1µM ABA or methanol (control) for 48 hours. Fluorol Yellow (FY) staining was performed to detect suberin in the wild type (WT) and *gpat2* T-DNA insertion lines.

3. Discussion and perspectives

In this study, we have further analyzed the expression patterns of *GPAT2, GPAT3,* and *GPAT7* upon ABA treatment in an attempt to elucidate their role in the root epidermis. We

have found that the expression of this set of *GPAT* genes can be enhanced by ABA, although not in the epidermal cells. The suppression of the expression in the epidermis in the reporter lines of *GPAT2*, *GPAT3* and *GPAT7* is questionable. The inconsistencies between the results of the transcriptional lines and the RT-qPCR data lead us to question whether this set of genes indeed is expressed in the differentiated root epidermis. In the p*GPAT2*: *MYB4* and p*GPAT3*: *MYB4* fusions, almost no GFP signal was detected in the differentiated epidermis. Still we could observe a strong expression in the meristematic epidermis (**Figure 24A-B**). Indeed, in young seedlings, the *gpat2* mutant shows defects in the root cap cuticle formation (Berhin, unpublished). Moreover, it has been shown recently that the lysophosphatidic acid, produced by *GPAT1* and *GPAT2*, regulates auxin-dependent embryonic and post-embryonic development. The *gpat1 gpat2* displays stunted root growth, shorter meristem, and abnormal cell development (Jia et al., 2022). Therefore, the expression of *GPAT3* in the meristematic root epidermis might also be linked to the regulation of auxin signaling.

Our data also highlights the importance of adequately assessing the spatial patterns of gene expression. Transcriptional lines, such as the reporter lines, show where the DNA is at the start of transcription. Hence, if RNA processing occurs quickly, there will be a difference between the levels and local of expression between the start and end of transcription (Wilusz et al., 2001). To overcome this hurdle, translational fusions of *GPAT2, GPAT3* and *GPAT7* should be generated and, the expression pattern in the root epidermis upon ABA should be assessed.

Although *GPAT2* might not have any role in the differentiated root epidermis, it may be involved in ABA-regulated processes, such as suberization. Despite the *gpat2* mutant did not show any delay in suberization, the induction of *GPAT2* in the cortex upon ABA treatment suggests involvement in suberin formation. In the root cap cuticle, *GPAT2* is involved in forming very long-chain fatty acids (Berhin, 2019). When the endodermal suberization was analyzed, *gpat2* single mutants showed no delay (**Figure 40**). The lack of phenotype could be due to gene redundancy, characteristic of the GPAT family. A way to circumvent this hurdle is to generate the higher order mutant *gpat2 gpat5 gpat7*. *GPAT5* is a well-characterized gene

involved in suberin formation in the endodermis (Beisson et al., 2007), and, recently, it has been shown that *GPAT7* shares the same function (Gully et al., unpublished).

Once the *gpat2 gpat5 gpat7* mutant is obtained, GC-MS should be carried out in comparison to the *gpat5 gpat7* mutant to determine if the level of suberin monomers has decreased and precisely which ones. Moreover, FY staining of the mutant roots upon ABA treatment should be done. The effects expected are mainly in the cortex cells due to the *GPAT2* expression pattern. Finally, endodermal cells would have to be analyzed with TEM after ABA treatment to evaluate the state of the suberin lamellae. When observing with TEM, suberin lamellae in the cortex are not obvious (Gully et al., unpublished), hence, differences are not necessarily expected.

Finally, *GPAT1* was not expressed in the root epidermis and only in stele cells. This expression pattern is similar to *GPAT3*, which is also expressed in the stele. In *Arabidopsis* seeds, *GPAT1* is reportedly involved in glycerolipid metabolism (Bai et al., 2021). Moreover, it also plays an important role in pollen grain development (Zheng et al., 2003). Generation of the mutant *gpat1 gpat3* would be necessary to investigate the role of these *GPATs* in the stele and to gain more insights into the function of *GPAT1* and *GPAT3* in polyester formation.

4. Collaborators and contributions

In this study, I designed, performed, and analyzed all the experiments.

General conclusions

Cell wall modifications of the root endodermis and vasculature have been studied thoroughly. Epidermal cell walls, however, have rarely been the focus of research and the most recent studies date to 15 years ago (Kramer et al., 2007; Ranathunge et al., 2008; Thomas et al., 2007). In addition, in the model plant *Arabidopsis thaliana,* there were no studies regarding the composition of the epidermal cell walls, and the only data available was the autofluorescence of the outer epidermal cell walls and a possible role as a permeability barrier (Franke et al., 2005; Kramer et al., 2007). In Chapter II, we have shown via histological stains, and genetic and pharmacological manipulations that the outer epidermal cell walls in *Arabidopsis* are modified with an atypical lignin (**Figure 41**). This modification is present in differentiated root epidermal cells from early development stages. We have also shown that the deposition of atypical lignin is higher in trichoblasts than atrichoblasts. Our results open a new chapter in the study of epidermal cell wall modifications in plants. However, many questions remain open, including: what is the role of atypical lignin deposition in epidermal walls? What is the precise composition of the atypical lignin? What is the role of the extra atypical lignin deposition in root hair cells?

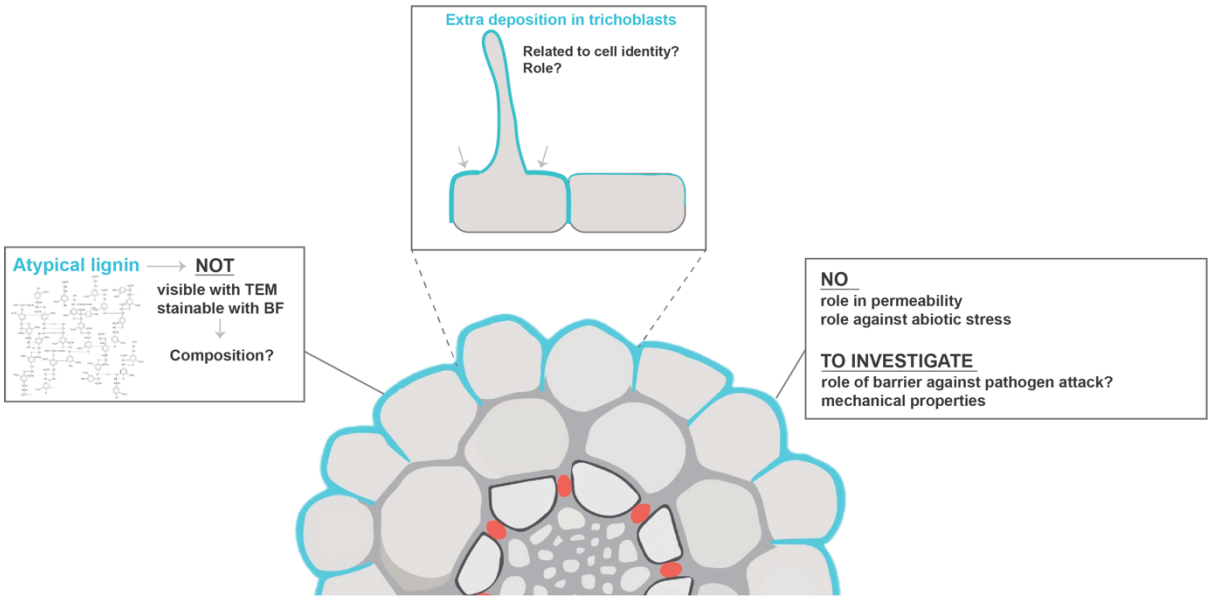

Figure 41. Summary model of the cell wall modification in root epidermal cell walls of *Arabidopsis*.

In Chapter III, we further explored the role of *GPAT2, GPAT3,* and *GPAT7* in the root epidermis, along with *GPAT1.* From expression data, the investigated *GPATs* may play essential roles in the defense against abiotic stress. However, contrasting data calls for the generation of translational reporter lines to better characterize the expression in the root epidermis for *GPAT2* and *GPAT3.* Moreover, the induction of the expression of *GPAT2* in the cortex upon ABA suggests a possible role of the latter in suberization. The development of high-order mutants might help to answer this question. Finally, the role of *GPAT1* in the stele should be further investigated.

In conclusion, our results pave the way for a better understanding of the cell wall modifications of the root epidermis of *Arabidopsis thaliana*. We provide evidence that the root epidermal cell wall may be more complex than previously appreciated. Further experiments should be performed to investigate the root epidermal outer cell wall in depth.

Material and methods

1. Growth conditions

For most experiments, plants were grown under sterile conditions. Seeds were surface-sterilized with chlorine gas. After 2 days of vernalization at 4°C, plants were grown on plates with $^1/_2$ MS (Murashige and Skoog, 500 mg/l MES, pH 5.8), 0.9% agar at 22°C, under continuous light (100 mmol m^{-2} s^{-1}). Plates were grown vertically. For transformation and seed propagation, plants were grown on soil under continuous light (100 mmol m^{-2} s^{-1}) at 20°C and 65% humidity.

2. Plant material

For all experiments, *Arabidopsis thaliana* (accession Col-0) was used. The following mutants were obtained from NASC: *gpat2-1* (SALK_118230) (Yang et al., 2012), *gpat2-2* (SALK_051152), *gpat7-3* (Yang et al., 2012), *ttg2* (SALK_148838), *gl1 rhd2* (Schiefelbein & Somerville, 1990)*, and ref4-3* (Bonawitz et al, 2012)*.* The following mutants were kindly provided by Niko Geldner (University of Lausanne): *rbohC* (SALK_018814), *rbohD* dSpm*, rbohF* dSpm and the respective cross *rbohD* dSpm *rbohF* dSpm*, rbohABFE, cad4 cad5 f5h1 f5h2 ccr1*, *myb36-2 sng3-3*, *5x-per*, *ahp6*, and *cif1 cif2*. *tt4* seeds were provided by Luis Lopez Molina (University of Geneva), and the *rhd6* mutant was kindly provided by Aurélien Bailly (University of Zurich).

The p*ASFT*: NLS-GFP-GUS transcriptional reporter line has been previously described (Naseer et al., 2012). The p*GPAT2/3/7*: NLS-GFP-GUS reporter lines were previously generated (Berhin, unpublished). The *gpat2-1 gpat7-3* double mutant was generated by crossing the respective single mutants. Gene numbers are described in Table S1. CS mutants were phenotyped by PI penetration assays or CIF2 treatment (Fujita et al., 2020).

3. Generation of transgenic lines

3.1 *GPAT3* knock-out

Three guide RNAs (sgRNAs) were used to target the first exon of *GPAT3*, aiming for deletions of 502bp and 607bp. Guides targeting either the beginning or end of the first exon of *GPAT3* were designed using the online platform Benchling (https://www.benchling.com) (**Figure 42**). Six primers were used for annealing the three guide RNAs; detailed information is available in Table S2. The plasmids were generated as previously described (Ursache et al., 2021b).

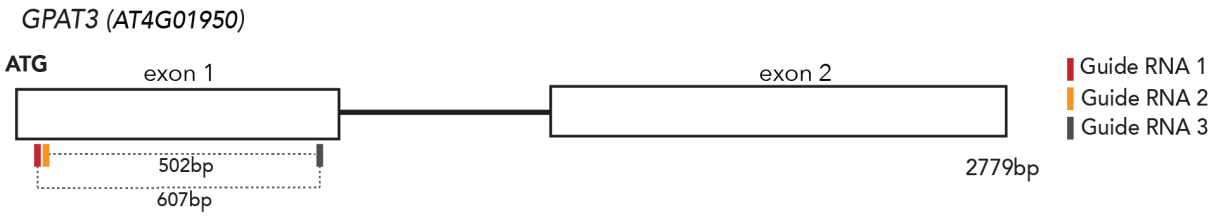

Figure 42. Schematic representation of CRISPR guide RNAs positioning to generate mutations in the *GPAT3* gene.

The protospacer to customize the sgRNA was cloned by annealing oligos and then ligated into *the Bbs*I linearized Gateway-Entry plasmid. For gene targeting, the three sgRNAs were cloned into an intermediate vector using Golden Gate assembly. Finally, the sgRNAs cassette was cloned into an expression vector containing Cas9, ubiquitin promoter, and fluorescent screenable marker FASTRed, which helps select the plasmid-containing seeds. The construct was transformed in *Agrobacterium tumefaciens* and then in Arabidopsis thaliana accession Col-0*, gpat2,* and *gpat2 gpat7* mutants using the floral dip method (Clough & Bent, 1998). T1 plants were selected based on their red fluorescence. T2 plants were selected based on their lack of Cas9 enzyme and screened by their lack of red fluorescence. Red seed selection was performed under the stereomicroscope Leica 6000 equipped with a DSR filter. To select CRISPR positive plants, primers were designed (Table S2) to amplify the region with

200bp upstream and downstream of the first and last guide RNAs, respectively. Genotyping was also done by sequencing the sgRNAs region using primers described in Table S2.

3.2 p*GPAT1* reporter line

To generate p*ENTRY* L4-p*GPAT1*-R1, a 2kb fragment upstream of GPAT1 was amplified and cloned into pDONR P4-P1 using *Kpn*I and *Xba*I as restriction enzymes. The promoter entry was recombined into the p*MMA-red* vector (Amjad Ali et al., 2012), together with a pDONR221 vector containing NLS-GFP-GUS. This was done via Gateway Technology (Lifesciences). Plants were transformed using the floral dip method (Clough & Bent, 1998). Red seeds were selected under the stereomicroscope Leica 6000 equipped with a DSR filter. Primers are available in Table S2. CRISPR and cloning

3.3 p*GPAT*: *MYB4* construct

To repress the phenylpropanoid in the root epidermis, a construct fusing the promoters of *GPAT2* or *GPAT3* to *MYB4-GFP* was generated. The *MYB4-GFP* clone has been previously generated (Andersen et al., 2021). The promoter entry clones had also been developed previously (Berhin, unpublished). These entry clones were recombined using LR-Clonase II (Invitrogen) into a destination vector containing a marker for FastRed seed selection.

4. Microscopy, histology, and quantitative analysis

Most fluorescence microscopy studies were performed using the confocal laser-scanning microscope ZEISS LSM 880 Airyscan. For Auramine O (AO, Sigma-Aldrich), Basic Fuchsin (BF, Sigma-Aldrich), and Safranine O (SF, Merck), sample clearing was performed with ClearSee, following a previously described methodology (Ursache et al., 2018). Roots were stained overnight with AO 0.5%, BF 0.2%, and SF 0.5%. AO, SF, and autofluorescence were visualized with an excitation at 488 nm and detection with BP 490-555 nm. The same parameters were also used for GFP and FY. For the BF, the signal was excited at 561 nm and

detected at 600–650 nm. Calcofluor white was excited at 405 nm and detected at 425-475 nm. Finally, for Propidium Iodide (PI), the excitation and detection wavelengths were 514 nm and the detection–610-620 nm. For fluorescence intensity quantification, the onset of elongation was defined as the point at which an epidermal cell in a median optical section was more than twice its width. Unless mentioned, the zone analyzed was +20. Permeability assays were performed using a Leica Stellaris 5 confocal microscope. Red seed selection was conducted under the stereomicroscope Leica 6000 equipped with a DSR filter.

4.1 Fluorol Yellow

For quantification of suberin deposition, 8-day-old roots were stained with Fluorol Yellow (FY, Santa Cruz Biotechnology). Seedlings were incubated in methanol at room temperature for at least 3 days, stained with FY (0.01%, in methanol) for 1 h at room temperature, rinsed in methanol, counterstained with aniline blue (0.5%, in methanol) at room temperature for 1 h in darkness, and washed. The samples were mounted in water for microscopic observation.

4.2 Autofluorescence

Autofluorescence visualization was performed as previously described (Naseer et al., 2012). 8-day-old seedlings were incubated in 0.24N HCl (in 20% methanol) at 57°C for 15 min. The solution was then replaced with 7% NaOH in 60% ethanol and incubated at room temperature for 15 min. Afterward, the seedlings were hydrated in subsequent baths for 5 min in 40%, 20%, and 10% ethanol. The seedlings were then transferred to 5% ethanol and 25% glycerol for 15 min. Finally, the samples were mounted in 50% glycerol for further analysis under the microscope.

4.3 Casparian strip functionality assay

Seedlings were incubated in the dark for 10 min in a fresh solution of PI (10mg/ml) and rinsed two times in water (Naseer et al., 2012). For quantification, the onset of elongation was

defined as the point where an endodermal was more than two times its length. From this point, cells in the file were counted until the PI signal was blocked in the stele.

5. Phenylpropanoid metabolites supply

The plants were grown vertically for 5 days on control conditions (½ MS, 0.9% agar) in a growth chamber under long-day conditions. Seedlings were then transferred for 3 more days on the same condition supplemented or not with the lignin inhibitor 10µM PA (Sigma-Aldrich), 10µM PA with 20µM *p*-coumaryl alcohol (Sigma-Aldrich), 10µM PA with 20µM coniferyl alcohol (Sigma-Aldrich), 10µM PA with 20µM sinapyl alcohol (Sigma-Aldrich), 10µM PA with 20µM p-coumaryl alcohol (Sigma-Aldrich) and coniferyl alcohol or 10µM PA with 20µM ferulic acid (Sigma-Aldrich). PA treatment needs to occur in the dark to inhibit PP synthesis properly. Hence the plates were covered in aluminum foil, and only the cotyledons were in contact with the light. Stock solutions of PA and monolignols were made in DMSO.

6. Inhibitor assays

Inhibition of lignin polymerization was done as previously described (Lee et al., 2013).For treatment with potassium iodide (Merck) and salicylhydroxamic acid (SHAM) (Sigma), 5-day-old seedlings were transferred to plates containing 5mM KI or 100µM SHAM and incubated for 72 h in the dark. For the DPI (NADPH oxidase inhibitor) and DDC (superoxide dismutase inhibitor) treatments, 5-day-old seedlings were preincubated in plates containing 10µM PA for 72 h in the dark and transferred to 1/2 MS solution including 5µM DPI or 250µM DDC together with 20µM of each coniferyl alcohol for 6h. Root hairs of 7-day-old seedlings were inhibited with 20µM of l-(2-aminoethoxyvinyl) glycine hydrochloride (AVG) (Sigma-Aldrich) for 24h.

7. Permeability assays

For apoplastic tracer assays with PI, wild-type seeds were grown under control conditions. Five days after sowing, seedlings were transferred to plates containing 10 µM PA for 72h in

the dark. To stain the cell walls, 8-day-old roots were incubated with 10µg/mL PI in the dark for 10 min. Afterward, roots were washed with water for 30 s and immediately observed with confocal microscopy, as described in section 4. Optical cross-sections of the roots were taken, and the intensity of the PI signal in the cortex radial cells was measured using Fiji. Calcofluor white staining and observation were performed on 8-day-old seedlings, following the methodology described in section 4. Optical cross-sections of the roots were taken, and the intensity of the calcofluor white signal in the epidermal, cortical, and endodermal outer cell walls was measured using Fiji.

8. Peptide treatments

The peptides AtPep1, flg22, chitin and CIF2 were kindly provided by Niko Geldner, and Kay Gully provided SCOOP1. For the peptide treatments, stock solutions were made in water and, the chemicals were diluted in ½ MS medium to the indicated concentration (1µM AtPep1, 1µM flg22, 1µM chitin, 100nM SCOOP12 and 1µM CIF2). Seedlings were grown for 7 days in control conditions and transferred for 24h to media containing the respective peptide. Roots were fixed and stained with Auramine O, following the methods described in section 4.

9. Abiotic stresses

For ABA treatments, 6-day-old seedlings were transferred and incubated for 48 in ½ MS medium supplemented with 1µM ABA or methanol (control). For salt experiments, 5-day-old seedlings were transferred and incubated for 72h in ½ MS medium supplemented with 100mM NaCl. For mannitol experiments, 5-day-old seedlings were transferred and incubated for 72h in ½ MS medium containing 150mM or 300mM of mannitol.

10. Mechanical analyses

For the osmotic shock with salt, 8-day-old seedlings were grown in control conditions, except for the PA-treated roots. Subsequently, roots were incubated for 10 min in10µg/mL PI

in the dark. The roots were mounted in water. Optical cross-sections of the roots were imaged with confocal microscopy, as described in section 4. Once imaging was done (ca. 5 min later), the water solution in the slide was removed with a paper towel and, a 0.4% NaCl solution was added. The incubation time was 20 min. Then, optical cross-sections of the roots, in similar regions were taken. The resulting images were pre-processed by applying filters, such as Gaussian smoothing and background subtraction, to enhance the image quality and reduce noise. Next, the edges of the sample were detected, and a mesh was created out of them. Pictures were next subdivided to obtain a cube size of 2 μm. For cell segmentation, MorphoGraphX offers an automatic segmentation feature. The software managed to label the cells accordingly. After automatic segmentation, results were reviewed and, manual adjudgments were done, if necessary. Subsequently, to image segmentation, the contours of each cell were generated, and the cell area data was extracted for further plotting and analysis.

For the bending assays, seedlings were grown vertically in control conditions, except for the PA-treated roots. When the seedlings reached 8-days-old, the plates were turned 90° to the left and imaging was automatized to take pictures every 30min. Photos were taken with an Arducam 12MP IMX477 Pan Tilt Zoom (PTZ) camera connected to a Raspberry Pi 3B. Imaging took place in semi-dark conditions. The output images were analyzed using the imaging software Fiji. Images were overlapped on each other to measure the bending angle and newly grown root length. The bending angle was analyzed by measuring the angle of the bent root using the angle tool in Fiji.

11. Electron Microscopy

8-day-old *Arabidopsis* seedlings were fixed in 2.5% glutaraldehyde solution (Electron Microscopy Services) in 0.1 M phosphate buffer pH 7.4 for 1 h at room temperature and post-fixed in a fresh mixture of osmium tetroxide 1% (Electron Microscopy Services) with 1.5% potassium ferrocyanide (Sigma) in phosphate buffer for 1 h at room temperature. The samples were then washed twice in distilled water and dehydrated in acetone solution (Sigma) at

graded concentrations (30%, 40 min; 50%, 40 min; 70%, 40 min; and 100%, 2 × 1 h). This was followed by infiltration in LR White resin (Electron Microscopy Science) at graded concentrations (LR White 33% in ethanol, 4 h; LR White 66% in ethanol, 4 h; LR White 100%, 2 × 8 h) and finally polymerized for 48 h at 60 °C in an oven under nitrogen atmosphere. 50-nm-thick sections were cut transversally 2 mm below the root tip, using a Leica UC7 (Leica Mikrosysteme), picked up on a copper slot grid 2 × 1 mm (Electron Microscopy Science) coated with a polystyrene film (Sigma).

Visualization of lignin deposition in the epidermal cell wall was done using permanganate potassium ($KMnO_4$) staining (Hepler et al., 1970). Ultrathin sections were post-stained using 1% $KMnO_4$ in H_2O (Sigma, St Louis, MO, US) for 45 min and rinsed several times with H_2O. Micrographs were taken with a transmission electron microscope FEI CM100 (FEI, Eindhoven, The Netherlands) at an acceleration voltage of 80kV and ×6.500 magnifications (pixel size of 3.136 nm), with a TVIPS TemCamF416 digital camera (TVIPS GmbH, Gauting, Germany) using the software EM-MENU 4.0 (TVIPS GmbH, Gauting, Germany). Panoramic images were aligned with the software IMOD (Kremer et al., 1996).

12. Expression analyses

qRT-PCR was used to analyze the expression levels upon ABA treatment. Wild-type 6-day-old seedlings grown under control conditions were transferred to plates containing 1µM ABA for 48 h. Subsequently, the roots were excised from the seedlings immediately below the hypocotyl. When necessary, the root tip was removed for analysis. Total RNA was extracted using the ReliaPrep™ RNA Tissue Miniprep System (Promega) following the manufacturer's instructions. cDNA was synthesized based on 1µg of RNA with M-MLV Reverse Transcriptase, RNase H Minus, Point Mutant (Promega). *GPAT* genes were amplified using adequate primers and the SYBR® Select Master Mix in the QuantStudioTM 3 Real-Time PCR System (Applied Biosystems). The level of expression was established by the $2^{-\Delta\Delta Ct}$ method (Schmittgen & Livak, 2008), where ΔΔCt is the difference between the raw threshold cycle

(Ct) obtained by the primers specific to the reference gene to that of the studied gene. Details of the primer sequences are available in Table S3. QuantStudioTM Software V1.3 was used for data acquisition. *The SAND* gene was used as a reference gene.

To study the expression pattern at the tissue level, GFP-fused reporter lines of the GPAT genes were stained with PI (10 µg/ml) for 10 min and visualized with confocal microscopy. Further details can be found in Section 4.

13. Statistical analyses

To quantify the staining or autofluorescence intensity, confocal images were analyzed using the Fiji package (v.2.1.0/1.54b (build:5f23140693; http://fiji.sc/Fiji) (47). The confocal microscopy settings were identical for all images of the same stain. To determine the fluorescence intensity of the outer cell wall of the root epidermis, a line was drawn along the epidermis, and the resulting mean intensity value was plotted. Two-way ANOVA with Tukey HSD and Student's t-test was used as a multiple-comparison procedure. Details of the statistical approaches used can be found in the figure legends. All statistical analyses were performed using GraphPad Prism software v.9.0.0 (https://www.graphpad.com/). Each experiment was repeated 2 to 4 times.

References

Alejandro, S., Lee, Y., Tohge, T., Sudre, D., Osorio, S., Park, J., Bovet, L., Lee, Y., Geldner, N., Fernie, A. R., & Martinoia, E. (2012). AtABCG29 is a Monolignol Transporter Involved in Lignin Biosynthesis. *Current Biology*, *22*(13), 1207–1212.

Amjad Ali, M., Hussain Shah, K., & Bohlmann, H. (2012). pMAA-Red: A New pPZP-Derived Vector for Fast Visual Screening of Transgenic Arabidopsis Plants at the Seed Stage. *BMC Biotechnology*, *12*(37). doi: 10.1186/1472-6750-12-37.

Andersen, T. G., Barberon, M., & Geldner, N. (2015). Suberization - The Second Life of an Endodermal Cell. *Current Opinion in Plant Biology*, *28*, 9–15.

Andersen, T. G., Molina, D., Kilian, J., Franke, R. B., Ragni, L., & Geldner, N. (2021). Tissue-Autonomous Phenylpropanoid Production Is Essential for Establishment of Root Barriers. *Current Biology*, *31*(5), 965-977.

Ayaz, A., Saqib, S., Huang, H., Zaman, W., Lü, S., & Zhao, H. (2021). Genome-Wide Comparative Analysis of Long-Chain Acyl-CoA Synthetases (LACSs) Gene Family: A Focus on Identification, Evolution and Expression Profiling Related to Lipid Synthesis. *Plant Physiology and Biochemistry*, *161*, 1–11.

Bai, Y., Shen, Y., Zhang, Z., Jia, Q., Xu, M., Zhang, T., Fang, H., Yu, X., Li, L., Liu, D., Qi, X., Chen, Z., Wu, S., Zhang, Q., & Liang, C. (2021). A GPAT1 Mutation in Arabidopsis Enhances Plant Height but Impairs Seed Oil Biosynthesis. *International Journal of Molecular Sciences, 22*(785).

Balcerowicz, D., Schoenaers, S., & Vissenberg, K. (2015). Cell Fate Determination and the Switch from Diffuse Growth to Planar Polarity in Arabidopsis Root Epidermal Cells. *Frontiers in Plant Science*, *6*. doi: 10.3389/fpls.2015.01163.

Baldacci-Cresp, F., Spriet, C., Twyffels, L., Blervacq, A. S., Neutelings, G., Baucher, M., & Hawkins, S. (2020). A Rapid and Quantitative Safranin-Based Fluorescent Microscopy Method to Evaluate Cell Wall Lignification. *The Plant Journal*, *102*(5), 1074–1089.

Barberon, M., & Geldner, N. (2014). Radial Transport of Nutrients: The Plant Root as a Polarized EEpithelium. *Plant Physiology*, *166*(2), 528–537.

Barberon, M., Vermeer, J. E. M., De Bellis, D., Wang, P., Naseer, S., Andersen, T. G., Humbel, B. M., Nawrath, C., Takano, J., Salt, D. E., & Geldner, N. (2016). Adaptation of Root Function by Nutrient-Induced Plasticity of Endodermal Differentiation. *Cell*, *164*(3), 447–459.

Barros, J., Serk, H., Granlund, I., & Pesquet, E. (2015). The Cell Biology of Lignification in Higher Plants. *Annals of Botany,* 115(7), 1053-1074.

Beisson, F., Li, Y., Bonaventura, G., Pollard, M., & Ohlrogge, J. B. (2007). The Acyltransferase GPAT5 is Required for the Synthesis of Suberin in Seed Coat and Root of Arabidopsis. *Plant Cell*, *19*(1), 351–368.

Beisson, F., Li-Beisson, Y., & Pollard, M. (2012). Solving the Puzzles of Cutin and Suberin Polymer Biosynthesis. *Current Opinion in Plant Biology, 15*(3), 329-337.

Berhin, A. (2019). *Characterization of atypical polyester depositions at the root of Arabidopsis thaliana* [Doctoral thesis, Université de Lausanne].

Berhin, A., de Bellis, D., Franke, R. B., Buono, R. A., Nowack, M. K., & Nawrath, C. (2019). The Root Cap Cuticle: A Cell Wall Structure for Seedling Establishment and Lateral Root Formation. *Cell*, *176*(6), 1367-1378.

Bernards, M. A. (2002). Demystifying Suberin. *Canadian Journal of Botany*, *80*(3), 227–240.

Boerjan, W., Ralph, J., & Baucher, M. (2003). Lignin Biosynthesis. *Annual Review of Plant Biology*, *54*, 519–546.

Bond, J., Donaldson, L., Hill, S., & Hitchcock, K. (2008). Safranine Fluorescent Staining of Wood Cell Walls. *Biotechnic and Histochemistry*, *83*(3–4), 161–171.

Briggs, C. L., & Ashford, A. E. (2001). Structure and Composition of the Thick Wall in Hair Root Epidermal Cells of *Woollsia pungens*. *New Phytologist*, *149*(2), 219–232.

Bruex, A., Kainkaryam, R. M., Wieckowski, Y., Kang, Y. H., Bernhardt, C., Xia, Y., Zheng, X., Wang, J. Y., Lee, M. M., Benfey, P., Woolf, P. J., & Schiefelbein, J. (2012). A Gene Regulatory Network for Root Epidermis Cell Differentiation in Arabidopsis. *PLoS Genetics*, *8*(1). doi: 10.1371/journal.pgen.1002446.

Brundrett, M. C., Enstone, D. E., & Peterson, C. A. (1988). A Berberine-Aniline Blue Fluorescent Staining Procedure for Suberin, Lignin, and Callose in Plant Tissue. *Protoplasma,* 146, 133–142.

Buer, C. S., Imin, N., & Djordjevic, M. A. (2010). Flavonoids: New Roles for Old Molecules. *Journal of Integrative Plant Biology*, *52*(1), 98–111.

Buer, C. S., & Muday, G. K. (2004). The transparent testa4 Mutation Prevents Flavonoid Synthesis and Alters Auxin Transport and the Response of Arabidopsis Roots to Gravity and Light. *Plant Cell*, *16*(5), 1191–1205.

Chen, H. C., Li, Q., Shuford, C. M., Liu, J., Muddiman, D. C., Sederoff, R. R., & Chiang, V. L. (2011). Membrane Protein Complexes Catalyze Both 4- and 3-Hydroxylation of Cinnamic Acid Derivatives in Monolignol Biosynthesis. *Proceedings of the National Academy of Sciences of the United States of America*, *108*(52), 21253–21258.

Chen, K., Song, M., Guo, Y., Liu, L., Xue, H., Dai, H., & Zhang, Z. (2019). MdMYB46 Could Enhance Salt and Osmotic Stress Tolerance in Apple by Directly Activating Stress-Responsive Signals. *Plant Biotechnology Journal*, *17*(12), 2341–2355.

Chezem, W. R., Memon, A., Li, F. S., Weng, J. K., & Clay, N. K. (2017). SG2-Type R2R3-MYB Transcription Factor MYB15 Controls Defense-Induced Lignification and Basal Immunity in Arabidopsis. *Plant Cell*, *29*(8), 1907–1926.

Choi, H. W., & Klessig, D. F. (2016). DAMPs, MAMPs, and NAMPs in Plant Innate Immunity. *BMC Plant Biology*, *16*(1). doi: 10.1186/s12870-016-0921-2.

Choudhury, F. K., Rivero, R. M., Blumwald, E., & Mittler, R. (2017). Reactive Oxygen Species, Abiotic Stress and Stress Combination. *The Plant Journal*, *90*(5), 856–867.

Chun, H. J., Baek, D., Cho, H. M., Lee, S. H., Jin, B. J., Yun, D. J., Hong, Y. S., & Kim, M. C. (2019). Lignin Biosynthesis Genes Play Critical Roles in the Adaptation of Arabidopsis Plants to High-Salt Stress. *Plant Signaling and Behavior*, *14*(8). doi: 10.1080/15592324.2019.1625697.

Clough, S. J., & Bent, A. F. (1998). Floral dip: A Simplified Method for Agrobacterium-Mediated Transformation of *Arabidopsis thaliana*. *The Plant Journal*, *16*(6), 735–743.

Considine, J., & Knox, R. (1979). Development and Histochemistry of the Cells, Cell Walls, and Cuticle of the Dermal System of Fruit of the Grape, *Vitis vinifera* L. *Protoplasma*, *99*, 347–365.

Cornelis, S., & Hazak, O. (2022). Understanding the Root Xylem Plasticity for Designing Resilient Crops. *Plant Cell and Environment, 45*(3), 664–676.

de Bellis, D., Kalmbach, L., Marhavy, P., Daraspe, J., Geldner, N., & Barberon, M. (2022). Extracellular Vesiculo-Tubular Structures Associated With Suberin Deposition in Plant Cell Walls. *Nature Communications*, *13*(1). doi: 10.1038/s41467-022-29110-0.

De Smet, S., Cuypers, A., Vangronsveld, J., & Remans, T. (2015). Gene Networks Involved in Hormonal Control of Root Development in *Arabidopsis thaliana*: A Framework for Studying its Disturbance by Metal Stress. *International Journal of Molecular Sciences*, *16*(8), 19195–19224.

Decaestecker, W., Buono, R. A., Pfeiffer, M. L., Vangheluwe, N., Jourquin, J., Karimi, M., van Isterdael, G., Beeckman, T., Nowack, M. K., & Jacobs, T. B. (2019). CRISPR-Tsko: A Technique for Efficient Mutagenesis in Specific Cell Types, Tissues, or Organs in Arabidopsis. *Plant Cell*, *31*(12), 2868–2887.

Deeken, R., Saupe, S., Klinkenberg, J., Riedel, M., Leide, J., Hedrich, R., & Mueller, T. D. (2016). The Nonspecific Lipid Transfer Protein AtLtpI-4 is Involved in Suberin Formation of *Arabidopsis thaliana* Crown Galls. *Plant Physiology*, *172*(3), 1911–1927.

Delaux, P. M., Varala, K., Edger, P. P., Coruzzi, G. M., Pires, J. C., & Ané, J. M. (2014). Comparative Phylogenomics Uncovers the Impact of Symbiotic Associations on Host Genome Evolution. *PLoS Genetics*, *10*(7). doi: 10.1371/journal.pgen.1004487.

Dharmawardhana, D. P., Ellis, B. E., & Carlson, J. E. (1992). Characterization of Vascular Lignification in *Arabidopsis thaliana*. *Canadian Journal of Botany, 70*(11), 2238-2244.

Dixon, R. A., & Paiva, N. L. (1995). Stress-Induced Phenylpropanoid Metabolism. *Plant Cell*, *7*, 1085–1097.

Doblas, V. G., Smakowska-Luzan, E., Fujita, S., Alassimone, J., Barberon, M., Madalinski, M., Belkhadir, Y., & Geldner, N. (2017). Root Diffusion Barrier Control by a Vasculature-Derived Peptide Binding to the SGN3 Receptor. *Science*, *355*, 280–284.

Dolan, L., Duckett, C. M., Grierson, C., Linstead, P., Schneider, K., Lawson, E., Dean, C., Poethig, S., & Roberts, K. (1994). Clonal Relationships and Cell Patterning in the Root Epidermis of Arabidopsis. *Development*, *120*, 2465–2474.

Dolan L, Janmaat K, Willemsen V, Linstead P, Poethig S, Roberts K, & Scheres B. (1993). Cellular Organisation of the *Arabidopsis thaliana* Root. *Development*, *119*, 71–84.

Dolan, L., & Roberts, K. (1995). The Development of Cell Pattern in the Root Epidermis. *Philosophical Transactions: Biological Sciences*, *350*(1331), 95–99.

Domergue, F., Vishwanath, S. J., Joubès, J., Ono, J., Lee, J. A., Bourdon, M., Alhattab, R., Lowe, C., Pascal, S., Lessire, R., & Rowland, O. (2010). Three Arabidopsis Fatty Acyl-Coenzyme a Reductases, FAR1, FAR4, and FAR5, Generate Primary Fatty Alcohols Associated With Suberin Deposition. *Plant Physiology*, *153*(4), 1539–1554.

Donaldson, L. (2020). Autofluorescence in Plants. *Molecules, 25*(10). doi: 10.3390/molecules25102393.

Dong, N. Q., & Lin, H. X. (2021). Contribution of Phenylpropanoid Metabolism to Plant Development and Plant–Environment Interactions. *Journal of Integrative Plant Biology*, *63*, 180–209.

Emonet, A., & Hay, A. (2022). Development and Diversity of Lignin Patterns. *Plant Physiology, 190*(1), 31–43.

Emonet, A., Zhou, F., Vacheron, J., Heiman, C. M., Dénervaud Tendon, V., Ma, K. W., Schulze-Lefert, P., Keel, C., & Geldner, N. (2021). Spatially Restricted Immune Responses Are Required for Maintaining Root Meristematic Activity upon Detection of Bacteria. *Current Biology*, *31*(5), 1012-1028.

Enstone, D. E., Peterson, C. A., & Ma, F. (2002). Root Endodermis and Exodermis: Structure, Function, and Responses to the Environment. *Journal of Plant Growth Regulation, 21*(4), 335–351.

Esch, J. J., Chen, M., Sanders, M., Hillestad, M., Ndkium, S., Idelkope, B., Neizer, J., & Marks, M. D. (2003). A Contradictory *GLABRA3* Allele Helps Define Gene Interactions Controlling Trichome Development in Arabidopsis. *Development*, *130*(24), 5885–5894.

Falcone Ferreyra, M. L., Rius, S. P., & Casati, P. (2012). Flavonoids: Biosynthesis, Biological Functions, and Biotechnological Applications. *Frontiers in Plant Science*, *3*. doi: 10.3389/fpls.2012.00222.

Fernandes, A. N., Chen, X., Scotchford, C. A., Walker, J., Wells, D. M., Roberts, C. J., & Everitt, N. M. (2012). Mechanical Properties of Epidermal Cells of Whole Living Roots of *Arabidopsis thaliana*: An Atomic Force Microscopy Study. *Physical Review E - Statistical, Nonlinear and Soft Matter Physics*, *85*(2 Pt 1). doi: 10.1103/PhysRevE.85.021916.

Fich, E. A., Segerson, N. A., & Rose, J. K. C. (2016). The Plant Polyester Cutin: Biosynthesis, Structure, and Biological Roles. *Annual Review of Plant Biology*, *67,* 207–233.

Foreman, J., Demidchik, V., Bothwell, J. H., Mylona, P., Miedema, H., Torres, M. A., Linstead, P., Costa, S., Brownlee, C., Jones, J. D., & al., et. (2003). Reactive Oxygen Species Produced by NADPH Oxidase Regulate Plant Cell Growth. *Nature*, *422*, 442–446.

Franke, R., Briesen, I., Wojciechowski, T., Faust, A., Yephremov, A., Nawrath, C., & Schreiber, L. (2005). Apoplastic Polyesters in Arabidopsis Surface Tissues - A Typical Suberin and a Particular Cutin. *Phytochemistry*, *66*(22), 2643–2658.

Franke, R., Höfer, R., Briesen, I., Emsermann, M., Efremova, N., Yephremov, A., & Schreiber, L. (2009). The DAISY Gene from Arabidopsis Encodes a Fatty Acid Elongase Condensing Enzyme Involved in the Biosynthesis of Aliphatic Suberin in Roots and the Chalaza-Micropyle Region of Seeds. *The Plant Journal*, *57*(1), 80–95.

Fraser, C. M., & Chapple, C. (2011). The Phenylpropanoid Pathway in Arabidopsis. *The Arabidopsis Book*, *9.* doi: 10.1199/tab.0152.

Fujita, S., De Bellis, D., Edel, K. H., Köster, P., Andersen, T. G., Schmid-Siegert, E., Dénervaud Tendon, V., Pfister, A., Marhavý, P., Ursache, R., Doblas, V. G., Barberon, M., Daraspe, J., Creff, A., Ingram, G., Kudla, J., & Geldner, N. (2020). SCHENGEN Receptor Module Drives Localized ROS Production and Lignification in Plant Roots. *The EMBO Journal*, *39*(9). doi: 10.15252/embj.2019103894.

Geldner, N. (2013). The Endodermis. *Annual Review of Plant Biology*, *64*, 531–558.

Girard, A. L., Mounet, F., Lemaire-Chamley, M., Gaillard, C., Elmorjani, K., Vivancos, J., Runavot, J. L., Quemener, B., Petit, J., Germain, V., Rothan, C., Marion, D., & Bakan, B. (2012). Tomato GDSL1 is Required for Cutin Deposition in the Fruit Cuticle. *Plant Cell*, *24*(7), 3106–3121.

Gorshkova, T. A., Salnikov, V. v, Pogodina, N. M., Chemikosova, S. B., Yablokova, E. v, Ulanov, A. v, Ageeva, M. v, van Dam, J. E. G., & Lozovaya, V. v. (2000). Composition

and Distribution of Cell Wall Phenolic Compounds in Flax (*Linum usitatissimum* L.) Stem Tissues. *Annals of Botany*, *85*(4), 477–486.

Graça, J., Cabral, V., Santos, S., Lamosa, P., Serra, O., Molinas, M., Schreiber, L., Kauder, F., & Franke, R. (2015). Partial Depolymerization of Genetically Modified Potato Tuber Periderm Reveals Intermolecular Linkages in Suberin Polyester. *Phytochemistry*, *117*, 209–219.

Grierson, C., Nielsen, E., Ketelaarc, T., & Schiefelbein, J. (2014). Root Hairs. *The Arabidopsis Book*, *12*. doi: 10.1199/tab.0172

Gully, K., Berhin, A., De Bellis, D., & Nawrath, C. (unpublished). GPAT4, GPAT6, and GPAT8 are Required for Suberin Deposition in Arabidopsis Roots with Non-Redundant Functions to GPAT5 and GPAT7.

Higuchi, T. (1990). Lignin biochemistry: Biosynthesis and biodegradation. *Wood Science and Technology*, *24*, 23–63.

Hilfiker, O., Groux, R., Bruessow, F., Kiefer, K., Zeier, J., & Reymond, P. (2014). Insect Eggs Induce a Systemic Acquired Resistance in Arabidopsis. *The Plant Journal*, *80*(6), 1085–1094.

Höfer, R., Briesen, I., Beck, M., Pinot, F., Schreiber, L., & Franke, R. (2008). The Arabidopsis Cytochrome P450 CYP86A1 Encodes a Fatty Acid ω-Hydroxylase Involved in Suberin Monomer Biosynthesis. *Journal of Experimental Botany*, *59*(9), 2347–2360.

Hong, L., Brown, J., Segerson, N. A., Rose, J. K. C., & Roeder, A. H. K. (2017). CUTIN SYNTHASE 2 Maintains Progressively Developing Cuticular Ridges in Arabidopsis Sepals. *Molecular Plant*, *10*(4), 560–574.

Hose, E., Clarkson, D. T., Steudle, E., Schreiber, L., & Hartung, W. (2001). The Exodermis: a Variable Apoplastic Barrier. *Journal of Experimental Botany*, *52*(365), 2245–2264.

Houston, K., Tucker, M. R., Chowdhury, J., Shirley, N., & Little, A. (2016). The Plant Cell Wall: A Complex and Dynamic Structure as Revealed by the Responses of Genes Under Stress Conditions. *Frontiers in Plant Science*, *7*. oi: 10.3389/fpls.2016.00984

Hruz, T., Laule, O., Szabo, G., Wessendorp, F., Bleuler, S., Oertle, L., Widmayer, P., Gruissem, W., & Zimmermann, P. (2008). Genevestigator V3: A Reference Expression Database for the Meta-Analysis of Transcriptomes. *Advances in Bioinformatics*, *2008*, 1–5. doi: 10.1155/2008/420747

Jia, Q., Bai, Y., Xu, H., Liu, Q., Li, W., Li, T., Lin, F., Shen, L., Xuan, W., Zhang, W., & Zhang, Q. (2022). Mitochondrial GPAT-Derived LPA Controls Auxin-Dependent Embryonic and Postembryonic Development. *Proceedings of the National Academy of Sciences of the United States of America*, *119*(49). doi: 10.1073/pnas.2212881119.

Jones, V. A. S., & Dolan, L. (2012). The Evolution of Root Hairs and Rhizoids. *Annals of Botany, 110*(2), 205–212.

Kajala, K., Gouran, M., Shaar-Moshe, L., Mason, G. A., Rodriguez-Medina, J., Kawa, D., Pauluzzi, G., Reynoso, M., Canto-Pastor, A., Manzano, C., Lau, V., Artur, M. A. S., West, D. A., Gray, S. B., Borowsky, A. T., Moore, B. P., Yao, A. I., Morimoto, K. W., Bajic, M., … Brady, S. M. (2021). Innovation, Conservation, and Repurposing of Gene Function in Root Cell Type Development. *Cell*, *184*(12), 3333 – 3348.

Karlsson, M., Melzer, M., Prokhorenko, I., Johansson, T., & Wingsle, G. (2005). Hydrogen Peroxide and Expression of hipl-Superoxide Dismutase are Associated with the Development of Secondary Cell Walls in *Zinnia elegans*. *Journal of Experimental Botany*, *56*(418), 2085–2093.

Karpinska, B., Karlsson, M., Schinkel, H., Streller, S., Süss, K. H., Melzer, M., & Wingsle, G. (2001). A Novel Superoxide Dismutase With a High Isoelectric Point in Higher Plants. Expression, regulation, and protein localization. *Plant Physiology*, *126*(4), 1668–1677.

Khandal, H., Singh, A. P., & Chattopadhyay, D. (2020). The MicroRNA 397b-LaCCASE2 Module Regulates root Lignification Under Water and Phosphate Deficiency. *Plant Physiology*, *182*(3), 1387–1403.

Kolattukudy, P. E. (2001). Polyesters in Higher Plants. *Advances in Biochemical Engineering/ Biotechnology, 71*, 1– 49.

Kosma, D., Murmu, J., Razeq, F., Santos, P., Bourgault, R., Molina, I., & Rowland, I. (2014). AtMYB41 Activates Ectopic Suberin Synthesis and Assembly in Multiple Plant Species and Cell Types. *The Plant Journal*, *80*, 216–229.

Kramer, E. M., Frazer, N. L., & Baskin, T. I. (2007). Measurement of Diffusion Within the Cell Wall in Living Roots of *Arabidopsis thaliana*. *Journal of Experimental Botany*, *58*(11), 3005–3015.

Krishnamurthy, P., Vishal, B., Bhal, A., & Kumar, P. P. (2021). WRKY9 Transcription Factor Regulates Cytochrome P450 Genes *CYP94B3* and *CYP86B1*, Leading to Increased Root Suberin and Salt tolerance in Arabidopsis. *Physiologia Plantarum*, *172*(3), 1673–1687.

Lai, C. P., Huang, L. M., Chen, L. F. O., Chan, M. T., & Shaw, J. F. (2017). Genome-Wide Analysis of GDSL-Type Esterases/Lipases in Arabidopsis. *Plant Molecular Biology*, *95*(1–2), 181–197.

Lee, M., Jeon, H. S., Kim, S. H., Chung, J. H., Roppolo, D., Lee, H., Cho, H. J., Tobimatsu, Y., Ralph, J., & Park, O. K. (2019). Lignin-Based Barrier Restricts Pathogens to the Infection Site and Confers Resistance in Plants. *The EMBO Journal*, *38*(23). doi: 10.15252/embj.2019101948.

Lee, S. B., Jung, S. J., Go, Y. S., Kim, H. U., Kim, J. K., Cho, H. J., Park, O. K., & Suh, M. C. (2009). Two Arabidopsis 3-Ketoacyl CoA Synthase Genes, KCS20 and KCS2/DAISY, are Functionally Redundant in Cuticular Wax and Root Suberin Biosynthesis, but Differentially Controlled by Osmotic Stress. *The Plant Journal*, *60*(3), 462–475.

Lee, Y., Rubio, M. C., Alassimone, J., & Geldner, N. (2013). A Mechanism for Localized Lignin Deposition in the Endodermis. *Cell*, *153*(2), 402–412.

Lepiniec, L., Debeaujon, I., Routaboul, J. M., Baudry, A., Pourcel, L., Nesi, N., & Caboche, M. (2006). Genetics and Biochemistry of Seed Flavonoids. *Annual Review of Plant Biology, 57*, 405–430.

Li-Beisson, Y., Pollard, M., Sauveplane, V., Pinot, F., Ohlrogge, J., & Beisson, F. (2009). Nanoridges that Characterize the Surface Morphology of Flowers Require the Synthesis of Cutin Polyester. *Proceedings of the National Academy of Sciences of the United States of America*, *106*(51), 22008–22013.

Lin, Y., & Schiefelbein, J. (2001). Embryonic Control of Epidermal Cell Patterning in the Root and Hypocotyl of Arabidopsis. *Development*, *128*, 3697–3705.

Liu, Q., Luo, L., & Zheng, L. (2018). Lignins: Biosynthesis and Biological Functions in Plants. *International Journal of Molecular Sciences, 19*(2). doi: 10.3390/ijms19020335.

Liu, S., Strauss, S., Adibi, M., Mosca, G., Yoshida, S., Dello Ioio, R., Runions, A., Andersen, T. G., Grossmann, G., Huijser, P., Smith, R. S., & Tsiantis, M. (2022). Cytokinin Promotes Growth Cessation in the Arabidopsis Root. *Current Biology*, *32*(9), 1974-1985.e3.

Long, Y., & Schiefelbein, J. (2020). Novel TTG1 Mutants Modify Root-Hair Pattern Formation in Arabidopsis. *Frontiers in Plant Science*, *11*. doi: 10.3389/fpls.2020.00383.

Lü, S., Song, T., Kosma, D. K., Parsons, E. P., Rowland, O., & Jenks, M. A. (2009). Arabidopsis CER8 EEncodes LONG-CHAIN ACYL-COA SYNTHETASE 1 (LACS1) that has Overlapping Functions with LACS2 in Plant Wax and Cutin Synthesis. *The Plant Journal*, *59*(4), 553–564.

Lucas, W. J., Groover, A., Lichtenberger, R., Furuta, K., Yadav, S. R., Helariutta, Y., He, X. Q., Fukuda, H., Kang, J., Brady, S. M., Patrick, J. W., Sperry, J., Yoshida, A., López-Millán, A. F., Grusak, M. A., & Kachroo, P. (2013). The Plant Vascular System: Evolution, Development and Functions. *Journal of Integrative Plant Biology, 55*(4), 294–388.

Mähönen, A., Bishopp, A., Higuchi, M., Nieminen, K., Kinoshita, K., Törmäkangas, K., Ikeda, Y., Oka, A., Kakimoto, T., & Helariutta, Y. (2006). Cytokinin signaling and its Inhibitor AHP6 Regulate Cell Fate During Vascular Development. *Science*, *311*(5757), 94–98.

Manzano, C., Morimoto, K. W., Shaar-Moshe, L., Mason, G. A., Cantó-Pastor, A., Gouran, M., De Bellis, D., Ursache, R., Kajala, K., Sinha, N., Bailey-Serres, J., Geldner, N., Carlos Del Pozo, J., & Brady, S. M. (2022). Regulation and Function of a Polarly Localized Lignin Barrier in the Exodermis. *BioRxiv*.

Marzec, M., Melzer, M., & Szarejko, I. (2013). Asymmetric Growth of Root Epidermal Cells is Related to the Differentiation of Root Hair Cells in *Hordeum vulgare* (L.). *Journal of Experimental Botany*, *64*(16), 5145–5155.

Masucci, J. D., & Schiefelbein, J. W. (1994). The rhd6 Mutation of *Arabidopsis thaliana* Alters Root-Hair Initiation through an Auxin- and Ethylene-Associated Process. *Plant Physiology*, *106*, 1335–1346.

Mathew, S., & Abraham, T. E. (2004). Ferulic Acid: An Antioxidant Found Naturally in Plant Cell Walls and Feruloyl Esterases Involved in its Release and their Applications. *Critical Reviews in Biotechnology*, *24*(2–3), 59–83.

McFarlane, H. E., Döring, A., & Persson, S. (2014). The Cell Biology of Cellulose Synthesis. *Annual Review of Plant Biology*, *65*, 69–94.

Meyer, C. J., Peterson, C. A., & Bernards, M. A. (2011). Spatial and Temporal Deposition of Suberin During Maturation of the Onion Root Exodermis. *Botany*, *89*(2), 119–131.

Mnich, E., Bjarnholt, N., Eudes, A., Harholt, J., Holland, C., Jørgensen, B., Larsen, F. H., Liu, M., Manat, R., Meyer, A. S., Mikkelsen, J. D., Motawia, M. S., Muschiol, J., Møller, B. L., Møller, S. R., Perzon, A., Petersen, B. L., Ravn, J. L., & Ulvskov, P. (2020). Phenolic Cross-Links: Building and De-Constructing the Plant Cell Wall. *Natural Product Reports*, *37*(7), 919–961.

Moghe, G., Kruse, L. H., Petersen, M., Scossa, F., Fernie, A. R., Gaquerel, E., & D'auria, J. C. (2023). BAHD Company: The Ever-Expanding Roles of the BAHD Acyltransferase Gene Family in Plants. *Annual Review of Plant Biology*, *74*(1). doi: 10.1146/annurev-arplant-062922-050122.

Molina, I., Li-Beisson, Y., Beisson, F., Ohlrogge, J. B., & Pollard, M. (2009). Identification of an Arabidopsis Feruloyl-Coenzyme a Transferase Required for Suberin Synthesis. *Plant Physiology*, *151*(3), 1317–1328.

Moura, J. C. M. S., Bonine, C. A. V., de Oliveira Fernandes Viana, J., Dornelas, M. C., & Mazzafera, P. (2010). Abiotic and Biotic Stresses and Changes in the Lignin Content and Composition in Plants. *Journal of Integrative Plant Biology, 52*(4), 360–376.

Müller, J., Toev, T., Heisters, M., Teller, J., Moore, K. L., Hause, G., Dinesh, D. C., Bürstenbinder, K., & Abel, S. (2015). Iron-Dependent Callose Deposition Adjusts Root Meristem Maintenance to Phosphate Availability. *Developmental Cell*, *33*(2), 216–230.

Naseer, S., Lee, Y., Lapierre, C., Franke, R., Nawrath, C., & Geldner, N. (2012). Casparian Strip Diffusion Barrier in Arabidopsis is Made of a Lignin Polymer Without Suberin. *Proceedings of the National Academy of Sciences of the United States of America*, *109*(25), 10101–10106.

Nawrath, C., Schreiber, L., Franke, R. B., Geldner, N., Reina-Pinto, J. J., & Kunst, L. (2013). Apoplastic Diffusion Barriers in Arabidopsis. *The Arabidopsis Book*, *11*. doi: 10.1199/tab.0167.

Önnerud, H., Zhang, L., Gellerstedt, G., & Henriksson, G. (2002). Polymerization of Monolignols by Redox Shuttle-Mediated Enzymatic Oxidation: A New Model in Lignin Biosynthesis I. *Plant Cell*, *14*(8), 1953–1962.

Pandey, J. L., Wang, B., Diehl, B. G., Richard, T. L., Chen, G., & Anderson, C. T. (2015). A Versatile Click-Compatible Monolignol Probe to Study Lignin Deposition in Plant Cell Walls. *PLoS ONE*, *10*(4). doi: 10.1371/journal.pone.0121334.

Panikashvili, D., Shi, J. X., Bocobza, S., Franke, R. B., Schreiber, L., & Aharoni, A. (2010). The Arabidopsis DSO/ABCG11 Transporter Affects Cutin Metabolism in Reproductive Organs and Suberin in Roots. *Molecular Plant*, *3*(3), 563–575.

Panikashvili, D., Shi, J. X., Schreiber, L., & Aharoni, A. (2009). The Arabidopsis DCR Encoding a Soluble BAHD acyltransferase is Required for Cutin Polyester Formation and Seed Hydration Properties. *Plant Physiology*, *151*(4), 1773–1789.

Payne, C. T., Zhang, F., & Lloyd, A. M. (2000). GL3 Encodes a bHLH Protein That Regulates Trichome Development in Arabidopsis Through Interaction with GL1 and TTG1. *Genetics*, *156*, 1349–1362.

Perumalla, C. J., Peterson, C. A., & Enstone, D. E. (1990). A Survey of Angiosperm Species to Detect Hypodermal Casparian bands. I. Roots With a Uniseriate Hypodermis and Epidermis. *Botanical Journal of the Linnean Society*, *103*, 93–112.

Pesquet, E., Ranocha, P., Legay, S., Digonnet, C., Barbier, O., Pichon, M., & Goffner, D. (2005). Novel Markers of Cylogenesis in *Zinnia* are Differentially Regulated by Auxin and Cytokinin. *Plant Physiology*, *139*(4), 1821–1839.

Peterson, C. A., & Emanuel, M. E. (1983). Casparian Strips Occur in Onion Root Hypodermal Cells: Evidence from Band Plasmolysis. *Annals of Botany, 51*(1).

Peterson, C. A., Peterson, R. L., & Robards, A. W. (1978). Correlated Histochemical and Ultrastructural Study of the Epidermis and Hypodermis of Onion Roots. *Protoplasma*, *96*, 1–21.

Philippe, G., de Bellis, D., Rose, J. K. C., & Nawrath, C. (2022). Trafficking Processes and Secretion Pathways Underlying the Formation of Plant Cuticles. *Frontiers in Plant Science*, *12*. doi: 10.3389/fpls.2021.786874.

Ranathunge, K., Thomas, R. H., Fang, X., Peterson, C. A., Gijzen, M., & Bernards, M. A. (2008). Soybean Root Suberin and Partial Resistance to Root Rot Caused by *Phytophthora sojae*. *Phytopathology*, *98*(11), 1179–1189.

Rani, S. H., Krishna, T. H. A., Saha, S., Negi, A. S., & Rajasekharan, R. (2010). Defective in Cuticular Ridges (DCR) of *Arabidopsis thaliana*, a Gene Associated With Surface Cutin Formation, Encodes a Soluble Diacylglycerol Acyltransferase. *Journal of Biological Chemistry*, *285*(49), 38337–38347.

Rautengarten, C., Ebert, B., Ouellet, M., Nafisi, M., Baidoo, E. E. K., Benke, P., Stranne, M., Mukhopadhyay, A., Keasling, J. D., Sakuragi, Y., & Scheller, H. V. (2012). Arabidopsis Deficient in Cutin Ferulate Encodes a Transferase Required for Feruloylation of ω-Hydroxy Fatty Acids in Cutin Polyester. *Plant Physiology*, *158*(2), 654–665.

Renard, J., Martínez-Almonacid, I., Queralta Castillo, I., Sonntag, A., Hashim, A., Bissoli, G., Campos, L., Muñoz-Bertomeu, J., Niñoles, R., Roach, T., Sánchez-León, S., Ozuna, C. v., Gadea, J., Lisón, P., Kranner, I., Barro, F., Serrano, R., Molina, I., & Bueso, E. (2021). Apoplastic Lipid Barriers Regulated by Conserved Homeobox Transcription Factors Extend Seed Longevity in Multiple Plant Species. *New Phytologist*, *231*(2), 679–694.

Renault, H., Werck-Reichhart, D., & Weng, J. K. (2019). Harnessing Lignin Evolution for Biotechnological Applications. *Current Opinion in Biotechnology, 56*, 105-111.

Reyt, G., Ramakrishna, P., Salas-González, I., Fujita, S., Love, A., Tiemessen, D., Lapierre, C., Morreel, K., Calvo-Polanco, M., Flis, P., Geldner, N., Boursiac, Y., Boerjan, W., George, M. W., Castrillo, G., & Salt, D. E. (2021). Two Chemically Distinct Root Lignin Barriers Control Solute and Water Balance. *Nature Communications*, *12*(1). doi: 10.1038/s41467-021-22550-0.

Rojas-Murcia, N., Hématy, K., Lee, Y., Emonet, A., Ursache, R., Fujita, S., De Bellis, D., & Geldner, N. (2020). High-Order Mutants Reveal an Essential Requirement for Peroxidases But Not Laccases in Casparian Strip Lignification. *Proceedings of the National Academy of Sciences of the United States of America*, *117*(46), 29166–29177.

Roppolo, D., Boeckmann, B., Pfister, A., Boutet, E., Rubio, M. C., Dénervaud-Tendon, V., Vermeer, J. E. M., Gheyselinck, J., Xenarios, I., & Geldner, N. (2014). Functional and Evolutionary Analysis of the CASPARIAN STRIP MEMBRANE DOMAIN PROTEIN Family. *Plant Physiology*, *165*(4), 1709–1722.

Rowe, J. H., Topping, J. F., Liu, J., & Lindsey, K. (2016). Abscisic Acid Regulates Root Growth Under Osmotic Stress Conditions via an Interacting Hormonal Network with Cytokinin, Ethylene and Auxin. *New Phytologist*, *211*(1), 225–239.

Ruegger, M., & Chapple, C. (2001). Mutations That Reduce Sinapoylmalate Accumulation in *Arabidopsis thaliana* Define Loci with Diverse Roles in Phenylpropanoid Metabolism. *Genetics*, *159*, 1741–1749.

Sapala, A., & Smith, R. S. (2020). Osmotic Treatment for Quantifying Cell Wall Elasticity in the Sepal of *Arabidopsis thaliana*. *Methods in Molecular Biology, 2094*, 101-112.

Schalk, M., Cabello-Hurtado, F., Pierrel, M. A., Atanossova, R., Saindrenan, P., & Werck-Reichhart, D. (1998). Piperonylic Acid, A Selective, Mechanism-Based Inactivator of the

Trans-Cinnamate 4-Hydroxylase: A New Tool to Control the Flux of Metabolites in the Phenylpropanoid Pathway. *Plant Physiology*, *118*(1), 209–218.

Scheres, B., Benfey, P., & Dolan, L. (2002). Root Development. *The Arabidopsis Book*, *1.* doi: 10.1199/tab.0101.

Scheres B, Di Laurenzio L, Willemsen V, Hauser M-T, Janmaat K, Weisbeek P, & Benfey PN. (1995). Mutations Affecting the Radial Organisation of the Arabidopsis Root Display Specific Defects Throughout the Embryonic Axis. *Development*, *121*, 53–62.

Schiefelbein, J. W., & Somerville, C. (1990). Genetic Control of Root Hair Development in *Arabidopsis thaliana*. *Plant Cell*, *2*, 235–243.

Schmittgen, T. D., & Livak, K. J. (2008). Analyzing Real-Time PCR Data by the Comparative CT Method. *Nature Protocols*, *3*(6), 1101–1108.

Schnurr, J., Shockey, J., & Browse, J. (2004). The Acyl-CoA Synthetase Encoded by LACS2 is Essential for Normal Cuticle Development in Arabidopsis. *Plant Cell*, *16*(3), 629–642.

Serra, O., & Geldner, N. (2022). The Making of Suberin. *New Phytologist*, *235*(3), 848–866.

Serra, O., Soler, M., Hohn, C., Franke, R., Schreiber, L., Prat, S., Molinas, M., & Figueras, M. (2009). Silencing of StKCS6 in Potato Periderm Leads to Reduced Chain Lengths of Suberin and Wax Compounds and Increased Peridermal Transpiration. *Journal of Experimental Botany*, *60*(2), 697–707.

Shibata, M., & Sugimoto, K. (2019). A Gene Regulatory Network for Root Hair Development. *Journal of Plant Research*, *132*(3), 301–309.

Shukla, V., Han, J.-P., Cléard, F., Lefebvre-Legendre, L., Gully, K., Flis, P., Berhin, A., Andersen, T. G., Salt, D. E., Nawrath, C., & Barberon, M. (2021). Suberin Plasticity to Developmental and Exogenous Cues is Regulated by a Set of MYB Transcription Factors. *Proceedings of the National Academy of Sciences of the United States of America*, *118*(39). doi: 10.1073/pnas.2101730118.

Siligato, R., Wang, X., Yadav, S. R., Lehesranta, S., Ma, G., Ursache, R., Sevilem, I., Zhang, J., Gorte, M., Prasad, K., Wrzaczek, M., Heidstra, R., Murphy, A., Scheres, B., & Mähönen, A. P. (2016). Multisite Gateway-Compatible Cell Type-Specific Gene-Inducible System for Plants. *Plant Physiology*, *170*(2), 627–641.

Somssich, M., Khan, G. A., & Staffan, S. P. (2016). Cell Wall Heterogeneity in Root Development of Arabidopsis. *Frontiers in Plant Science*, *7*(1242). doi: 10.3389/fpls.2016.01242.

Song, S.-K., Hui Ryu, K., Hee Kang, Y., Hyo Song, J., Cho, Y.-H., Yoo, S.-D., Schiefelbein, J., & Min Lee, M. (2011). Cell Fate in the Arabidopsis Root Epidermis Is Determined by Competition between WEREWOLF and CAPRICE. *Plant Physiology*, *157*(3), 1196–1208.

Spicer, R., & Groover, A. (2010). Evolution of Development of Vascular Cambia and Secondary Growth. *New Phytologist*, *186*(3), 577–592.

Stout, J., Romero-Severson, E., Ruegger, M. O., & Chapple, C. (2008). Semidominant Mutations in Reduced Epidermal Fluorescence 4 Reduce Phenylpropanoid Content in Arabidopsis. *Genetics*, *178*(4), 2237–2251.

Swamy, P. M., & Smith, B. N. (1999). Role of Abscisic Acid in Plant Stress Tolerance. *Current Science*, *76*(9), 1220–1227.

Takeuchi, M., Watanabe, A., Tamura, M., & Tsutsumi, Y. (2018). The Gene Expression Analysis of *Arabidopsis thaliana* ABC Transporters by Real-Time PCR for Screening Monolignol-Transporter Candidates. *Journal of Wood Science*, *64*(5), 477–484.

Tamminen, T., Poppius-Levlin, K., Aurela, B., & Kcl, B. H. (1997). Oxidative Degradation of Lignin by Potassium Permanganate-Method Improvement. *Holzforschung*, *51*(2), 155–157.

Tanimoto, M., Roberts, K., & Dolan, L. (1995). Ethylene is a Positive Regulator of Root Hair Development in *Arabidopsis thaliana*. *The Plant Journal*, *8*(6), 943–948.

Thomas, R., Fang, X., Ranathunge, K., Anderson, T. R., Peterson, C. A., & Bernards, M. A. (2007). Soybean Root Suberin: Anatomical Distribution, Chemical Composition, and Relationship to Partial Resistance to *Phytophthora sojae*. *Plant Physiology*, *144*(1), 299–311.

Tognolli, M., Penel, C., Greppin, H., & Simon, P. (2002). Analysis and Expression of the Class III Peroxidase Large Gene family in *Arabidopsis thaliana*. *Gene*, *288*, 129–138.

Tuladhar, A., Ohtsuka, S., & Nii, N. (2014). Formation of Exclusive Pattern During Accumulation of Ligno-Suberic Material in Cell Wall of Myrtaceae Root Tissues Including Epidermis, Exodermis, Endodermis and Polyderm. *Plant Root*, *8*, 24–32.

Ursache, R., Andersen, T. G., Marhavý, P., & Geldner, N. (2018). A Protocol for Combining Fluorescent Proteins with Histological Stains for Diverse Cell Wall Components. *The Plant Journal*, *93*(2), 399–412.

Ursache, R., De Jesus Vieira Teixeira, C., Dénervaud Tendon, V., Gully, K., De Bellis, D., Schmid-Siegert, E., Grube Andersen, T., Shekhar, V., Calderon, S., Pradervand, S., Nawrath, C., Geldner, N., & Vermeer, J. E. M. (2021). GDSL-Domain Proteins Have Key Roles in Suberin Polymerization and Degradation. *Nature Plants*, *7*(3), 353–364.

Ursache, R., Fujita, S., Dénervaud Tendon, V., & Geldner, N. (2021). Combined Fluorescent Seed Selection and Multiplex CRISPR/Cas9 Assembly for Fast Generation of Multiple Arabidopsis Mutants. *Plant Methods*, *17*(1). https://doi.org/10.1186/s13007-021-00811-9

Üstüner, S., Schäfer, P., & Eichmann, R. (2022). Development Specifies, Diversifies and Empowers Root Immunity. *EMBO Reports*, *23*(12). doi: 10.15252/embr.202255631

Verbon, E. H., Liberman, L. M., Zhou, J., Yin, J., Pieterse, C. M., Benfey, N., Stringlis, I. A., & de Jonge, R. (2022). Cell-Type Specific Transcriptomics Reveals Roles for Root Hairs and Endodermal Barriers in Interaction with Beneficial Rhizobacterium. *BioRxiv*.

Vogt, T. (2010). Phenylpropanoid Biosynthesis. *Molecular Plant*, *3*(1), 2–20.

Walker, T. S., Bais, H. P., Grotewold, E., & Vivanco, J. M. (2003). Root Exudation and Rhizosphere Biology. *Plant Physiology, 132*(1), 44-51.

Wallace, G., & Fry, S. C. (1994). Phenolic Components of the Plant Cell Wall. *International Review of Cytology*, *151*, 229-267.

Wendrich, J. R., Yang, B. J., Vandamme, N., Verstaen, K., Smet, W., Velde, C. van de, Minne, M., Wybouw, B., Mor, E., Arents, H. E., Nolf, J., van Duyse, J., van Isterdael, G., Maere, S., Saeys, Y., & Rybel, B. de. (2020). Vascular Transcription Factors Guide Plant Epidermal Responses to Limiting Phosphate Conditions. *Science*, *370*(6518). doi: 10.1126/science.aay4970

Wilson, C. A., & Peterson, C. A. (1983). Chemical Composition of the Epidermal, Hypodermal, Endodermal and Intervening Cortical Cell Walls of Various Plant Roots. *Annals of Botany*, *51*(6), 759-769.

Wilusz, C. J., Wormington, M., & Peltz, S. W. (2001). The Cap-To-Tail Guide To mRNA Turnover. *Nature Reviews*, *2*, 237–246.

Wunderling, A., Ripper, D., Barra-Jimenez, A., Mahn, S., Sajak, K., Targem, M. ben, & Ragni, L. (2018). A Molecular Framework to Study Periderm Formation in Arabidopsis. *New Phytologist*, *219*(1), 216–229.

Yang, W., Pollard, M., Li-Beisson, Y., Beisson, F., Feig, M., & Ohlrogge, J. (2010). A Distinct Type of Glycerol-3-Phosphate Acyltransferase with sn-2 Preference and Phosphatase Activity Producing 2-Monoacylglycerol. *Proceedings of the National Academy of Sciences of the United States of America*, *107*(26), 12040–12045.

Yang, W., Simpson, J. P., Li-Beisson, Y., Beisson, F., Pollard, M., & Ohlrogge, J. B. (2012). A Land-Plant-Specific Glycerol-3-Phosphate Acyltransferase Family in Arabidopsis: Substrate specificity, sn-2 preference, and evolution. *Plant Physiology*, *160*(2), 638–652.

Yu, X. H., Gou, J. Y., & Liu, C. J. (2009). BAHD Superfamily of Acyl-CoA Dependent Acyltransferases in Populus and Arabidopsis: Bioinformatics and gene expression. *Plant Molecular Biology*, *70*(4), 421–442.

Zhang, F., Gonzalez, A., Zhao, M., Payne, C. T., & Lloyd, A. (2003). A Network of Redundant bHLH Proteins Functions in all TTG1-Dependent Pathways of Arabidopsis. *Development*, *130*(20), 4859–4869.

Zhang, J., Li, Y., Bao, Q., Wang, H., & Hou, S. (2022). Plant Elicitor Peptide 1 Fortifies Root Cell Walls and Triggers a Systemic Root-to-Shoot Immune Signaling in Arabidopsis. *Plant Signaling and Behavior*, *17*(1):2034270. doi: 10.1080/15592324.2022.2034270.

Zhang, J. W., Xu, L., Wu, Y. R., Chen, X. A., Liu, Y., Zhu, S. H., Ding, W. N., Wu, P., & Yi, K. K. (2012). OsGLU3, a Putative Membrane-Bound EEndo-1,4-Beta-Glucanase, is Required for Root Cell Elongation and Division in Rice (*Oryza sativa* L.). *Molecular Plant*, *5*(1), 176–186.

Zhao, Q., Nakashima, J., Chen, F., Yin, Y., Fu, C., Yun, J., Shao, H., Wang, X., Wang, Z. Y., & Dixon, R. A. (2013). LACCASE is Necessary and Nonredundant with PEROXIDASE for Lignin Polymerization During Vascular Development in Arabidopsis. *Plant Cell*, *25*(10), 3976–3987.

Zheng, Z., Xia, Q., Dauk, M., Shen, W., Selvaraj, G., & Zou, J. (2003). Arabidopsis AtGPAT1, a Member of the Membrane-Bound Glycerol-3-Phosphate Acyltransferase Gene Family, is Essential for Tapetum Tifferentiation and Male Fertility. *Plant Cell*, *15*(8), 1872–1887.

Zhou, J., Lee, C., Zhong, R., & Ye, Z. H. (2009). MYB58 and MYB63 are Transcriptional Activators of the Lignin Biosynthetic Pathway During Secondary Cell Wall Formation in Arabidopsis. *Plant Cell*, *21*(1), 248–266.

Zhou, X., Xiang, Y., Li, C., & Yu, G. (2020). Modulatory Role of Reactive Oxygen Species in Root Development in Model Plant of *Arabidopsis thaliana*. *Frontiers in Plant Science*, *11*:485932. doi: 10.3389/fpls.2020.485932

Supplementary data

Table S1. Gene names and numbers

Gene number	Gene name	Gene number	Gene name
AT1G80100	*AHP6*	AT2G48110	*MED5B*
AT3G19450	*CAD4*	*AT4G38620*	*MYB4*
AT4G34230	*CAD5*	*AT1G05260*	*PER3*
AT1G15950	*CCR1*	*AT1G44970*	*PER9*
AT2G16385	*CIF1*	*AT4G11290*	*PER39*
AT4G34600	*CIF2*	*AT5G42180*	*PER64*
AT5G13930	*CHS*	*AT5G66390*	*PER72*
AT2G34770	*F5H1*	AT5G07390	*RBOHA*
AT5G04330	*F5H2*	AT5G51060	*RBOHC/RHD2*
AT1G06520	*GPAT1*	AT5G47910	*RBOHD*
AT1G02390	*GPAT2*	AT1G64060	*RBOHF*
AT4G01950	*GPAT3*	AT1G19230	*RBOHE*
AT2G38110	*GPAT7*	AT1G66470	*RHD6*
AT3G27920	*GL1*	*AT2G37260*	*TTG2*

Table S2. CRISPR and cloning

Name	Sequence	Purpose
pGPAT1-KpnI_F	CAT AGG TAC CAC AAT GAC CGG GAG AAG	Cloning
pGPAT1-XmaI_R	CAT ACC CGG GAG CTA TGG CGT AGA GAG	Cloning
GPAT3_sgRNA1_F	ATT GCT CTT GTC TTT CTA TTC TAC	Cloning
GPAT3_sgRNA1_R	AAA CGT AGA ATA GAA AGA CAA GAG	Cloning
GPAT3_sgRNA2_F	GTC AAC ATT GAT CTT CAA CGT AGA	Cloning
GPAT3_sgRNA2_R	AAA CTC TAC GTT GAA GAT CAA TGT	Cloning
GPAT3_sgRNA3_F	ATT GAG TGA TGC CAA TAA CAC GAC	Cloning
GPAT3_sgRNA3_R	AAA CGT CGT GTT ATT GGC ATC ACT	Cloning
GPAT3_F1	CGG TTT CAG TTT CGC TTT GT	Genotyping
GPAT3_R1	TCG CAA TCA AGC AAG TTG TC	Genotyping
GPAT3_F2	ACG GTT TCA GTT TCG CTT TGT	Genotyping
GPAT3_R2	TGT CCG TGT TTC ATC ACC GT	Genotyping
GPAT3_sg3_R	TGTTGCTTTTTACTAATTATC	Sequencing

Table S3. qPCR primers

Name	Sequence	Reference
SAND_F	AACTCTATGCAGCATTTGATCCACT	Hilfiker et al., 2014
SAND_R	TGATTGCATATCTTTATCGCCATC	Hilfiker et al., 2014
GPAT1_F	CCTCCTCGACCCAGTTTTCC	This study
GPAT1_R	TGCCTCACCGTCTTTCTTCC	This study
GPAT2_F	GAA AGA CTT GGT AGT GGT CGT CG	Berhin, unpublished
GPAT2_R	TTA GGG TAT TGA TCT TGT GGT AGG G	Berhin, unpublished
GPAT3_F	CTC CAT TAT TAC CGG CCA AGA TC	Berhin, unpublished
GPAT3_R	ACT TGA CCC GCT TTT CTT CCT C	Berhin, unpublished
GPAT5_F	TCGTTATGTGAGGAGCATATTCATG	Kosma et al., 2014
GPAT5_R	TTGTTGGTCACCGTGGTTGT	Kosma et al., 2014
GPAT7_F	GGTCTAGGACGACATATTATCTCGG	Berhin, unpublished
GPAT7_R	GCCGCTGGTTATGACCG	Berhin, unpublished